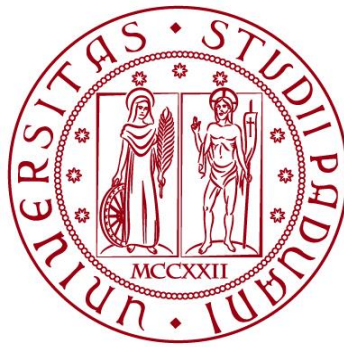


**UNIVERSITÀ DEGLI STUDI DI PADOVA**

**DIPARTIMENTO DI BIOLOGIA**

**Corso di Laurea magistrale in MARINE BIOLOGY**



**TESI DI LAUREA**

**Assessing the structure of the circalittoral  
epibenthic community in the Slovenian Sea  
using video sledge**

**Relatore:** Professoressa Laura Airoidi

Dipartimento di Biologia

**Correlatore:** Doc. dr. Borut Mavrič

National Institute of Biology, Marine Biology Station Piran, Slovenia

**Laureanda:** Neža Leban

**ANNO ACCADEMICO 2023/2024**

## Table of contents

Abstract .....	3
Introduction .....	5
Benthic community .....	5
Granulometry and sediment classification .....	7
Study area .....	8
Sedimentation and sediment classification in the study area .....	9
Benthic community observation in the North Adriatic and study area .....	11
Aim of study .....	14
Materials and methods .....	15
SKIKAM – video sledge .....	15
Data collection .....	16
Video analysis .....	17
Categorization of the sea bottom .....	20
The muddy-sand type .....	22
The transitional type .....	24
The sandy-mud type .....	24
Statistical analysis .....	27
Results .....	30
Faunistic description and community structure of the study area .....	30
Faunistic description and community structure of communities associated with sea bottom types .....	38
The muddy-sand type .....	38
The transitional type .....	40
The sandy-mud type .....	40
Discussion .....	48
Acknowledgements .....	58
References .....	59
Appendix A .....	67
Data collected during sampling .....	67
Appendix B .....	77
List of species with comments on identification process .....	77

## Abstract

Keywords: circalittoral, soft bottom, epibenthic community, video sledge, , Northern Adriatic

One of the main factors shaping a marine benthic community is sediment composition of the seafloor. In this study, we observed an epibenthic community in an offshore area of the Slovenian Sea represented mainly by sandy bottom with gradually increasing pelite fraction in the sediment towards the coastline. The observations were carried out along linear transects using a video sledge (SKIKAM) in the spring of 2022 and 2023. The video sledge is comprised of three video cameras, two laser pointers and lights fixed to a metal construction, with a pair of skis attached on the bottom. At each location, the videos of the sea bottom were recorded together with additional data on GPS position, speed and duration of survey. Each video transect was divided into sub-sections with the duration of approximately 3 minutes, which were then analysed separately. The video analysis included taxonomic identification of organisms, their size and abundance together with a visual observation of changes in community structure, the amount and distribution of organic detritus, comprised of mollusc shells and dead organism skeletons, along with changes in the seafloor topography including presence of bumps and recessions on the bottom.

The overall number of taxa observed was 129, of which 91 were determined to the species level. The highest species diversity belonged to Tunicata (24 taxa, 19%) followed by Porifera (23 taxa, 18%) and Cnidaria (18 taxa, 14%). The echinoderms had the highest abundance (3036/100m<sup>2</sup>, 76%) followed by sponges (409/100m<sup>2</sup>, 10%) and cnidarians (171/100m<sup>2</sup>, 4%). The dominant species was the brittle star *Ophiothrix quinque maculata* (2900/100m<sup>2</sup>, 70%). In the area surveyed, we have observed visible changes in species composition and distribution, changes in the seafloor topography and the amount and distribution of coarse detritus material on the bottom. We recognised similar community characteristics in transects, sampled in the areas with similar pelite fraction in the sediment. We distinguished between the community type found on muddy-sand (from up to 20% to up to 40% pelite), sandy-mud (from up to 50% to up to 60% pelite) and transitional area (from up to

30% to up to 50% pelite) which included the characteristics of both groups. The muddy-sand sea bottom type (MS) was most recognisable by the overall high abundance of *O. quinquemaculata*, great quantity of small organic detritus particles and overall flat bottom surface. We recognised the transitional sea bottom type (T) by the overall high abundance of *O. quinquemaculata*, high quantity of detritus, with the prevalence of coarse detritus material, and a variance in the roughness of the bottom surface. The sandy-mud sea bottom type (SM) was characterized by low abundance of *O. quinquemaculata*, along with a general low abundance of epifaunal species, low quantity of detritus material and uneven bottom surface with frequent occurrence of sediment mounds and regressions in the seafloor. *O. quinquemaculata* contributed to the majority of the difference between sea bottom types. We applied a non-parametrical test (ANOSIM) based on the Bray-Curtis distance measure, which presented a significant difference between the three sea bottom types, along with the result of the SIMPER analysis, which the highest dissimilarity (0.66) between muddy-sand and sandy-mud type. *O. quinquemaculata* contributed to the greatest difference (77%) between the sandy-mud and transitional sea bottom types and presented a dominant species in abundance measures. Finally, in some areas we observed damages on the seabed that can be associated with fishing activity.

## Introduction

### Benthic community

Marine communities are collections of plants and animals within an area of the ocean that interact with one another more than with other such collections (Snelgrove, 2003). The species distribution and community structure are influenced by environmental factors, food availability, trophic interactions, habitat properties and outside disturbances (Craig & Jones, 1966; Pan & Pratolongo, 2021).

When observing the benthic community, we focus on the benthic zone, described as the lowest ecological zone in the water body including the sediment and sub-sediment levels. The seafloor is divided into hard and soft substrata, which can differ in sediment particle accumulation rate, benthic community structure and the degree of ecological and biogenic processes (Pan & Pratolongo, 2021).

The term "benthos" can also be used when describing the organisms that inhabit the benthic habitats ranging from bacteria, algae and plants to invertebrates and vertebrates. Based on the size and living space of organisms, they can be classified as microbenthos, which includes photosynthetic organisms and bacteria smaller than 40µm living mostly attached to sediment particles; meiobenthos, including organisms living in the interstitial space between sediment grains ranging from 40µm to 500µm; and macrobenthos, organisms bigger than 500µm living in or on the sediment surface (Pan & Pratolongo, 2021; Watling, 2019). Additionally, all truly benthic species are considered to be mostly sessile with specific adaptations associated with living on or in the substrate: elongated body forms, calcareous shells and appendages along with body musculature enabling movement over and into the sediment (Parsons *et al.*, 1984).

Benthic marine organisms can be further divided into two ecologically different groups: the epifauna and the infauna (Thorson, 1957). Most epibenthic (*i.e.* organisms living on the sediment surface, attached or capable of movement) and endobenthic (*i.e.* organisms living within the sediment, capable of moving freely through the sediment and building burrows and tubes ) organisms have developed some adaptations relating to sessile life on the sediment floor (Baynes & Szmant, 1989). Alongside browsers and occasional predators, most of the epibenthic species

are passive or active suspension-feeders, relying on the current speed for food availability in the water column (Craig & Jones, 1966). Strong currents near the seabed containing high concentration of suspended organic matter favour the establishment of suspension-feeding macrofauna, whereas areas with low speed bottom-currents enable the settlement of organic matter on the seafloor alongside the high sediment accumulation rate, favouring sub-surface deposit feeders (McCave, 1984; Rosenberg, 1995).

The idea of communities came from Petersen (1915) who observed a homogenous combination of benthic species inhabiting wide area of the Danish Sea, based on the quantitative sampling by a sediment grab. These communities were characterized and described based on the most numerous, most conspicuous, and for the area most "characteristic" species of animals found (Thorson, 1957). Petersen's communities mostly represented statistical units, consisting of random species with overlapping distributions with no ecological relation, characterized by the most common species and often under-representative of the small, rare species. Nevertheless, Petersen's communities are used as a base for describing a framework of areas with similar biotic and abiotic characteristics (Thorson, 1957).

The term biocenosis is used based on the definition of Pérès & Picard (1964) to describe "a group of living beings corresponding by its composition, number of species and individuals to certain average conditions of the environment; a group of beings which are linked by a reciprocal dependence and maintain themselves by reproducing in a certain place in a permanent way". Briefly, it defines a group of organisms adapted to the average conditions in a particular environment with its fluctuations (Bellan-Santini *et al.*, 2015), thus relating a community composition to the habitat that it is present in. Therefore, due to a close connection between the animal population (biocenose) and the substratum (biotope), the division of organisms into communities has to be supported by sediment sample analysis, among other environmental parameters (Thorson, 1957).

Two of the most adopted classification systems for the European and the Mediterranean Seas – The European Nature Information System (EUNIS) and The Barcelona Convention marine benthic habitat classification for the Mediterranean (UNEP/MED) – use a hierarchic classification system, defining different habitats

based on substrate composition, bionomic zonation in which they occur and levels defining species composition characteristic of the area (Montefalcone *et al.*, 2021). The classifications follow a hierarchical system including the environment (marine benthic, marine pelagic, transitional water, freshwater and terrestrial), the depth zone in the marine environment (from littoral to abyssal), the region (Mediterranean, Atlantic, etc.) and the habitat type. The latter is defined based on the environmental features such as sedimentology or seabed morphology, or by the dominating biological assemblages, (*i.e.* biocenoses) which are considered as a higher level, within which the assemblages of certain species of animals (facies) or plants (assemblages) are defined as representative for a certain habitat. The representative species of biocenoses, assemblages and facies are provided as examples for easy visual identification of habitats (Bellan-Santini *et al.*, 2015; Montefalcone *et al.*, 2021; UNEP/MAP & SPA/RAC, 2021; UNEP/MED, 1998).

#### Granulometry and sediment classification

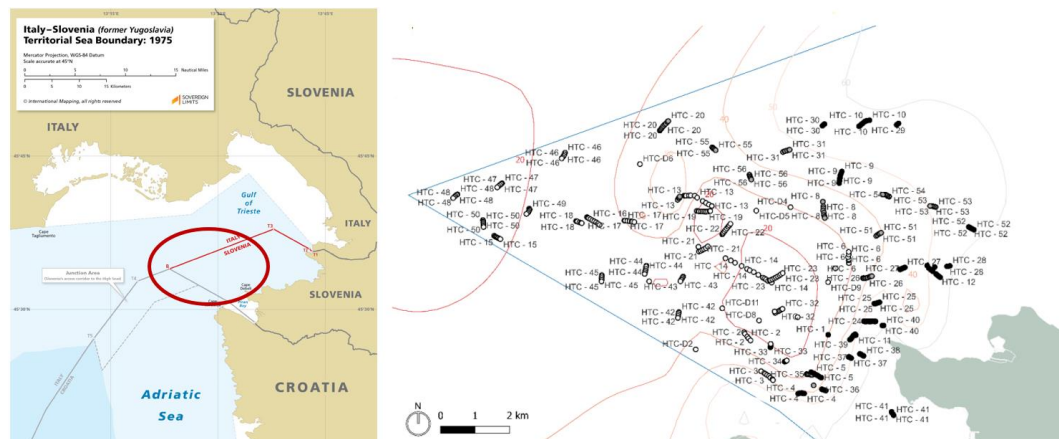
Internationally used grain size scale from Wentworth (1922) provides a classification based on sediment particle size, including gravel (particles bigger than 2mm), sand (particles between 2mm and 63µm), silt (particles from 63µm to 3.9µm) and mud class including clay (particles from 3.9µm to 0.06µm).

Based on Wentworth's grain size scale, Folk (1954), proposed 15 "textural groups" based on the proportion of gravel, sand and mud. In the latter, he included all material finer than 63µm, combining Wentworth's silt and mud/clay classes, arguing that the proportion of silt to clay can be difficult to measure and proposing the use of "mud" as the mixture of both. To define the prevalence of silt over clay in the mud class the terms "silty" or "clayey" should be used if the clay fraction is bigger than the silt fraction; for intermediate mixtures, the term "muddy" would mark a prevalence of mud over the other fraction. Therefore, "muddy sand" would consist of more than 50% sand, whereas "sandy mud" would consist of 10-50% sand. Halder (2020) uses the term "pelite" to describe a fine-grained sediment mainly consisting of silt and clay, with a grain size less than 63µm. In this classification, he includes silt, clay and their mixture of mud as unbound, loose sediments.

In the EUNIS classification system (Davies *et al.*, 2004), the particles follow a grain size scale from gravel (16-4mm) to sand (4mm-63µm) and mud (particles smaller than 63µm). The habitats are divided based on the dominating particle size of the substrate; "fine sand or muddy sand" describes the habitat with sediment particle size less than 1mm and with less than 30% silt content ("silt" *i.e.* mud) and "mud" as the habitat with more than 30% silt content present in the sediment (Davies *et al.*, 2004). However, in the recent classification (EUNIS, 2022), the "sand" class includes a habitat "fine sands", with less than 5% silt or clay fraction, and "muddy sands" with 5-20% of silt fraction. Furthermore, the "mud" class includes a habitat "sandy mud" with more than 20% silt or clay fraction (EEA, 2022). Due to the lack of information on the proportion of clay to silt in our sediment composition data, in this study the terms from Folk (1954) will be used to describe the nature of the observed sea bottom types, and the term "pelite" (S. K. Halder, 2020) to describe the fraction in the sediment consisting of silt and clay.

### Study area

The study area is located in the southernmost area of the Slovenian Sea, on the southern opening of the Gulf of Trieste (**Figure 1**). The Slovenian Sea lies in the southeast of the Gulf of Trieste with a surface area of 214km<sup>2</sup> and a mean depth of 17m (Kovačič & Radovan, 2019).



**Figure 1** Map of the study area with locations of sampling stations. (adapted from (Mavrič *et al.*, 2023)).

The Gulf of Trieste lies on the northernmost part of the Adriatic Sea with an average depth of 20m, surrounded by Italian, Slovenian and Croatian coasts (Trobec



*et al.*, 2018). Most of the freshwater input comes from the adjacent eastern rivers (Adige, Isonzo) along with high nutrient and sediment supply, resulting in seasonal vertical stratification and anoxia-related events due to low current activity in the inner part of the Gulf (Zuschin & Stachowitsch, 2009).

The area is also characterised by high variations of salinity and temperatures. Temperatures can vary from below 10°C in winter up to 30°C during summer, while the salinity typically ranges between 25 and 38 PSU, being with an average value of 35 PSU among the lowest in the Mediterranean (Boicourt *et al.*, 1999; Cozzi *et al.*, 2012). The variations are however less pronounced above the bottom in the deeper parts of the gulf. During a period of stable summer weather, a water column gets thermally stratified (Cardin & Celio, 1997). The influence of the open part of the Adriatic Sea gradually declines towards the closed area of the Gulf of Trieste on the northeast, observed by a decrease in the current velocity and sediment grain size correlating with the increase in pelite content (Cushman-Roisin *et al.*, 2001; Ogorelec *et al.*, 1991).

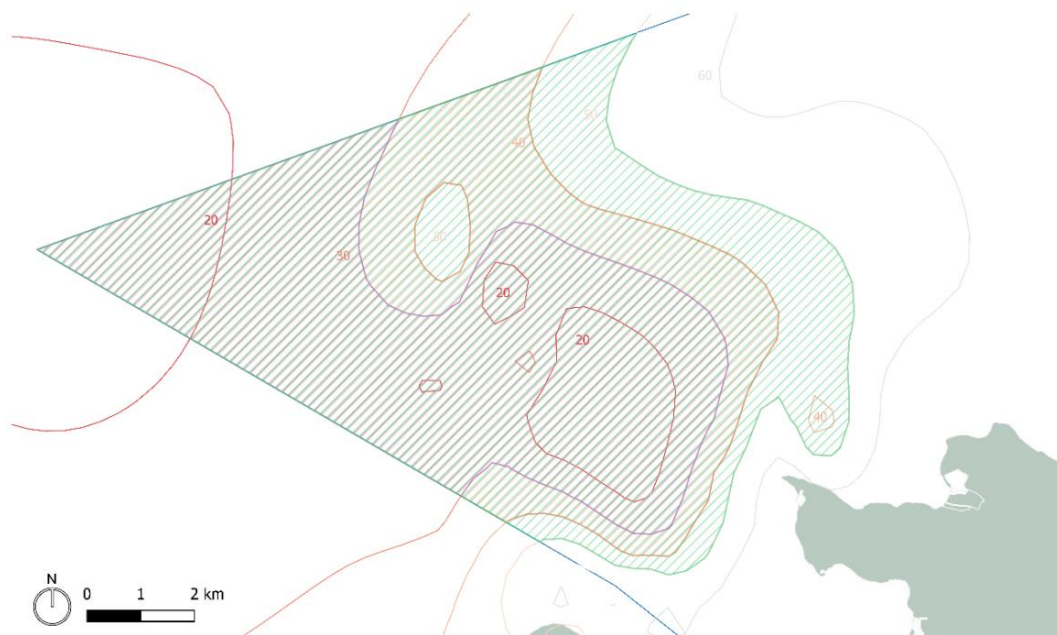
#### Sedimentation and sediment classification in the study area

The sediment deposits in the North Adriatic are mostly of terrestrial origin, supplied by the adjacent Alpine rivers (*e. g.* Adige, Brenta, Isonzo, Piave) and the River Po in the west (Syvitski & Kettner, 2007; Trincardi *et al.*, 1994). In addition to river runoff, the sedimentation in the North Adriatic is influenced by wind shears and water circulation (McKinney, 2007; Poulain *et al.*, 2001). The dominant winds of Bora, dry wind coming from the northeast, and Sirocco, warm wind blowing from the southeast, produce a counter clockwise gyre in the North Adriatic. The wind-produced current re-suspends and transports the sediments from the mouth of the River Po towards the East, resulting in a fine-grain thin deposit formed in the Gulf of Trieste (Harris *et al.*, 2008; McKinney, 2007; Orlić *et al.*, 1994; Poulain *et al.*, 2001).

Vatova (1949) described the sediment in the area off the Gulf of Trieste as predominantly silty and muddy sediments, also muddy-sand with different detrit quantities ("fondi prevalenza melmosi o fangosi, ma anche fangoso – sabbiosi con maggiore o minore numero di detriti"), where he used the term "melma" to describe

terrigenous muds and "fango" to describe mud comprised of different portions of silt and clay. According to Fedra *et al.* (1976) the bottom of the central and eastern part of the Gulf of Trieste consists of muddy sediment (mean grain size 70µm, with 65% of sediment particles smaller than 32µm) with observed structures such as burrows and piles, while sandy deposits (mean grain size 360µm, with 7% of sediment particles smaller than 32µm) were characteristic of the more open part of the bay in the Southwest. Similarly to Fedra *et al.* (1976), Ogorelec *et al.* (1991) described the sediment composition from the Bay of Koper to Cape Savudria based on sand, silt and clay composition. The silt and clay content decreases from the coastal area with the highest (40% inside the bays, up to 20% in the transitional zones named "silt" and "coarse silt"), to the sediment of the open part of the Gulf of Trieste with the lowest silt and clay content (10% named "silty sand"). On the other hand, the sand component increases from the coastal area (5-20% sand) towards the open part of The Gulf where the sand fraction in the sediment prevails, along with the highest carbonate content (50-80%) which includes biogenic fragments of thin shells, foraminifera and molluscs.

Combining the available results of sediment sampling in the Gulf of Trieste, Mavrič *et al.* (2023) mapped the areas with different sediment compositions based on particle size. They divided the study area into 5 classes with pelite content ranging from 10 to 60% (10-20%, 20-30%, 30-40%, 40-50%, 50-60%) by combining the information on the sediment composition and performing a spatial interpolation, applying the information to the map of the sampling area (**Figure 2**).



**Figure 2** The study area with applied areas of different pelite content, derived from the spatial interpolation of the data collected on the sediment composition in the area (Mavrič *et al.*, 2023). Purple filled area – 20-30%, orange filled area – 30-40%, green filled area – 40-50% pelite. (from Mavrič *et al.* (2023)).

Based on the EUNIS classification of sediment (EEA, 2022), the study area would be classified as muddy sand and mud. Therefore, the area mapped by Mavrič *et al.* (2023) would be divided into muddy sand (classes of 10-20% and 20-30% of pelite content) and mud (the classes of 30-40%, 40-50%, 50-60% pelite content). Following the classification of Folk (1954), the areas from Mavrič *et al.* (2023) would fall into muddy sand (first three classes of 10-20%, 20-30% and 30-40% of pelite content) and sandy mud (the classes of 40-50% and 50-60% of pelite content). As mentioned above, in this study Folk's classification will be used to describe the nature of the sea bottom types.

#### Benthic community observation in the North Adriatic and study area

The sublittoral soft bottom of the North Adriatic is characterized by well-developed megafauna, consisting of not only high abundant infauna (Orel & Mennea, 1969; Vatova, 1935) but also of epifaunal suspension-feeding sponges, ascidians and ophiurids (Fedra *et al.*, 1976; Orel & Mennea, 1969; Stachowitsch & Fuchs, 1995; Zuschin & Stachowitsch, 2009). The benthic fauna was primarily observed by sediment grab samples (Orel & Mennea, 1969; Vatova, 1935), enabling a good estimation of the infaunal community structure, however not representable of the

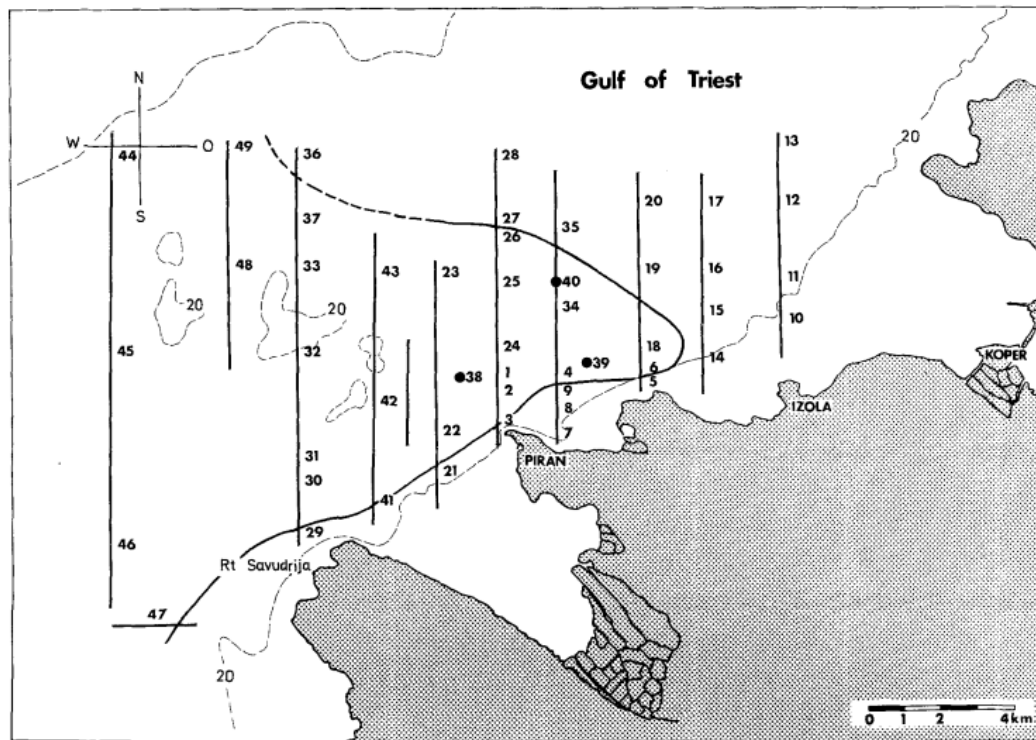
epifauna dominated communities (Fedra, 1978). The studies of the epibenthos progressed with the observation with a televised camera sled (Machan & Fedra, 1975), leading to improvement in the observations of the epifaunal communities (Stachowitsch & Fuchs, 1995).

Records of studies on benthic community structure date back to Vatova (1935) sampling with a "prendisaggio" (also Petersen grab from Petersen (1915), Van Veen grab) near the Gulf of Rovinj. He described six different biocenoses based on species present in the samples, including sediment composition in the sampling area. However, due to the sampling method, Fedra (1978) argued that Vatova's description of biocenoses could not apply to epibenthic communities as most of the organisms living on top of the sediment get swept away during grab sampling. Improving the method for benthic community observation, Machan & Fedra (1975) introduced a remote controlled camera on sled followed by sediment and underwater sampling with SCUBA sampling, which presented a better idea of epibenthic community structure in the area south of the Gulf of Trieste (Fedra *et al.*, 1976).

As mentioned above, Vatova (1935) studied sediment types in the vicinity of Rovinj and in the Lim Channel in the Croatian Istra. From the results obtained by the Van Veen grab, he introduced the biocenosis of *Schizaster chiajei*, a community structure named by the most common species found – *Schizaster canaliferus* and *Amphiura chiajei* – in the area of predominantly muddy bottoms with high detritic component extending along the coastline. In a later work (Vatova, 1949), the range of the biocenosis was extended from the coast of Istra towards the North including the Gulf of Trieste between 14m and 37m deep. It is described as a transitional zoocenosis between the coastal and the offshore area, found on predominantly muddy sediment, also on muddy-sand with various amounts of detritic content.

In an attempt to classify marine benthic ecology in the Mediterranean, Pérès & Picard (1964) introduced the biocenoses present on the circalittoral movable sediment. The biocenosis of coastal detritic was described by a high amount of various detritic material (molluscs, bryozoans, coralligenous algae) while the biocenosis of muddy detritic bottom included the facies of *Ophiothrix quinque maculata* which presented 90% of the total biomass.

Later, Fedra *et al.* (1976) focused on the observation of epibenthic fauna in the Northern part of the Gulf of Trieste, obtaining televised footage of the bottom floor along with samples of sediment and organisms collected by hand. Based on the TV-observations they divided the sampling area into a central region and a peripheral zone, the division was clear due to organism density and distribution differences along with different species composition between the areas (**Figure 3**). The homogenous community of the central area was named the Ophiothrix-Reniera-Microcosmus (ORM) community, based on the most common species observed in the area: *Ophiothrix quinquemaculata*, *Reniera* spp. (*Haliclona* spp.) *Microcosmus* spp.. The community was described on a predominantly sandy area, which stretched from the southern open part of the Gulf of Trieste towards the northeast, where it bordered to the peripheral zone, associated mostly with muddy bottoms. Later, Fedra (1978) proposed new classifications for communities present in the Northeast Adriatic and in the Gulf of Trieste. As an alternative to the established name of the ORM community, he proposed "The suspension feeding *Ophiothrix* communities" which would include the areas of the ORM in the south. Additionally, the peripheral areas of the ORM, expanding east and northeast towards Trieste, were named "The detritus feeding *Ophiura* communities" due to the overall decrease in suspension feeder biomass and increase in deposit feeders and carnivore species, including the dominant *Ophiura lacertosa* (*Ophiura ophiura*), by which the community was named.



**Figure 3** The sampling area of Fedra, 1976. The curved thick line marks the northeastern border of the ORM community (from Fedra *et al.* (1976), Fig. 1).

Combining the information of past community descriptions in the study area with the recent EUNIS classifications (EEA, 2022), Lipej *et al.* (2018) outlined two biocenoses present in the northern part of The Gulf of Trieste. Firstly, the biocenosis of coastal detritic bottom appears on predominantly sandy bottoms with a lower mud component, and more or less coincides with the area of the ORM community. Secondly, the biocenosis of muddy detritic bottoms in the eastern part of the Gulf of Trieste appears on sediment with higher mud fraction and characteristic species such as *Amphiura chiajei* and *Schizaster canaliferus*, similar to Vatova's description of *Schizaster chiajei* zoocenosis. Additionally, facies with *Ophiothrix quinque maculata* can be recognised as a part of the biocenosis, described by a dense population of the brittle star (Lipej *et al.*, 2006, 2018).

#### Aim of study

The aim of this study was to evaluate the composition and structure of the epibenthic community of the circalittoral muddy sand in the Slovenian Sea. We predict a significant difference in the community structure correlated with pelite fraction in the sediment. We also expect to observe the impact of fishing gears on

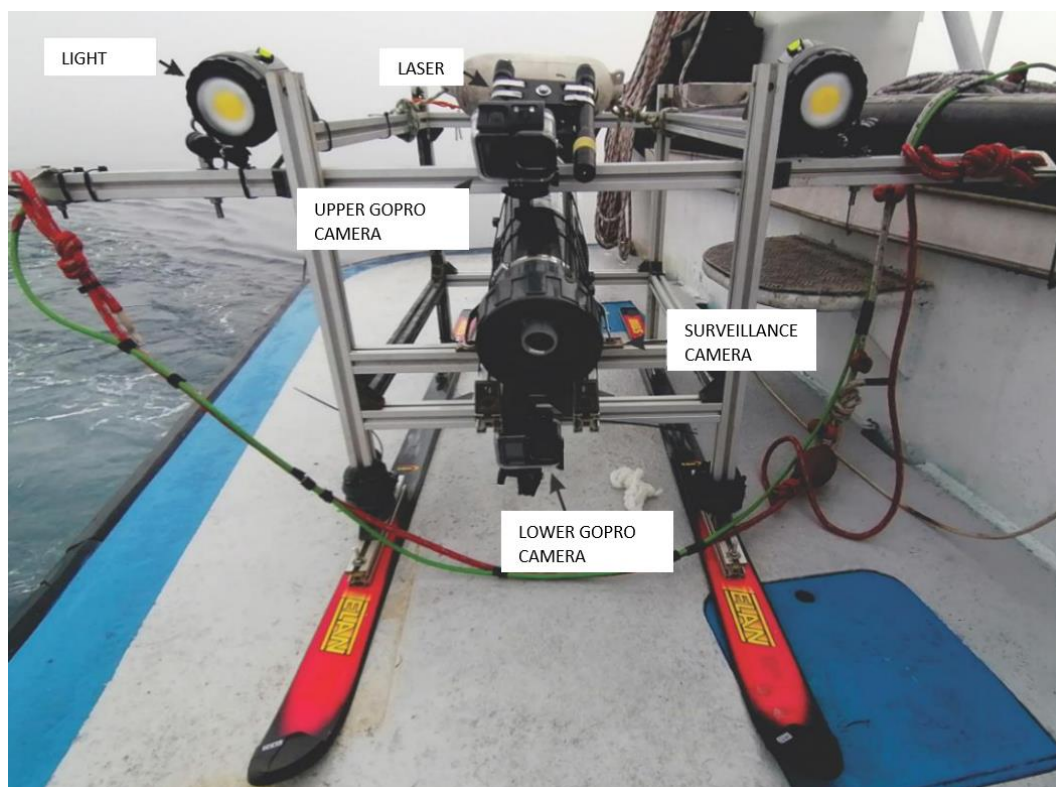
the sea bottom and on the structure of the community. This study, along with the project of Mavrič *et al.* (2023) and Premrl (2024) are the first surveys focusing on the epibenthic fauna in this area, since Fedra *et al.* (1976).

## **Materials and methods**

This study is based on the project "An upgrade on knowledge of biotic and abiotic characteristics and extent of benthic habitat types circalittoral coarse sediments (MC3), circalittoral mixed sediments (MC4) and circalittoral sands (MC5)" (Mavrič *et al.*, 2023) carried out by the Marine Biology Station, Piran (National Institute of Biology, Slovenia) from 2021 to 2023. This work was conducted based on the sampling carried out in the course of this project and agrees with the methods presented in the project report (Mavrič *et al.*, 2023). This study extends the number of the video transects analysed from 25 (Mavrič *et al.*, 2023) to 41.

### SKIKAM – video sledge

This study is based on the video surveys of the seafloor. The observations were carried out along linear transects using a video sledge (SKIKAM), constructed in the Marine Biology Station Piran, with the main goal of developing a non-destructive sampling method that would enable a stable drag on the seafloor and providing good quality videos of the bottom community. The SKIKAM (**Figure 4**) consists of a metal construction with attached filming equipment, which includes two GoPro cameras for recording and an additional surveillance camera for the transmission of the video directly to the sampling vessel. Two laser pointers are attached above the cameras, so that the beams, which are approximately 10 cm apart, fall inside the recording field of the cameras and serve as a calibration method for later determination of the size of the organisms and the filmed surface of the seafloor. Two lights are added to illuminate the recorded area of the floor for better recognition of organisms and bottom structures.



**Figure 4** The front side of the SKIKAM-video sledge (from Mavrič et al. (2023)).

### Data collection

The sampling was carried out using video survey methods in the spring of 2022 and 2023, at 56 sampling sites randomly distributed in the southwestern part of the Slovenian Sea (**Figure 1**). At each sampling station, we noted the starting GPS position when the SKIKAM was lowered to the seafloor. The cameras, lights and laser pointers were turned on at the same time beforehand to ensure calibration of the footage. When the sledge hit the bottom the boat moved in the desired direction until the rope, with which the SKIKAM was attached, was long enough to enable a stable pull on the seafloor. Again, the GPS position was written down once the sledge started moving. The transect duration was agreed to 12 minutes after a few experimental samplings, with a constant trawl speed 0.4 – 0.5 knots. The GPS location of the boat and depth of the sledge were marked every 3 minutes through the duration of trawling. To stop the trawling activity the boat slowed down so the rope loosened, which brought the SKIKAM to a full stop. When the boat was in a position directly above the sledge, the final GPS location was marked before the sledge was lifted back on the vessel. The GPS positions, speed and duration of



trawling marked throughout the sampling are important for the calculation of the direction of trawling and the surface of the seafloor recorded (Appendix A **Table 8**).

Each transect was filmed with three cameras, which were positioned at different viewpoints and captured different angles of the seafloor. In the analysis, we used primarily the footage of the bottom GoPro camera in the lowest position on the metal construction, capturing the closest footages of the seabed overall, thus enabling the easiest recognition of organisms. We used footage of the top camera as an additional point of view, if the organisms were unrecognisable from the bottom camera. The third camera was connected to the sampling vessel by a cable, which enabled a live transmission of the video, and was used as a surveillance method to prevent any obstruction of the sledge and ensure undisturbed recording of transects.

#### Video analysis

The analysis of video transects was based on the methods described in Mavrič *et al.* (2023) and Premrl (2024).

The first step of the video analysis consisted of looking over the 56 transect videos we recorded and dividing them into sub-sections. Some of the videos had to be discharged due to non-optimal video quality, therefore only 41 out of 56 transects were analysed. Firstly, each video transect was divided into sub-transects of approximately 3 minutes. The 3 minute mark was clear in transects with little to no change in community structure visible throughout the video. However, if we observed a noticeable change in the number of species, their abundance or changes in the seafloor morphology (described in detail later in the Methods section) throughout the duration of the transect, the transect was divided into sub-transects, that captured the observed change (*e.g.* if the frequency of sediment mounds increased in the  $x_1$  minute of the video transect and decreased in the  $x_2$  minute of the transect, a sub-transect lasted from the  $x_1$  minute to the  $x_2$  minute, capturing the time of the highest frequency of the sediment mounds). We only considered capturing a change in an individual sub-transect, if the duration of the change lasted more than 30s.

Furthermore, we marked the presence and abundance of organisms, recognised from the video recordings. The videos were analysed using the VLC media player (VideoLan, 2006) and slowed down for easier recognition and identification of the organisms. We mostly included organisms, which we could observe were alive by vivid colour or signs of movement in mobile species. To ensure a standard protocol throughout the analysis, only the organisms passing the line of the two laser pointers were accepted for the analysis. We identified the organisms to the lowest possible taxon with the help of identification keys and other reliable sources. We also collected screenshots of organisms, representable for each taxon and organised them similarly to an identification key for accessible identification in similar studies (Appendix B **Table 9**). For taxa, where specific identification was impossible or presented a high uncertainty if identified to a lower taxonomic level, we used the modifier sp. or spp. to indicate the higher taxonomic level to which the observed organisms were assigned with greater confidence. We used the qualifier cf. as an indication of the correlation of identifying factors of the specimen with the given species (Sigovini *et al.*, 2016).

The organisms were counted upon occurrence. However, due to the high abundance of *Ophiothrix quinquemaculata*, the brittle stars were only counted in the first 10 seconds of every minute of the sub-transect. We multiplied the counted value by 6, providing us with an estimated number of individuals in 1 minute, which we then applied to the duration of each sub-transect, respectively. Some of the organisms and other structures proved to be uncountable, therefore only their presence and absence was marked. Most of the marked species represented the infaunal community, which was not the main point of observation for this study; therefore, the marks are merely informative and not included in the community analysis. Shells of irregular sea urchins (Irregularia) present on the surface of the sediment, did not coincide with our standard of counting only live organisms, however, their presence was notated due to the high occurrence of this taxa in previous studies of benthic communities in this area (Vatova, 1935). We assumed the presence of *Solecurtus strigilatus* based on the occurrence of two round holes in the sediment (**Figure 8**), which have been related to the occurrence of this species in the sample area (Dworschak, 1987). In some areas, *Peyssonnelia squamaria* was observed, which occasionally covered a large portion of the seafloor. We have recorded its

occurrence with a mark of presence and absence in transects and separately also its dominant presence. Additionally, we marked any occurrence and number of damages on the seafloor, which mostly presented in the form of a narrow ditch or a strip of barren surface (**Figure 10**), where we observed unusual patterns in the epibenthic community such as aggregation or a decline in organism abundance.

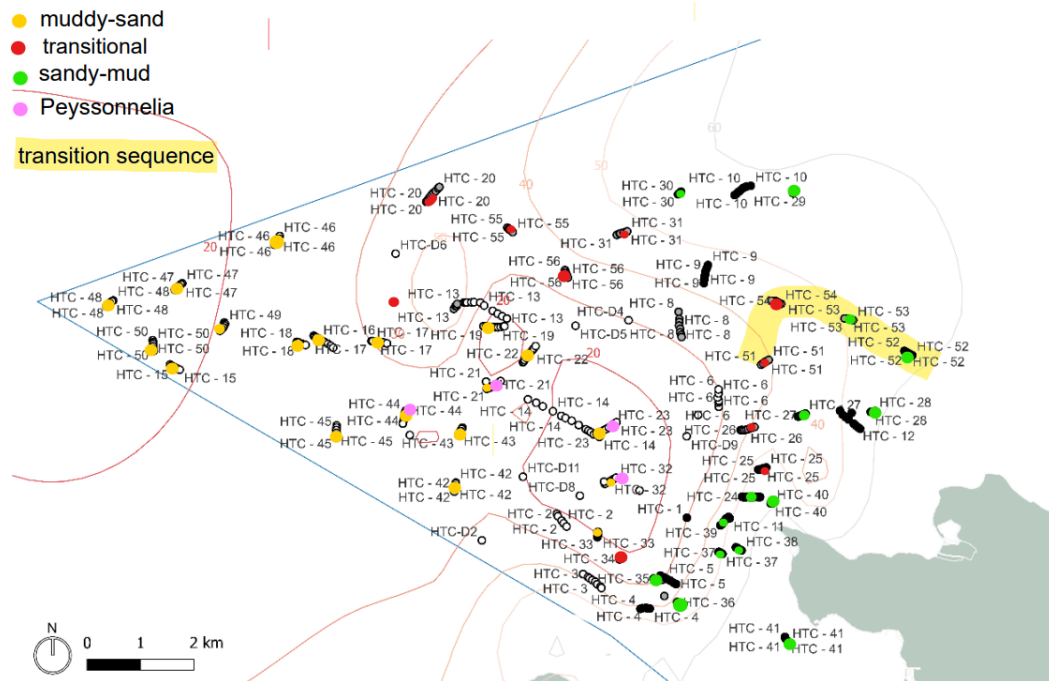
We also described each sub-transect based on the observed characteristics of the community and seafloor structure. As mentioned above, each video transect was divided into sub-transects of approximately 3 minutes, if no noticeable changes in the community and bottom structure were observed. Otherwise, video transects were divided based on visual observation, where each sub-transect represented the duration of the observed change. We visually estimated the quantity, quality and distribution pattern of coarse detritus material, composed of the shells and skeletal remains of organisms. We observed the general amount of detritus particles, where we compared the quantity between sub-transects by being higher or lower than the previous, and the general size of the particles, which we divided into fine (small, broken pieces, usually mixed with sediment) and coarse (big pieces of mollusc shells). Regarding the distribution, we observed if the detritus particles aggregated into piles or in pits, present on the surface, or were distributed evenly on the surface of the sea floor. Thirdly, we observed the local topography of the bottom based on the presence of bumps and pits on the surface. We also observed the presence of sediment mounds and holes, again marking their frequency. Finally, we noted any damage to the seafloor we observed. We distinguished between shallow, narrow ditches and strips of barren surface where it was obvious, that the organisms were scraped from the bottom due to the difference in the quantity of material present on the bottom on both sides of the strip (**Figure 10a**).

Based on described characteristics, we recognised three different types of sea bottom in the study area. Due to later associations between transects, where we recognised a certain type of sea bottom, and the pelite fraction assigned to those transects, we named two out of the three types based on the prevailing textural group following Folk (1954) classifications. The muddy-sand type was assigned mainly to transects with low pelite fraction in the sediment (10-20%, 20-30%), therefore, the textural group "sand" prevailed over "mud", justifying the name

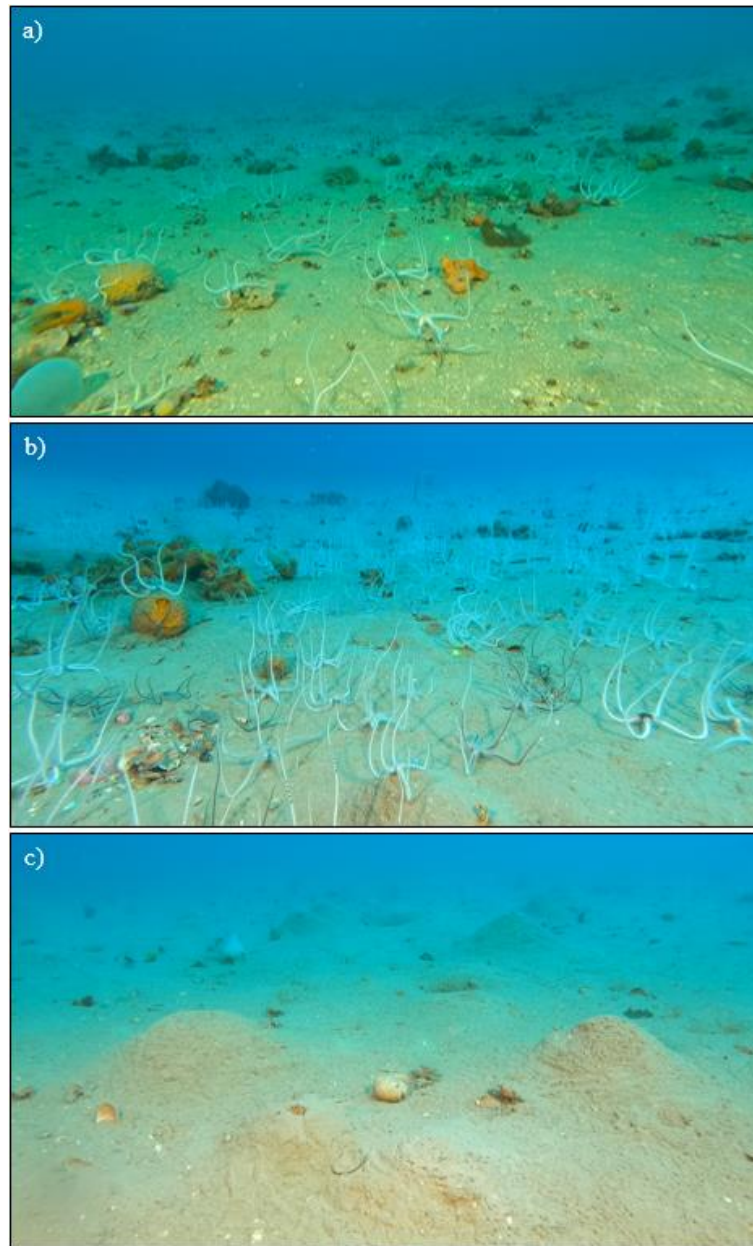
muddy-sand. Similarly, we mostly assigned the sandy-mud type to transects with high pelite fraction in the sediment (40-50%, 40-60%), where the textural group "mud" prevailed over "sand". However, in some transects, we observed a combination of the characteristics from both muddy-sand and sandy-mud types, which made it difficult to assign one of the established types of sea bottom to these areas with interchanging features. Nevertheless, after mapping the GPS positions of all transects sampled in the study and associating them with the observed sea bottom types, the transects, where we observed mixed characteristics, were located in the geographical area between the areas of transects assigned to sandy-mud and muddy-sand sea bottom type. As the community and seafloor characteristics gradually progressed from muddy-sand to sandy-mud attributes, this type was named transitional.

#### Categorization of the sea bottom

We distinguished between three sea bottom types (muddy-sand, transitional, sandy-mud) based on the observation of the quantity and distribution of different size detritus particles and the characteristics of the seafloor morphology. **Figure 5** presents the study area, with each transect sampling station marked with colour representing the sea bottom type observed in the video transect. Additionally, we also marked the transects, where we observed the presence of *Peyssonnelia squamaria*.



**Figure 5** A map of study area with sampling stations. The different sea bottom types associated with the transects are marked with colour, as well as the transects, with the presence of *P. squamaria*. The sequence of transects with gradual change are highlighted (adapted from Mavrič et al. (2023)).

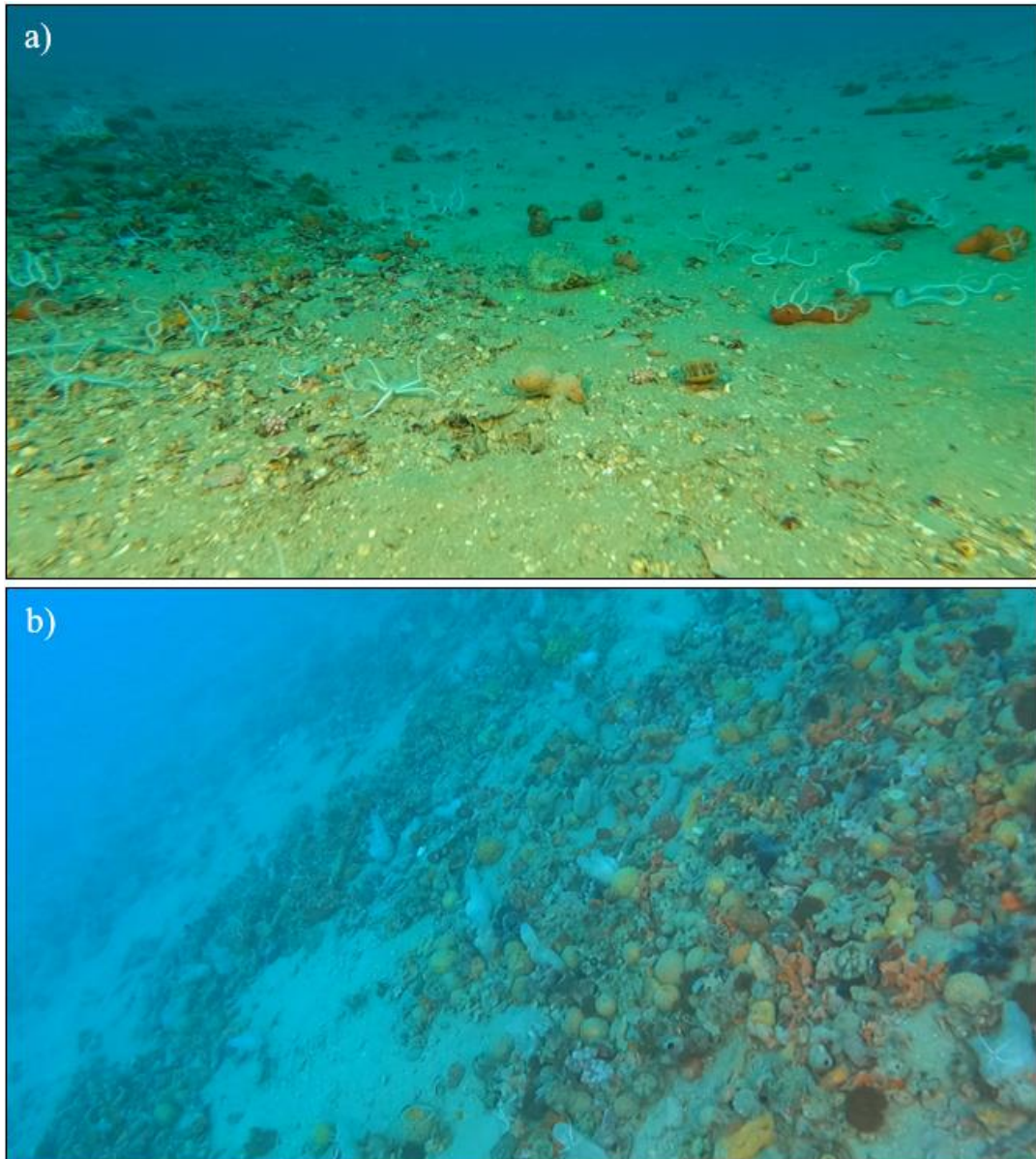


**Figure 6** Screenshot pictures of the transects, representative for the sea bottom type a) muddy-sand b) transitional c) sandy-mud.

#### The muddy-sand type

The muddy-sand sea bottom type was most recognisable by the high quantity of small organic detritus particles and overall flat bottom surface (**Figure 6a**). The detritus material was present in the shape of small, broken mollusc shells, distributed evenly on the surface. We also observed a high quantity of pebbles and other coarse-grain sediment on the bottom surface. However, in some areas we

observed distinct aggregations of coarse detritus, mostly mollusc shells and other organic material, and organisms (sponges and tunicates in piles or wide strips) (**Figure 7a**), similar to deposition areas, caused by current activity. One transect in particular had an unusually large amount of organisms, aggregated in piles or distributed in a dense layer on the bottom (**Figure 7b**). The bottom surface was mostly flat.



**Figure 7** Screenshot photos, complimentary to the description of the sea bottom type muddy-sand. a) aggregation of coarse detritic material, deposition area b) dense layer on the bottom.



### The transitional type

We recognised the transitional sea bottom type by the high quantity of detritus material, with the prevalence of coarse detritus material, and a variance in the roughness of the bottom surface (**Figure 6b**). We observed a high quantity of coarse detritus, with whole mollusc shells and skeletal remains of organisms, in particular irregular sea urchins (Irregularia), which occasionally appeared on the bottom surface. A recognisable characteristic of the transects in the transitional sea bottom type was the variation in the sea bottom structure, which ranged from mostly flat bottom with occasional regressions and pits, to slightly bumpy, with deeper pits and small bumps in the surface and occasional mounds of sediment present on the surface. Rarely, the transition could be seen within the duration of one transect, where we could observe a change in bottom morphology from one sub-transect to another by the increased number of sediment mounds. However, most of the time the changes were observed throughout multiple transects, as they were sampled on a smaller scale and could not capture such transitions in the bottom topography of the area. Occasionally, we observed a pair of holes in the sediment surface (**Figure 8**), usually not more than 5cm apart, which we could relate to siphon openings of a burrowing bivalve *Solecurtus strigilatus* present in the area (Dworschak, 1987).



**Figure 8** A pair of holes observed in the sediment, related to siphon openings of *S. strigilatus*.

### The sandy-mud type

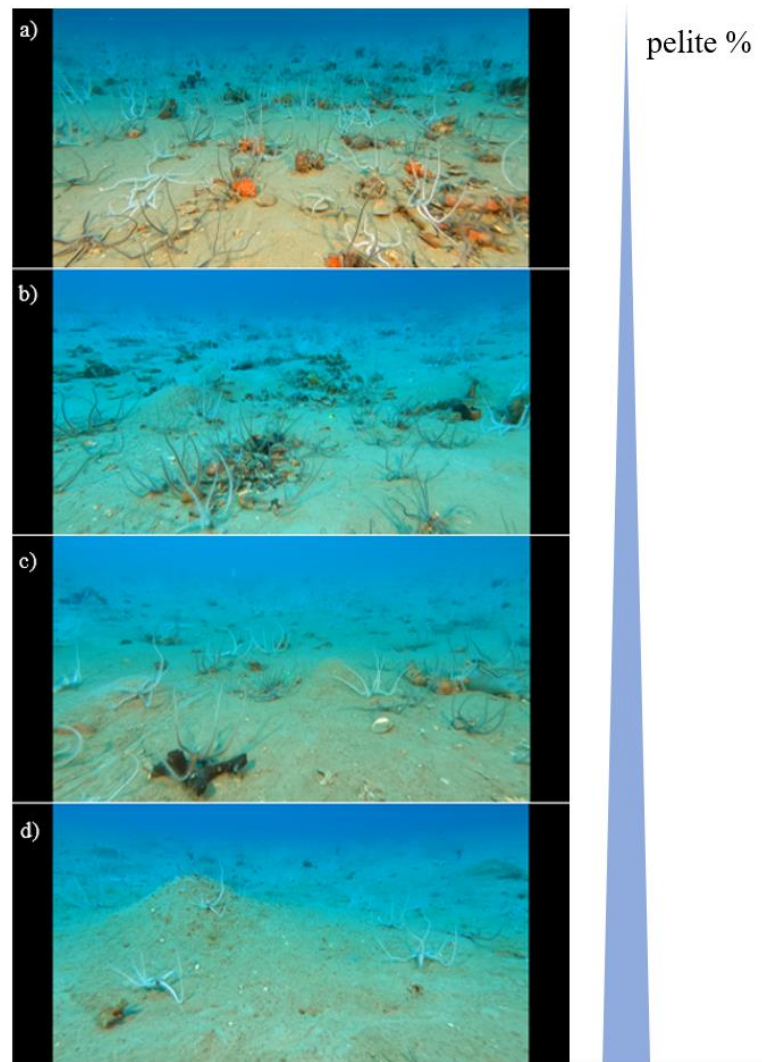
The sandy-mud sea bottom type was characterized by low quantity of detritus material and uneven bottom surface with frequent occurrence of sediment mounds and regressions in the seafloor (**Figure 6c**). We observed mostly coarse detritus on the bottom surface, occasionally aggregated in piles or in regressions, but more



frequently as individual pieces of shells and skeletal remains of organisms (Irregularia) on the sediment surface. The surface of the seafloor was uneven, with regressions, pits and high frequency of sediment mounds that could grow as high as the position of the top recording camera (50cm). We also came upon areas with high abundance of band fish (*Cepola marophthalma*) swimming in and out of vertical burrows in the sediment floor.

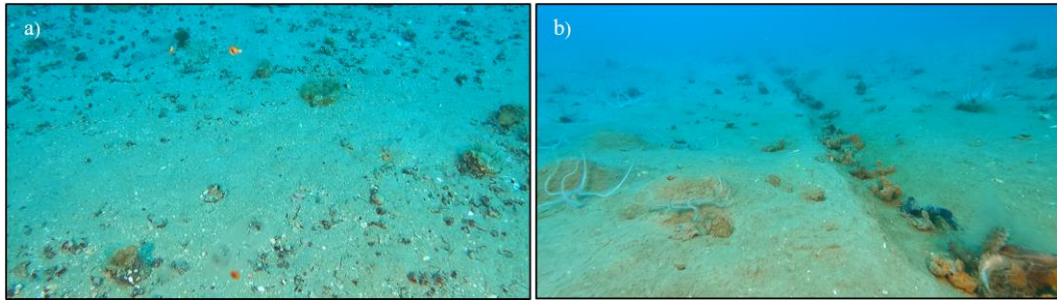
During the video analysis, we documented each sub-transect by a screenshot photo, representative of the description we made for each sub-transect. With the observation of the screenshot photos, we could link some transects into sequences, from which we could observe a gradual change in sea floor characteristics throughout the area. We arranged the sequence to start with a transect, sampled in the area with lower pelite fraction, and continued with transects in a semi-linear direction towards the areas with a higher pelite fraction in the sediment (**Figure 5** "transitions").

A sequence of transects in the Northeast, towards the middle of the Gulf of Trieste, started from a transect on transitional sea bottom type to a transect on sandy-mud sea bottom type (**Figure 9**). We can observe a decrease in the quantity of detritus material from the first two frames (**Figure 9a-b**) to the last two frames (**Figure 9c-d**). Furthermore, the overall decrease in the epifaunal abundance from the transitional transect (**Figure 9a**) towards sandy-mud transect (**Figure 9d**), along with the gradual change in the sea bottom structure with an increase in the frequency of sediment mounds.



**Figure 9** A sequence of screenshot photos made during video analysis, depicting a change from transects in the transitional type (a, b, c) to the transect in the sandy-mud type (d) in the northeastern part of the study area. a) Transitional sea bottom type with lower quantity of coarse detritic material and mostly flat sea floor surface. b) A transitional area with a high quantity of coarse detritus material, aggregating in clumps; the occurrence of bumps in the bottom surface. c) A decrease in the quantity of detritus material in transect, sampled in the area closer to the sandy-mud sea bottom type area. d) The appearance of the sandy-mud sea bottom type, with low detritus quantity and the frequent occurrence of sediment mounds.

Overall, we observed 20 individual signs of damage to the seafloor in 11 sub-transects, 7 strips of barren surface and 13 ditches. Strips of barren surfaces were observed in the areas of *Peyssonnelia* beds, where the algal matt was stripped from the surface along with other surface organisms, usually leaving *Cereus pedunculatus* unharmed (**Figure 10a**). Ditches were seen in parallel pairs, usually filled with organisms or detritic material (**Figure 10b**).



*Figure 10 Screenshot photos of transects with observed damage a) strip b) ditch.*

### Statistical analysis

The description of the community structure is based on species composition and abundance data derived from the video analysis

Based on the data recorded during the sampling activity and the calibration of the laser pointers in each video we were able to calculate the organism density for each sub-transect. We combined the trawling speed data and the duration of each sub-transect to calculate the trawling distance covered in each transect. Based on the distance between the laser pointers we were able to calculate the width of the recorded area, which we combined with the recorded distance to obtain the surface of the recorded area in each sub-transect (Appendix A **Table 8**). With the given surface area and the number of organisms in each sub-transect, we calculated the density of organisms per 100 m<sup>2</sup>.

For the interpretation of data on community structure we followed the strategies described by Clarke & Warwick (2001). We obtained a broad picture of the community composition in the study area with a faunistic description of the community, also analysing communities of the three observed types of sea bottom. Using Excel, we performed a faunistic description of the community in the sampled area.

Firstly, we observed the overall biodiversity and abundance of organisms in the overall study area. We identified the organisms to the lowest possible taxa (T2), which we then assigned to thirteen higher taxonomic groups (T1), of which five on the level of Phylum (Porifera, Cnidaria, Bryozoa, Echinodermata and Platyhelminthes), four Classes (Polychaeta, Gastropoda, Bivalvia and Cephalopoda), two Subphyla (Crustacea and Tunicata), one Parvphylum

(Osteichthyes) and one common name (Macroalgae). The abundance data of all organisms was pooled for the abundance and biodiversity analysis; the average density for each T2 taxa was used as an abundance measure of a taxa.

We counted the overall number of lower taxa (T2) in each taxonomic group (T1), specifying the number of T2 taxa identified to the level of species, genus and family or higher. To observe the proportion of sample diversity represented by each T1 taxonomic group, we calculated the relative diversity of each T1 taxonomic group, in relation to the overall number of T2 taxa in the sample. Similarly, we calculated the relative abundance of each T1 taxonomic group in relation to the sum of average abundances of T2 taxa in the sample. Furthermore, we calculated the relative abundance of each T2 taxa in relation to the sum of average abundances of T2 taxa. To observe the dominant T2 taxa in each T1 taxonomic group, we calculated the relative abundance of T2 taxa within each T1 taxonomic group.

Secondly, we looked at the biodiversity and abundance patterns of the community in the study area. We observed the overall biodiversity in the area by calculating the Shannon-Weiner Species Diversity Index ( $H'$ ) and evenness with Pielou's evenness index ( $J'$ ). The abundance data were transformed by taking the square root of the values, to equivalently weight the contribution of common and rare species on the similarity values (Clarke & Warwick, 2001). We applied a similarity coefficient (Bray-Curtis dissimilarity index) on the transformed data to obtain a dissimilarity matrix, to which we applied a Non-metric Multidimensional Scaling (NMDS) for a graphic presentation of ordinated data.

We observed the dominance in abundance of *Ophiothrix quinquemaculata* very early into the data analysis. To observe the underlying abundance patterns of the rest of the community, potentially masked by the dominance of the ophiurid, we have also performed the analysis of diversity and dissimilarity on the data without *O. quinquemaculata*.

Following the results of the NMDS visualization, we applied the information on the pelite content and sea bottom type associated with each sub-transect as factor with three levels (muddy-sand, transitional, sandy-mud) (Appendix A **Table 8**). We observed the biodiversity and abundance patterns of each sea bottom type

separately, following the faunistic analysis described above. We observed species diversity within each sea bottom type by calculating the Shannon-Weiner Species Diversity Index ( $H'$ ) and evenness with Pielou's evenness index ( $J'$ ). We compared the abundance and diversity patterns of taxa between the sea bottom types by performing an Indicator Species Analysis (ISA), which calculates the proportion of abundance of each taxa in a group in relation to the total abundance of taxa with the output of individual value. The highest values are assigned for taxa, common in only one group (Bakker, 2024), which are presented as characteristic species of the group. Characteristic species are species that are special to or especially abundant in a particular situation or biotope, which can usually be easily identified (Park, 2007). The similarity between sea bottom types was tested with a non-parametric Analysis of Similarity (ANOSIM). Finally, we used a Similarity Percentage analysis (SIMPER) to assess the contribution of individual species to overall dissimilarity between the sea bottom types. In the statistical testing the cut-off P-value for statistical significance was  $>0.001$ .

For further analysis of diversity and dissimilarity along with the visualization of the results we used the program PAST (Paleontological Statistics) (Hammer *et al.*, 2001) and R program (R Core Team, 2024) with RStudio integrated development environment (IDE) (RStudio Team, 2019), with the packages *vegan* (Oksanen *et al.*, 2024) and *tidyverse* (Wickham *et al.*, 2019).

## Results

### Faunistic description and community structure of the study area

The overall number of taxa present in the study area is 129, from which 16 taxa were identified to a taxonomic level higher than Family, 22 to the level of Genus and 91 to the level of Species (**Table 1**).

Overall, the subphylum Tunicata had the highest biodiversity with the highest number of T2 taxa (24; 19%), of which 17 (74%) were identified to the species level, followed by the phylum Porifera (23; 18%), of which 17 (78%) were identified to the species level and the phylum Cnidaria (18; 14%), of which 14 (78%) were identified to the species level (**Table 1**). The T1 taxonomic group with the highest abundance of organisms was the phylum Echinodermata (avg. 3036 org./100m<sup>2</sup>, 76%), followed by Porifera (avg. 409 org./100m<sup>2</sup>, 10%) and Cnidaria (avg. 171 org./100m<sup>2</sup>, 4%). The T2 taxon with the highest abundance was *Ophiothrix quinquemaculata* (avg. 2900 org./100m<sup>2</sup>, 70%), then *Paguristes eremita* (avg. 156 org./100m<sup>2</sup>, 4%) and *Cereus pedunculatus* (avg. 146 org./100m<sup>2</sup>, 4%).

**Table 1** A summary of diversity and abundance data for all sub-transects in the study area. T1 – higher taxonomic group; T2 – the lowest possible identified taxa. The number of all T2 within T1 ( $N_{T2}$ ), number of taxa identified to a level of family or higher ( $N_F$ ), genus ( $N_G$ ) and species ( $N_S$ ) within each T1 taxonomic group. The average density of T1 taxonomic group ( $A_{T1}$ ) is presented as the average number of organisms per 100m<sup>2</sup>. The first three most abundant T2 taxa in each T1 taxonomic group are presented (T2) along with their average density per T1, presented as the average number of organisms per 100m<sup>2</sup> ( $A_{T2}$ ).

T1	$N_{T2}$	$N_F$	$N_G$	$N_S$	$A_{T1}$	T2	$A_{T2}$
Porifera	23	2	4	17	409	cf. <i>Clathria compressa</i>	78
						<i>Ulosa digitata</i>	72
						<i>Haliclona</i> spp.	58
Cnidaria	18	3	1	14	171	<i>Cereus pedunculatus</i>	2146
						<i>Epizoanthus</i> spp.	10
						<i>Hydrozoa</i>	9
Polychaeta	7	2	1	4	7	<i>Filograna</i> sp./ <i>Salmacina</i> sp.	3
						<i>Myxicola infundibulum</i>	2
						<i>Sabellidae</i>	2

<b>Gastropoda</b>	10	2	0	8	12	<i>Aporrhais pespelecani</i>	7
						<i>Bolinus brandaris</i>	2
						<i>Doris pseudoargus</i> / <i>Geitodoris planata</i>	1
<b>Bivalvia</b>	5	0	1	4	68	<i>Aequipecten opercularis</i>	38
						<i>Mimachlamys varia</i>	23
						<i>Flexopecten flexuosus</i>	5
<b>Cephalopoda</b>	1	0	0	1	0	<i>Seppia officinalis</i>	<1
<b>Bryozoa</b>	8	1	1	6	14	<i>Schizobrachiella sanguinea</i>	6
						<i>Bugulina</i> cf. <i>turbinata</i>	3
						<i>Schizomavella</i> sp.	2
<b>Crustacea</b>	10	0	4	6	163	<i>Paguristes eremita</i>	156
						<i>Inachus</i> spp.	4
						<i>Pagurus prideaux</i>	2
<b>Echinodermata</b>	10	1	2	7	3036	<i>Ophiothrix quinquemaculata</i>	2900
						<i>Ophiura</i> sp.	80
						<i>Psammechinus microtuberculatus</i>	49
<b>Tunicata</b>	24	1	7	16	86	cf. <i>Diplosoma spongiforme</i>	13
						<i>Polycarpa</i> cf. <i>mamillaris</i>	13
						<i>Phallusia mammillata</i>	9
<b>Osteichthyes</b>	9	3	1	5	3	<i>Gobius niger</i>	1
						<i>Serranus hepatus</i>	<1
						<i>Teleostei</i>	<1
<b>Platyhelminthes</b>	2	0	0	2	0	<i>Pseudoceros maximus</i>	<1
						<i>Yungia aurantiaca</i>	<1
<b>Macroalgae</b>	2	1	0	1	17	<i>Corallinales</i>	15
						<i>Valonia utricularis</i>	2
<b>Total</b>	129	16	22	91			

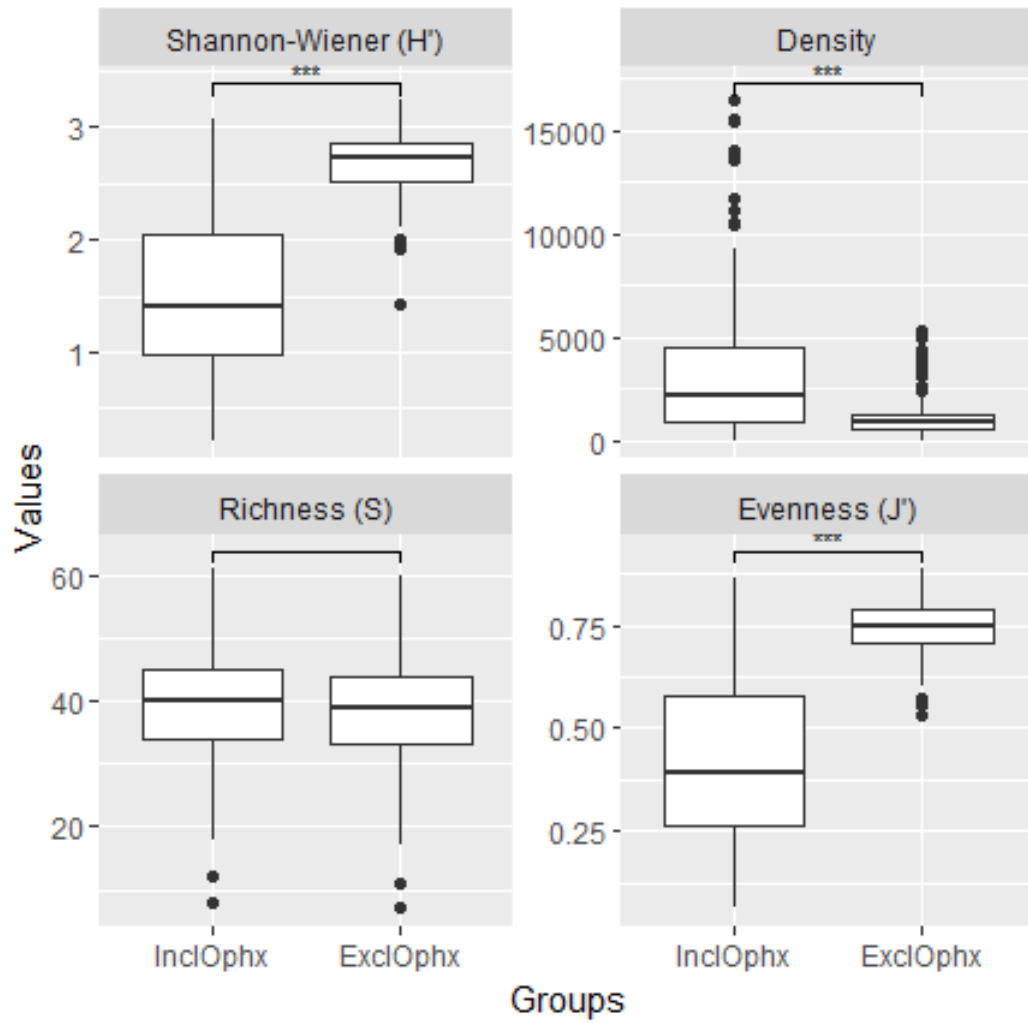
**Table 2** shows the different structural parameters of the community in the study area. The mean density of organisms per sub-transect was 3373.4 org./100m<sup>2</sup> (min: 4, max: 16459.9, median: 2236.3). The mean number of taxa was 39.1 (min: 8, max: 61, median: 40). The mean value of evenness was 0.42 (min: 0.06, max: 0.87, median: 0.39). The mean *H'* diversity within sub-transects in the study area was 1.52 (min: 0.22, max: 3.07, median: 1.4) (Figure 11, Table 2). After removing the

abundance value for *Ophiothrix quinquemaculata* from the data set, the mean density of organisms per sub-transect was 1085.7 org./100m<sup>2</sup> (min: 4, max: 5321.2, median: 857.1). The mean number of taxa was 38.1 (min: 7, max: 60, median: 39). The mean value of evenness was 0.53 (min: 0.53, max: 0.89, median: 0.75). The mean *H'* diversity within sub-transects in the study area was 2.68 (min: 1.42, max: 3.23, median: 2.74). When comparing the data with (InclOphx) and without (ExclOphx) the abundance value of *O. quinquemaculata*, the mean values of density, evenness and Shannon-Wiener diversity were significantly different between the groups (**Figure 11**).

**Table 2** Faunistic parameters for the data including abundance values for *Ophiothrix quinquemaculata* and the data obtained after the removal of abundance values. The density of organisms is presented as the average number of organisms per 100m<sup>2</sup>. The diversity is presented with Species richness (*S*), Pielou's evenness index (*J'*) and Shannon–Wiener diversity index (*H'*) for data with (including) and without (excluding) abundance of *Ophiothrix quinquemaculata*.

		Density	Richness ( <i>S</i> )	Evenness ( <i>J'</i> )	Diversity ( <i>H'</i> )
including <i>Ophiothrix quinquemaculata</i>	mean	3373.4	39.1	0.42	1.52
	min	4	8	0.06	0.22
	max	16459.9	61	0.87	3.07
	median	2236.3	40	0.39	1.41
excluding <i>Ophiothrix quinquemaculata</i>	mean	1085.7	38.1	0.75	2.68
	min	4.0	7	0.53	1.42
	max	5321.2	60	0.89	3.23
	median	857.1	39	0.75	2.74





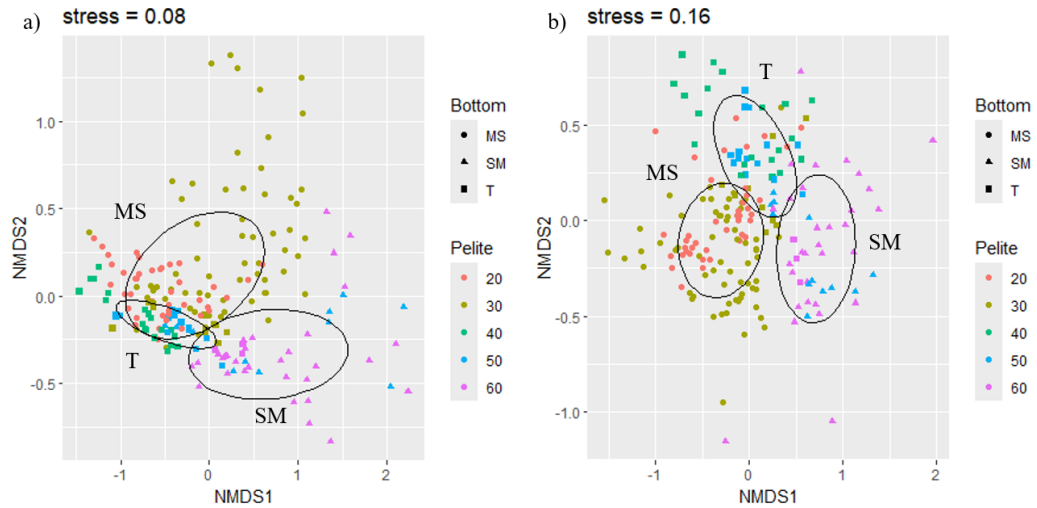
**Figure 11** Means and confidence intervals (95%) for density (avg. org./100m<sup>2</sup>), species richness (S), Pielou's evenness index (J') and Shannon-Wiener diversity index (H') for data with (InclOphx) and without (ExclOphx) abundance of *Ophiothrix quinquemaculata*. MS:muddy-sand, T:transitional, SM:sandy-mud, blank:  $p > 0.05$ , \*:  $p \leq 0.05$ , \*\*:  $p \leq 0.01$ , \*\*\*:  $p \leq 0.001$ , \*\*\*\*:  $p \leq 0.0001$ .

In the NMDS ordination plot (**Figure 12a**) presents a slight aggregation of points in the bottom-left corner of the plot, while the points on the right side of the plot are more scattered. The distance between the ordination points correlates to the Bray-Curtis dissimilarity between the sub-transects. Based on the information on the pelite fraction associated with the sub-transects (10-20%, 20-30%, 30-40%, 40-50%, 50-60%) the aggregation in the down-left corner is made up of sub-transects with 30-40% pelite, and some sub-transects with lower (10-20%, 20-30%) and higher (40-50%) pelite fraction in the sediment. The scattered area on the right is mostly composed of sub-transects with 20-30% and 50-60% pelite, where the points representing each level of pelite are segregated. The NMDS plot based on the data

without abundance values of *Ophiothrix quinquemaculata* (**Figure 12b**) showed a more uniform aggregation of all points, with smaller and more uniform distances between them as in the ordination plot with unaltered data. However, it also shows slight grouping of points with low pelite (10-20% and 20-30%) in the bottom-left side of the cluster and points with higher pelite (30-40%, 40-50% and 50-60%) in the top-right.

Furthermore, we applied the information about the assigned sea bottom type to each sub-transect as a shape-code. The ordination points representing the muddy-sand sea bottom type were shaped as circles, sandy-mud as triangles and transitional as squares. Comparing the two factors, sea bottom type and pelite fraction, we can see that the sea bottom types quite distinctly coincide with certain levels of pelite. Sub-transects within muddy-sand type are mainly associated with pelite of 10-20% and 20-30%, sub-transects within the transitional sea bottom type are mainly associated with 10-20%, 30-40% and 40-50% pelite and sub-transects associated with the sandy-mud sea bottom type with 40-50% and 50-60% pelite fraction. We could observe, that the grouping of sub-transects can be associated with the sea bottom types (**Figure 12a**). The 60% confidence interval ellipse of transitional sea bottom type (T) coincides with the aggregation of points in the bottom-left corner, while the ellipses of sandy-mud (SM) and muddy-sand (MS) type partially capture the scattered area on the right, respectively.

When observing the ellipses based on the observed sea bottom types on the ordination plot without the abundance values of *Ophiothrix quinquemaculata* (**Figure 12b**), a higher degree of separation and smaller overlap between the three ellipses can be seen. Due to the smaller distances between the sub-transect ordination points, the 60% confidence interval ellipse of the associated sea bottom type transitional coincide with the grouping of points of 20% and 30% pelite, points of 30-40%, 40-50% and 50-60% pelite coincide with the ellipse of transitional and points with 40-50% and 50-60% pelite coincide with the ellipse of sandy-mud sea bottom type.



**Figure 12** NMDS ordination plot based on the data a) including and b) excluding abundance value of *Ophiothrix quinquemaculata*, with applied colour-coded pelite classes (10-20%, 20-30%, 30-40%, 40-50%, 50-60%), shape-coded sea bottom type information (MS:muddy-sand, T:transitional, SM:sandy-mud) and statistical ellipses with 60% confidence interval. The ordination stress value is presented above each plot.

The dissimilarity matrix calculated based on the Bray-Curtis dissimilarity index showed the average distance 0.53 within and 0.60 between sea bottom types. After the exclusion of the abundance values of *Ophiothrix quinquemaculata*, the average of mean distance was 0.54 within and 0.67 between sea bottom types. The highest dissimilarity was observed between muddy-sand and sandy-mud sea bottom types, while muddy-sand and transitional had the lowest dissimilarity between them (**Table 3**). After the removal of abundance values of *O. quinquemaculata* from the data, the dissimilarity values between the types increased. The R-value calculated with ANOSIM presents the highest difference between transitional and sandy-mud types, which decreases after the exclusion of abundance values of *O. quinquemaculata*. Furthermore, the difference between muddy-sand and transitional types increases remarkably when excluding the abundance values of *O. quinquemaculata*. The ANOSIM test showed a significant difference between muddy-sand, sandy-mud and sandy-mud, transitional type regardless the abundance of *O. quinquemaculata*. However, the difference between muddy-sand and transitional type was significant only when performed on the data without abundance values of *O. quinquemaculata*.

**Table 3** Bray-Curtis dissimilarity values and ANOSIM pairwise comparison of sea bottom types. Dissimilarity values between types ( $D_{BC}$ ) are obtained from a Bray-Curtis dissimilarity matrix for data with (including) and without (excluding) abundance of *Ophiothrix quinquemaculata*.  $R$  values and significance levels are presented ( $p < 0.001^{***}$ ) derived from a pairwise ANOSIM analysis. MS:muddy-sand, T:transitional, SM:sandy-mud.

	Groups	Dissimilarity ( $D_{BC}$ )	R-value	Significance level
including <i>Ophiothrix quinquemaculata</i>	MS,SM	0.66	0.36	0.0001***
	MS,T	0.50	0.01	0.3077
	T,SM	0.64	0.44	0.0001***
excluding <i>Ophiothrix quinquemaculata</i>	MS,SM	0.72	0.70	0.0001***
	MS,T	0.62	0.40	0.0001***
	T,SM	0.65	0.39	0.0001***

The results of the SIMPER analysis presented the species that contributed most to the differences between sea bottom types (**Table 4**). Overall, *Ophiothrix quinquemaculata* contributed to the dissimilarity between all types; the highest contribution (77%) to the dissimilarity between transitional and sandy-mud type and the lowest (57%) to the dissimilarity between muddy-sand and sandy-mud sea bottom type. Other species contributing to the dissimilarity between the types were *Cereus pedunculatus*, *Paguristes eremita*, *Ophiura* sp. and various sponges (*Ulosa digitata*, cf. *Clathria compressa*, *Haliclona* spp.).

**Table 4** The results of SIMPER analysis performed with the programme PAST. Av. Diss – average dissimilarity of the species in the group; Contrib. % - proportion of the dissimilarity between groups explained by a species; Cumulative % - cumulative contribution of species to the dissimilarity between groups; Mean – the mean of abundances of the species in each group. MS: muddy-sand, T: transitional, SM: sandy-mud.

MS,SM					
T2	Av. dissim	Contrib. %	Cumulative %	Mean MS	Mean SM
<i>Ophiothrix quinquemaculata</i>	37.36	56.81	56.81	2,99E03	942
<i>Cereus pedunculatus</i>	5.45	8.29	65.10	265	9.22
<i>Paguristes eremita</i>	2.15	3.26	68.36	197	114
cf. <i>Clathria compressa</i>	1.86	2.83	71.19	118	8.87
<i>Ulosa digitata</i>	1.54	2.34	73.53	95.40	13.30
<i>Ophiura</i> sp.	1.35	2.05	75.58	73.60	25.80
<i>Psammechinus microtuberculatus</i>	1.34	2.04	77.62	64.30	13.90
<i>Aequipecten opercularis</i>	1.20	1.82	79.44	63.20	4.82
<i>Mycale tunicata</i>	1.19	1.81	81.25	73.40	10.70
<i>Haliclona</i> spp.	0.94	1.43	82.68	65.70	21.70
MS,T	Av. dissim	Contrib. %	Cumulative %	Mean MS	Mean T
<i>Ophiothrix quinquemaculata</i>	33.65	67.21	67.21	2,99E03	4,53E03
<i>Cereus pedunculatus</i>	3.07	6.12	73.33	265	7.18
<i>Paguristes eremita</i>	1.35	2.70	76.03	197	103
<i>Ophiura</i> sp.	1.28	2.55	78.59	73.6	146
<i>Ulosa digitata</i>	0.99	1.97	80.56	95.4	72.70
cf. <i>Clathria compressa</i>	0.98	1.96	82.52	118	51.80
<i>Haliclona</i> spp.	0.72	1.44	83.96	65.7	72.80
<i>Aequipecten opercularis</i>	0.63	1.26	85.21	63.2	11.90
<i>Psammechinus microtuberculatus</i>	0.61	1.23	86.44	64.3	46.50
<i>Mycale tunicata</i>	0.60	1.21	87.64	73.4	49
T, SM	Av. dissim	Contrib. %	Cumulative %	Mean T	Mean SM
<i>Ophiothrix quinquemaculata</i>	49.95	77.46	77.46	4,53E03	942
<i>Ophiura</i> sp.	1.52	2.35	79.81	146	25.80
<i>Paguristes eremita</i>	1.18	1.83	81.64	103	114
<i>Haliclona</i> spp.	0.86	1.33	82.97	72.80	21.70
<i>Ulosa digitata</i>	0.83	1.29	84.26	72.70	13.30
<i>Psammechinus microtuberculatus</i>	0.73	1.14	85.39	46.50	13.90
<i>Raspailia viminalis</i>	0.73	1.13	86.53	46.80	11
cf. <i>Clathria compressa</i>	0.71	1.09	87.62	51.80	8.87
<i>Mycale tunicata</i>	0.69	1.07	88.69	49	10.70
<i>Tedania anhelans</i>	0.52	0.80	89.49	33.30	13.50

## Faunistic description and community structure of communities associated with sea bottom types

### The muddy-sand type

The muddy-sand sea bottom type included 104 sub-transects, 41 (100%) were sampled in the area with 10-20% pelite and 63 (88%) in the area with 20-30% pelite fraction in the sediment. Furthermore, *Peyssonnelia squamaria* was present in 38 (36%) sub-transects, of which 17 associated with sediment with 10-20% and 21 with 20-30% pelite. We have observed damage of the seafloor on 6 sub-transects (6%), of which 4 in the shape of a strip and 2 ditches. The overall surface covered with transects was 7388 m<sup>2</sup>.

The overall number of taxa present was 119, of which 85 we identified to the species level (**Table 5**). The subphylum Tunicata had the highest biodiversity with the highest number of T2 taxa (24; 21%), followed by the phylum Porifera (21; 18%) and the phylum Cnidaria (15; 13%). The most abundant T2 taxon was *Ophiothrix quinquemaculata* (avg. 2987 org./100m<sup>2</sup>, 68%), followed by *Cereus pedunculatus* (avg. 265 org./100m<sup>2</sup>, 6%), and *Paguristes eremita* (avg. 196 org./100m<sup>2</sup>, 4%) (**Table 6**).

Overall, we observed a high abundance of sponges (cf. *Clathria compressa*, *Ulosa digitata*, *Mycale tunicata*), cnidarians (*Cereus pedunculatus*), tunicates (*Asciidiella* spp.), the dominant *O. quinquemaculata* and occasional flat fish (*Pleuronectiformes*). The ophiurid formed a carpet-like coverage, where the organisms covered the seafloor in a layer over all other organisms present on the bottom. In some areas, the dense carpet-cover transitioned into patchy cover, where the ophiurid was less abundant, however still distributed evenly on the bottom. Rarely, when *O. quinquemaculata* was less abundant, we observed aggregations of the organisms on large sponges (*U. digitata*, cf. *C. compressa*, *Tedania anhelans*) and tunicates (*Phallusia mammillata*). In some areas, we observed a high abundance of the red algae *Peyssonnelia squamaria* covering the seafloor, occasionally forming a dense layer mixed with tunicates (*P. mammillata*), fragments of sponges (cf. *C. compressa*, *U. digitata*, *M. tunicata*) and an even coverage of *O. quinquemaculata* on top (**Figure 13a**). Furthermore, distinct patches



with high abundance of *C. pedunculatus* could be seen in areas with *Peyssonnelia squamaria* presence, where numerous cnidarians were evenly distributed on the seafloor, with less other organisms (sponges, tunicates) present (**Figure 13b**). In these areas with the dominance of *C. pedunculatus*, *O. quinquemaculata* was absent or present in very low quantities, where it aggregated on big sponges and tunicates.



**Figure 13** Screenshot photos, complimentary to the description of the sea bottom type muddy-sand. a) *Peyssonnelia squamaria* bed b) patches of *Cereus pedunculatus*.

### The transitional type

The transitional type included 46 sub-transects, 9 (12%) were sampled in the area with 20-30% pelite, 20 (100%) in the area with 30-40% pelite, 14 (53%) in the area with 40-50% pelite, 3 (8%) in the area with up to 50-60% pelite fraction in the sediment. *Peyssonnelia squamaria* was not present in the sub-transects of this sea bottom type. We have observed damage on the seafloor in 4 sub-transects (9%), of which 1 in the shape of a strip and 3 ditches. The overall surface covered with transects was 3040m<sup>2</sup>.

The overall number of taxa present was 112, of which 76 were identified to the species level. The subphylum Tunicata and Porifera had the highest biodiversity with the highest number of T2 taxa (22; 20%) followed by the phylum Cnidaria (13; 12%) (**Table 5**). The most abundant T2 taxa was *Ophiothrix quinque maculata* (avg. 4533 org./100m<sup>2</sup>, 84%), followed by *Ophiura sp.* (avg. 146 org./100m<sup>2</sup>, 3%), and *Paguristes eremita* (avg. 103 org./100m<sup>2</sup>, 2%) (**Table 6**).

In the areas with high abundance, *Ophiothrix quinque maculata* formed a dense carpet-like coverage that became thinner in areas with lower abundance of the ophiurid. Besides the dominant *O. quinque maculata*, we observed high abundance of sponges (*Tedania anhelans*, *Raspailia viminalis*, *Ulosa digitata*), tunicates (*Phallusia mammillata*, *Ascidiella spp.*), hermit crabs (*Paguristes eremita*) and bivalves (*Mimachlamys varia*, *Aequipecten opercularis*) with epibiont sponges (*Suberitidae*) overgrowing the shells.

### The sandy-mud type

The sandy-mud sea bottom type included 43 sub-transects, 12 (46%) were sampled in the area with 40-50% pelite and 31 (91%) in the area with 50-60% pelite fraction in the sediment. *Peyssonnelia squamaria* was not present in sub-transects on this sea bottom type. We have observed damage of the seafloor on 3 sub-transects (7%) all of them ditches; in one sub-transect we observed a set gill net. The overall surface covered with transects was 1980m<sup>2</sup>.

The overall number of taxa present was 104, of which 73 we identified to the species level. The subphylum Tunicata had the highest biodiversity with the highest number of T2 taxa (21; 20%) followed by the phylum Porifera (20; 19%) and the phylum



Cnidaria (16; 15%) (**Table 5**). The most abundant T2 taxa was *Ophiothrix quinquemaculata* (avg. 942 org./100m<sup>2</sup>, 66%), followed by *Paguristes eremita* (avg. 113 org./100m<sup>2</sup>, 8%), and *Ophiura* sp. (avg. 26 org./100m<sup>2</sup>, 2%) (**Table 6**).

*Ophiothrix quinquemaculata* appeared in very low quantity, mostly in aggregations on sponges (*Tedania anhelans*) and tunicates (*Phallusia mammillata*). We observed an overall low abundance of epibenthic organisms, mostly represented by hermit crabs (*Paguristes eremita*) and occasional brittle stars (*Ophiura* sp., *O. quinquemaculata*) along with individual sponges (*T. anhelans*, *Mycale tunicata*), tunicates (*P. mammillata*, *Diplosoma spongiforme*) and cnidarians (*Epizoanthus* spp.).

**Table 5** Biodiversity and abundance data of the observed sea bottom types. T1 – higher taxonomic group; T2 – the lowest possible identified taxa. The number of all T2 within T1 ( $N_{T2}$ ), number of taxa identified to a level of species ( $N_S$ ) within each T1 taxonomic group. The density of T1 taxonomic groups ( $A_{T1}$ ) is presented as the average number of organisms per 100m<sup>2</sup>.

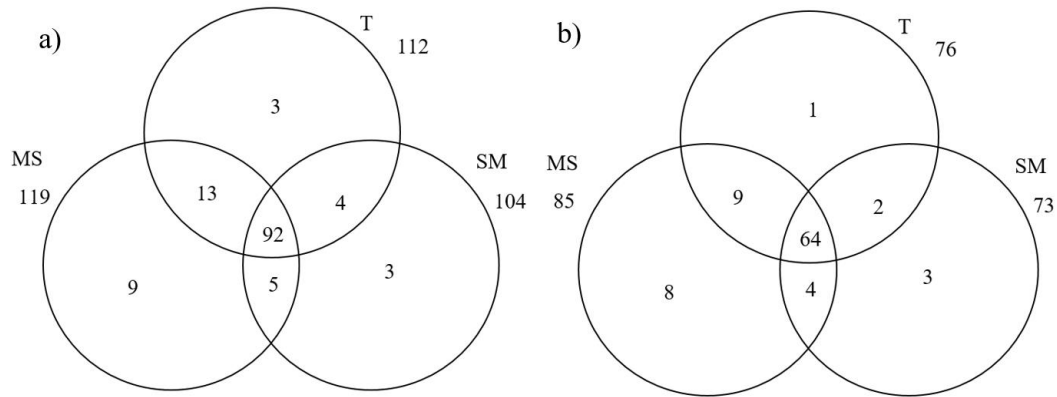
	MUDDY-SAND			TRANSITIONAL			SANDY-MUD		
T1	$N_{T2}$	$N_S$	$A_{T1}$	$N_{T2}$	$N_S$	$A_{T1}$	$N_{T2}$	$N_S$	$A_{T1}$
Porifera	21	16	533	22	16	402	20	15	117
Cnidaria	15	12	282	13	10	32	16	13	53
Polychaeta	6	4	2	6	3	8	5	2	20
Gastropoda	10	8	9	10	8	13	9	7	19
Bivalvia	5	4	105	5	4	35	3	3	12
Cephalopoda	1	1	0	1	1	0	1	1	0
Bryozoa	7	5	7	7	5	11	8	6	36
Crustacea	10	6	207	7	4	107	7	4	118
Echinodermata	10	7	2709	9	6	3797	8	5	293
Tunicata	24	16	107	22	14	54	21	14	70
Osteichthyes	7	4	2	7	3	4	5	3	6
Platyhelminthes	1	1	0	1	1	0	0	0	0
Macroalgae	2	1	25	2	1	14	1	0	0
Total	119	85	4413	112	76	5409	104	73	1438

**Table 6** The most abundant T2 taxa in each T1 taxonomic group on each sea bottom type. Their abundance is presented as the average number of organisms per 100m<sup>2</sup> (A<sub>T2</sub>). The relative abundance of a T2 taxa within each T1 taxonomic group is presented (AR<sub>T2</sub>). Values of undetected species are marked with "/".

	MUDDY-SAND			TRANSITIONAL			SANDY-MUD		
T1	T2	A <sub>T2</sub>	AR <sub>T</sub> 2	T2	A <sub>T2</sub>	AR <sub>T</sub> 2	T2	A <sub>T</sub> 2	AR <sub>T</sub> 2
<b>Porifera</b>	<i>Clathria compressa</i>	118	22	<i>Ulosa digitata</i>	73	18	<i>Haliclona</i> spp.	22	19
<b>Cnidaria</b>	<i>Cereus pedunculatus</i>	265	94	<i>Epizoanthus</i> spp.	12	39	<i>Epizoanthus</i> spp.	25	47
<b>Polychaeta</b>	<i>Sabellidae</i>	1	62	<i>Sabellidae</i>	4	46	<i>Filograna</i> sp. / <i>Salmacina</i> sp.	12	55
<b>Gastropoda</b>	<i>Aporrhais pespelecani</i>	3	36	<i>Aporrhais pespelecani</i>	8	64	<i>Aporrhais pespelecani</i>	15	77
<b>Bivalvia</b>	<i>Aequipecten opercularis</i>	63	60	<i>Mimachlamys varia</i>	20	57	<i>Mimachlamys varia</i>	6	478
<b>Cephalopoda</b>	<i>Seppia officinalis</i>	<1	100	<i>Seppia officinalis</i>	<1	100	<i>Seppia officinalis</i>	<1	100
<b>Bryozoa</b>	<i>Schizobranchiel a sanguinea</i>	4	54	<i>Schizobranchiel a sanguinea</i>	4	38	<i>Schizobranchiel a sanguinea</i>	13	36
<b>Crustacea</b>	<i>Paguristes eremita</i>	196	95	<i>Paguristes eremita</i>	103	96	<i>Paguristes eremita</i>	11 3	96
<b>Echinodermat a</b>	<i>Ophiothrix quinquemaculata</i>	298 7	95	<i>Ophiothrix quinquemaculata</i>	453 3	95	<i>Ophiothrix quinquemaculata</i>	94 2	95
<b>Tunicata</b>	<i>Polycarpa</i> cf. <i>mamillaris</i>	22	21	<i>Phallusia mamillata</i>	8	15	cf. <i>Diplosoma spongiforme</i>	21	30
<b>Osteichthyes</b>	<i>Gobius niger</i>	<1	38	<i>Gobius niger</i>	2	40	<i>Serranus hepatus</i>	2	39
<b>Platyhelminthes</b>	<i>Pseudoceros maximus</i>	<1	100	<i>Yungia aurantiaca</i>	<1	100	/	/	/
<b>Macroalgae</b>	<i>Corallinales</i>	22	86	<i>Corallinales</i>	14	99	<i>Corallinales</i>	<1	77

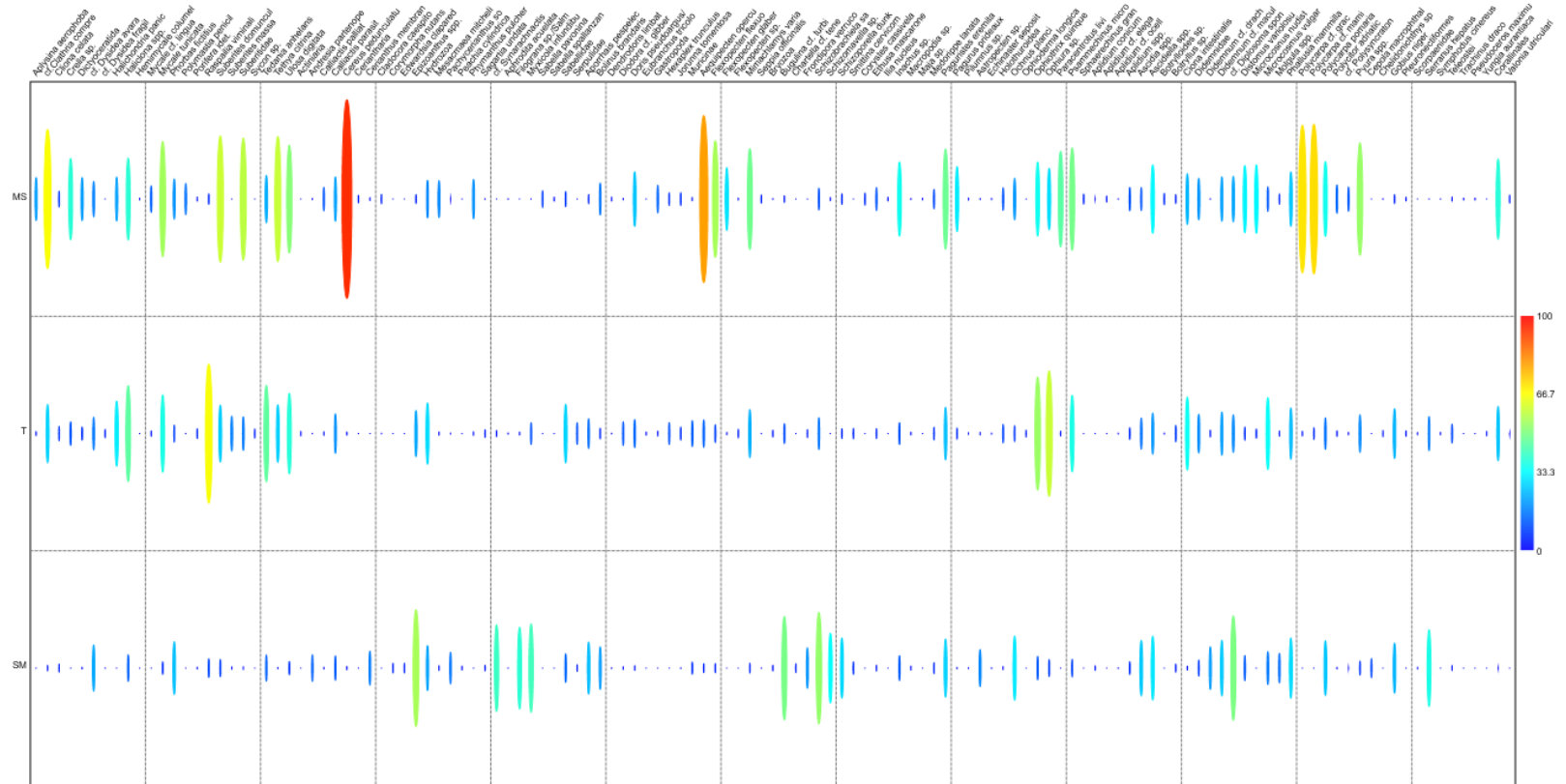
We compared the number of T2 taxa recorded on each individual sea bottom type, in pairs and the number of taxa present on all three sea bottom types (**Figure 14a**). Out of all taxa identified, 92 were recorded on all sea bottom types observed. Muddy-sand and transitional sea bottom type had 13 taxa in common, sandy-mud had 4 taxa in common with transitional and 5 with muddy-sand sea bottom type. 9 taxa were present only on the muddy-sand, 3 on transitional and 3 on sandy-mud bottom type. When observing the taxa identified to the species level (**Figure 14b**), 64 species were recorded on all sea bottom types. Muddy-sand and transitional sea

bottom type had 9 species in common, sandy-mud had 2 species in common with transitional and 4 with muddy-sand sea bottom type. 8 taxa were present only on the muddy-sand, 1 on transitional and 3 on sandy-mud bottom type.



**Figure 14** Comparison of the number of a) taxa and b) species present exclusively on each individual sea bottom type, in pairs and the number of taxa present on all three sea bottom types. The total number of a) taxa and b) species for each sea bottom type is presented outside of the circle. MS:muddy-sand, T:transitional, SM:sandy-mud.

We performed an Individual value analysis (ISA) to obtain the information on the distribution of the species among sea bottom types and their affinity to them (**Figure 15**). The highest individual value on muddy-sand sea bottom type was found for *Cereus pedunculatus* (98%), *Polycarpa* cf. *gracilis* (85%) and *Paracentrotus lividus* (68%) (**Table 7**). These species were significantly ( $p < 0.001$ ) more associated with the muddy-sand type than with any other sea bottom types. The species with the highest individual value on transitional type was *Raspailia viminalis* (81%). For sandy-mud sea bottom type the species with the highest individual value were cf. *Synarachnactis lloydii* (64%), *Filograna* sp./*Salmacina* sp. (62%) and *Schizomavella* sp. (58%).



**Figure 15** Species and their individual value calculated with RStudio and presented with PAST. MS: muddy-sand, T: transitional, SM: sandy-mud.

**Table 7** Indicator species for each sea bottom type and for pairs of types. Individual value is displayed as the proportion of the T2 taxa abundance in the cluster, relative to the overall abundance of the T2 taxa in the study area. Only taxa with statistically significant ( $p < 0.0001$ ) indicator value are displayed.

MUDDY-SAND		TRANSITIONAL		SANDY-MUD	
T2	Ind. Val. [%]	T2	Ind. Val. [%]	T2	Ind. Val. [%]
<i>Cereus pedunculatus</i>	98	<i>Raspailia viminalis</i>	81	cf. <i>Synarachnactis lloydii</i>	64
cf. <i>Polycarpa gracilis</i>	85			<i>Filograna</i> sp. / <i>Salmacina</i> sp.	62
<i>Paracentrotus lividus</i>	68			<i>Schizomavella</i> sp.	60

Species density (average number of organisms per 100m<sup>2</sup>), richness ( $S$ ), evenness ( $J'$ ) and Shannon-Wiener diversity ( $H'$ ) varied between sea bottom types (**Figure 16**).

The mean density of organisms per sub-transect between the sea bottom types was significantly different between transitional, sandy-mud and muddy-sand, transitional sea bottom type. The mean density of organisms in the sandy-mud sea bottom type was 3987.3 org./100m<sup>2</sup> (min: 765.8, max: 16459.9, median: 3074.2), in transitional 4476.4 org./100m<sup>2</sup> (min: 243.8, max: 15455.8, median: 3514.4) and in sandy-mud 708.4 org./100m<sup>2</sup> (min: 4, max: 3012.5, median: 590.5).

The mean number of taxa was significantly different between transitional, sandy-mud and muddy-sand, transitional sea bottom type. The mean number of taxa in muddy-sand sea bottom type was 41 (min: 18, max: 61, median: 42), in transitional 40.52 (min: 24, max: 56, median: 40) and in sandy-mud 33 (min: 8, max: 49, median: 34).

The mean value of evenness was significantly different between muddy-sand, transitional and sandy-mud, transitional. The mean number of evenness in muddy-sand sea bottom type was 0.44 (min: 0.12, max: 0.85, median: 0.42), in transitional 0.27 (min: 0.06, max: 0.49, median: 0.25) and in sandy-mud 0.53 (min: 0.18, max: 0.87, median: 0.47).

The mean value of Shannon-Wiener diversity ( $H'$ ) was significantly different between muddy-sand, transitional and sandy-mud, transitional. The mean diversity

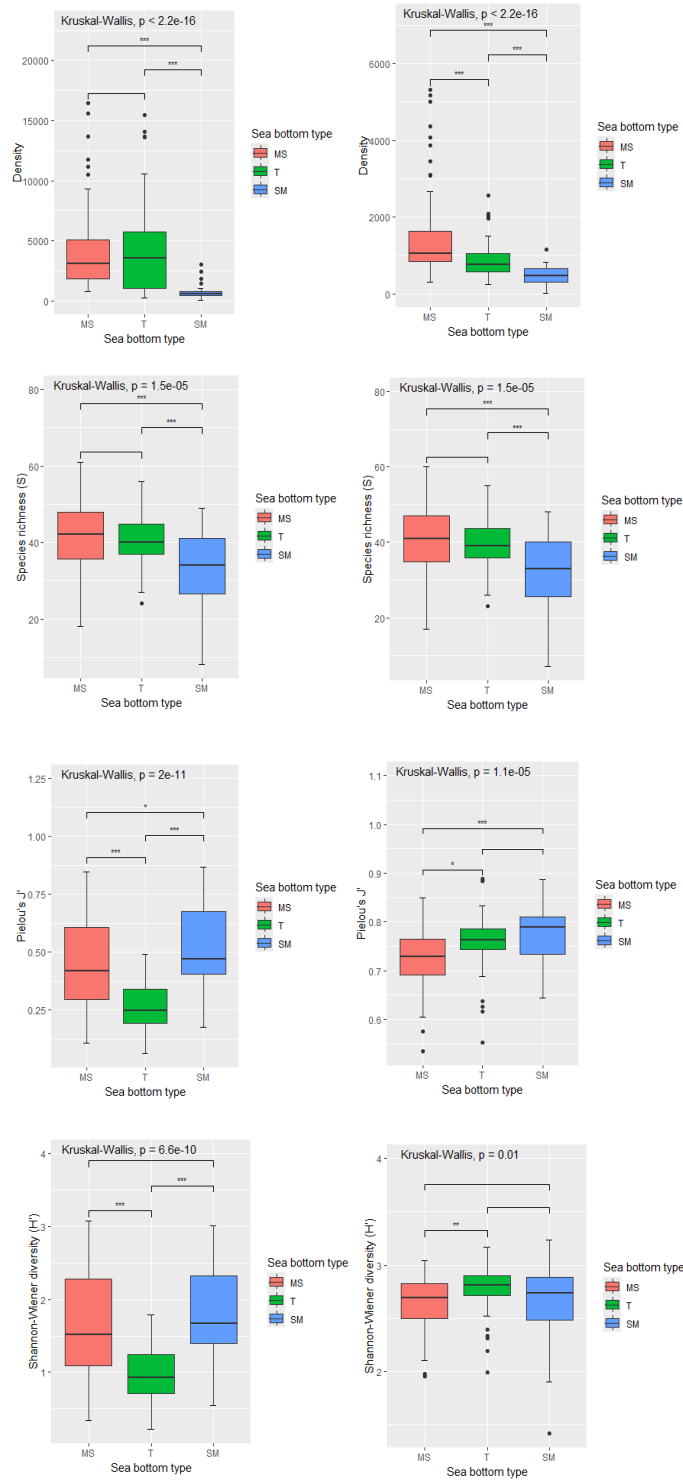
in muddy-sand was 1.63 (min: 0.34, max: 3.07, median: 1.51), in transitional 0.99 (min: 0.22, max: 1.79, median: 0.93) and in sandy-mud 1.80 (min: 0.54, max: 3.0, median: 1.67).

After removing the abundance value for *O. quinquemaculata* from the data set, the mean density of organisms between muddy-sand and transitional became significantly different. The mean density of organisms in the sandy-mud sea bottom type was 1425.6 org./100m<sup>2</sup> (min: 297.7, max: 5321.2, median: 1047.3), in transitional 876.3 org./100m<sup>2</sup> (min: 243.8, max: 2553.5, median: 761.9) and in sandy-mud 487.7 org./100m<sup>2</sup> (min: 4, max: 1163.6, median: 477.4).

The mean number of taxa between the sea bottom types did not change significantly after removing the abundance value for *O. quinquemaculata* from the data set.

The mean value of evenness was significantly different between muddy-sand, and sandy-mud after removing the abundance value for *O. quinquemaculata* from the data set, but muddy-sand, transitional and transitional, sandy-mud mean values of evenness were not significantly different. The mean number of evenness in muddy-sand sea bottom type was 0.73 (min: 0.53, max: 0.85, median: 0.73), in transitional 0.76 (min: 0.55, max: 0.89, median: 0.76) and in sandy-mud 0.78 (min: 0.64, max: 0.88, median: 0.79).

The mean values of Shannon-Wiener diversity (H') between the sea bottom types after removing the abundance value for *O. quinquemaculata* from the data set were not significantly different. The mean diversity in muddy-sand was 2.65 (min: 1.96, max: 3.04, median: 2.67), in transitional 2.77 (min: 1.99, max: 3.17, median: 2.82) and in sandy-mud 2.65 (min: 1.42, max: 3.23, median: 2.73).



**Figure 16** Means and confidence intervals (95%) for density (avg. org./100m<sup>2</sup>), species richness (S), Pielou's evenness index ( $J'$ ) and Shannon-Wiener diversity index ( $H'$ ) for data with (left column) and without (right column) abundance of *Ophiothrix quinquemaculata*. MS:muddy-sand, T:transitional, SM:sandy-mud, blank:  $p > 0.05$ , \*:  $p < 0.05$ , \*\*:  $p < 0.01$ , \*\*\*:  $p < 0.001$ , \*\*\*\*:  $p < 0.0001$ .

## Discussion

The most abundant taxonomic group were the echinoderms, which included the most abundant species, *Ophiothrix quinquemaculata*. The dominance of the ophiurid was also recorded by Fedra *et al.* (1976), who explored an epifauna-rich community off the coast of Slovenia, describing it as the *Ophiothrix*-*Reniera*-*Microcosmus* community (ORM), based on the high biomass of the suspension-feeding macrofauna. The ORM community was dominated by *Ophiothrix quinquemaculata* in number (avg. 10,000 org./100m<sup>2</sup>) and wet weight (10 kg/100m<sup>2</sup>), which represented 28% of the total macrofaunal biomass. The sponge *Reniera* spp. (now *Haliclona* spp.) (no available density data, 10 kg/100m<sup>2</sup>) and the ascidian *Microcosmus* spp. (avg. 250 org./100m<sup>2</sup>, 5 kg/100m<sup>2</sup>) were the second and third most dominant organisms, representing 20% and 16% of the total biomass, respectively. In our study, of the three most dominant species mentioned by Fedra *et al.* (1976), only *O. quinquemaculata* stands out in abundance and was by far the most abundant species. However the density was much lower than documented by Fedra *et al.* (1976). *Haliclona* spp. (avg. 58 org./100m<sup>2</sup>) and *Microcosmus* spp. (avg. 5 org./100m<sup>2</sup>) were also less abundant than mentioned by Fedra *et al.* (1976) and were even not among the most abundant organisms overall. However, when observing the higher taxonomic levels, we still observed a high average abundance of sponges (409.26 org./100m<sup>2</sup>, 10%) and tunicates (85.82 org./100m<sup>2</sup>, 2%) represented by *Ulosa digitata*, cf. *Clathria compressa*, *Diplosoma spongiforme*, *Polycarpa* cf. *mamillaris* and *Phallusia mammillata*.

Our observations show an overall lower overall abundance of epifaunal species in the area of the described ORM community than the recorded abundance in 1976. This might be due to the slow recovery rate of the community after repeated anoxia-related disturbances in the Gulf of Trieste, such as the mass mortality event in 1983, which has severely altered the community structure in the areas (Blasnig *et al.*, 2013; Stachowitsch, 1984). Although *Microcosmus* spp. population was seen to re-establish itself, the sponge *Haliclona* spp. had visibly lower abundance in the samplings between 1991 and 1994 than recorded by Fedra *et al.* in 1976 (Stachowitsch & Fuchs, 1995). Interestingly, we recorded a high abundance of *Cereus pedunculatus*, which Fedra *et al.* (1976) does not mention in his study. The



sea anemone has been observed to withstand short-term anoxic conditions (Blasnig *et al.*, 2013) and having the longest survival rate recorded in the area of the anoxia (Stachowitsch, 1984). Our observation of the high density of *C. pedunculatus* could be related to its resilience towards oxygen depletion; however, the difference in observations may also be due to the sampling method used in Fedra's studies, where they collected the samples by SCUBA diving and therefore excluding the sessile sea anemone from their observations.

The overall species diversity in the study area was low (1.53), along with low species evenness (0.16). However, species evenness and diversity increased after removing the abundance values of *Ophiothrix quinquemaculata*, which seemed to affect the species diversity values with its dominance in abundance measures. Therefore, the density of the most abundant species should be taken into account when observing the overall species diversity in the area.

Based on the Bray-Curtis dissimilarity index we saw that some of the sub-transects were more similar to each other. Grouping of the sub-transects correlated quite well to the five pelite classes and the three determined sea bottom types.

The sub-transects with lower pelite (10-20%, 20-30%) correlated with the ellipse representing muddy-sand type and the highest pelite (40-50%, 50-60%) correlated with sandy-mud sea bottom type. On the transitional sea bottom type, a mixture of sub-transects with different associated pelite fractions were found (10-20%, 20-30%, 30-40%, 40-50%). We have shown, that the epibenthic community differs significantly between the three sea bottom types, even more if *Ophiothrix quinquemaculata* is excluded from the analyses.

In the area of the described muddy-sand sea bottom type, we observed a high abundance of suspension-feeding macrofauna, represented by solitary tunicates (*Polycarpa* cf. *mamillaris*), ascidians (*Cereus pedunculatus*), sponges (cf. *Clathria compressa*) and the overall dominating *Ophiothrix quinquemaculata* (**Table 2**). Overall, the diversity of species was the highest on the muddy-sand sea bottom type, with the highest value of species, present only in this area (**Figure 15**). The characteristic species of the muddy-sand sea bottom type was the sea anemone *Cereus pedunculatus*, with 98% of all recorded individuals found in the area (**Table**

7). This shows high site fidelity of the anemone, usually found buried in the sediment, which has been associated to circalittoral muddy mixed sediment and maërl beds on infralittoral mud (JNCC, 2015) and commonly found in the Adriatic Sea (Kružić, 2002). The observation of the absence of *O. quinque maculata* from the areas with high abundance of *C. pedunculatus*, might be due to the observed predation avoidance behaviour of the brittle star, including evasion of contact (Riedel, Stachowitsch, *et al.*, 2008).

The observed transitional sea bottom type was observed to have the highest abundance of *Ophiothrix quinque maculata*, which appeared in dense, carpet-coverage like assemblages. Although in lower abundance than the muddy-sand, the transitional sea bottom type was still covered by relatively dense suspension-feeding macrofauna, comprised of sponges (*Ulosa digitata*), bivalves (*Mimachlamys varia*) and solitary tunicates (*Phallusia mammillata*). The sponge *Raspailia viminalis* was a characteristic species of the transitional sea bottom type. The growth form of the sponge is usually described as erect, with a tree-like branching pattern, developing as a response of reduced water mixing, stretching into the water column to reach areas with better nutrient supply (Schönberg, 2021). Interestingly, the observed individuals were mostly lying flat on the sea floor surface, with no sign of die-off (exposed spongin fibres) (Cebrian *et al.*, 2011) (**Figure 17**). The phenomenon remains unexplained due to the lack of information available. Sponges were overall very abundant on muddy-sand and transitional sea bottom types, which might be related to suitable habitat conditions with relatively high hydrodynamic activity in the area (Cushman-Roisin *et al.*, 2001). Furthermore, it might also be related to the occurrence of *Peyssonnelia squamaria* and other coralligenous algae on the sea bottom types. The dense *P. squamaria* beds, as well as coralligenous material, provide suitable habitat as a secondary hard bottom as well as a constant source of dissolved organic matter, produced by the red algae and released into the water column (Díaz *et al.*, 2024). Although we observed a high abundance of sponges on the *Peyssonnelia* beds, most of them were fragmented, which can relate to unsuitability of the movable algal beds for the establishment of big erect sponges, which require a more stable substrate (Schönberg, 2021) or to the possible higher fishery activity in the area, causing physical damage to the bigger forms and tearing them into fragments. Several species of *Peyssonnelia* have

been observed as important bioconstruction species in coralligenous assemblages along the Eastern Italian coast (Ingrosso *et al.*, 2018). However, some free living non-calcareous species (*e.g.* *P. squamaria*) have been observed to develop on coastal debris deposits between 90m and 40m deep in the Western Mediterranean (Ballesteros, 2008) and from 15m to 100m along the Italian coast (Ingrosso *et al.*, 2018), depending on water transparency. Due to the high content of suspended organic matter brought into the Northern Adriatic by the adjacent rivers and overall low water transparency, the biocenosis otherwise present in the circalittoral area could be observed in shallower depths (Gamulin-Brida, 1967), thus relating to our observation of the *Peyssonnelia* beds in shallow waters of the Gulf of Trieste.



**Figure 17** Screenshot picture of *Raspailia viminalis*, lying on the bottom.

The density of the ophiurid seemed to increase in the transitional area, but decreased noticeably, along with the overall organism abundance, in the northernmost part, towards the middle of the Gulf of Trieste. There, the epifaunal community was mostly comprised of hermit crabs (*Paguristes eremita*), colonial tunicates (*Diplosoma spongiforme*) and cnidarians (*Epizoanthus* spp.). Although the density of *O. quinquemaculata* on sandy-mud sea bottom type was the lowest out of the three, it was still the most abundant taxon, due to overall low abundance of organisms in the area (**Table 6**). The dominance in abundance of the ophiurid was obvious on all sediment types, especially in transitional type (**Table 6**). The species, characteristic of the sandy-mud sea bottom type, are usually found on soft substrates, buried in the substrate (cf. *Synarachnactis lloydii*) (Picton & Morrow, 2024) or forming assemblages on the seafloor (*Filograna* sp./*Salmacina* sp.) (Enrichetti *et al.*, 2019). Another taxa, associated with the sandy-mud and transitional sea bottom type was *Epizoanthus* spp. which mostly appeared as an

epibiont on hermit crabs shells, which provide a suitable hard habitat on the soft bottom floor (Stachowitsch, 1980).

The abundance of *Ophiothrix quinquemaculata* contributed greatly to the difference in community composition between sea bottom types. The transitional and sandy-mud types appear to be more similar without the presence of *O. quinquemaculata*, which contributed almost 80% to the difference between the types (**Table 4**). This could be explained by the high difference in the average abundance of the ophiurid between the types, where the abundance in transitional type was five times higher than in the sandy-mud type (**Table 4**). On the other side, *O. quinquemaculata* seemed to contribute to greater similarity between the other two pairs of sea bottom types, the muddy-sand and transitional, where the difference between the types was not significant prior to the data alteration (**Table 3**). The overall dominance in the abundance of *O. quinquemaculata* seemed to mask the underlying difference in the structure of the community between muddy-sand and transitional as well as between sandy-mud and transitional sea bottom types.

The sandy-mud and muddy-sand sea bottom types show a great difference in community composition, regardless of the abundance of *Ophiothrix quinquemaculata* (**Table 3**). This was also observed by Fedra *et al.* (1976), who divided the study area in the central community with a high abundance of suspension-feeding organisms and a peripheral area in the east and northeast towards the Gulf of Trieste, represented by the decrease in suspension-feeders and an increase in deposit feeders (Fedra, 1978). Previous studies (Orel & Mennea, 1969; Vatova, 1935, 1949) described the area extending along the west coast of Istria and north towards the Gulf of Trieste as the transitory area from the coastal to the open area, represented by silty and muddy sediment with a *Schizaster chiajei* zoocenosis, first described in the Gulf of Rovinj (Vatova, 1935). However, both descriptions (Orel & Mennea, 1969; Vatova, 1935, 1949) fail to mention the presence of the epifauna-rich community seen off the coast of Slovenia, observed by Fedra *et al.* (1976), describing it as the *Ophiothrix*-*Reniera*-*Microcosmus* community (ORM), based on the high biomass of the suspension-feeding macrofauna. This could be due to the sampling method with the Van Veen sediment grab that Vatova (1935) and Orel & Mennea (1969), which failed to properly

sample the epifaunal species, as most of the organisms got swept away while sampling (Fedra, 1978; Zuschin & Stachowitsch, 2009). The use of a televised camera sledge on the other hand provided a good observation of the epibenthic community in the Northern Adriatic (Fedra *et al.*, 1976; Machan & Fedra, 1975).

The differences in community structure and sea bottom types were also highly correlated with the pelite content in the sediment. We observed a correlation between sub-transect associated with low pelite fraction and muddy-sand sea bottom type with an overall high abundance of suspension-feeding organisms, and between sub-transects associated with higher pelite fraction and sandy-mud sea bottom type, with lower abundance of epifaunal species, along with a lower abundance of *Ophiothrix quinquemaculata* (**Figure 12**).

The observed change in the community biodiversity and organism abundance in relation to increasing pelite sediment component might be related to the passive effect of hydrodynamic patterns on the composition of the seafloor. The bottom current from the Southern Adriatic, directed along the western Istrian and Slovenian coast towards the north and into the Gulf of Trieste, reaches a speed of  $3 \pm 1$  cm/s in the southern opening of the Gulf, and decreases to 1 cm/s in the middle of the Gulf of Trieste (Cushman-Roisin *et al.*, 2001). Areas with a high rate of water circulation, induced by near-bottom currents containing high concentration of nutrients, favour the establishment of a suspension-feeding epifaunal community (Rosenberg, 1995). Furthermore, higher water flow velocity prevents the settlement of fine-grain sediment particles, therefore the sediment in areas with higher current activity mostly comprise of coarse-grain sediment particles (McCave, 1984). Therefore, the observed high abundance of suspension-feeding taxa (*Cereus pedunculatus*, *Polycarpa* cf. *mamillaris*, cf. *Clathria compressa*, *Ulosa digitata*, *Ophiothrix quinquemaculata*) in the area of muddy-sand sea bottom type can be related to hydrodynamic conditions in the area with low pelite content. Interestingly, the transect where we observed abnormal abundance of organisms (**Figure 7b**), lies in the sheltered areas of the sandy dunes formed by the Southern Adriatic current, directed towards the Gulf of Trieste (Kolega *et al.*, 2014; Malačič & Petelin, 2009; Trobec *et al.*, 2017; Zavatarelli *et al.*, 2002). Therefore, the dense

layer of organisms on the bottom floor, could be related to the decrease in bottom current patterns causing a variation in deposition rate in the area (McCave, 1984).

On the other hand, in the areas with low current activity and low water circulation, enabling high settlement rate of sediment particles, the sediment is predominantly composed of fine-grain deposits (Pan & Pratolongo, 2021). In the study area, the pelite component in the sediment increased from the offshore area towards the middle of the Gulf of Trieste. The sedimentation and sediment resuspension in the otherwise low-energy North Eastern Adriatic continental shelf, is mostly induced by seasonal winds Bora and Sirocco, along with current-induced sediment movement from the Po river towards the Northeast (Zuschin & Stachowitsch, 2009). Along with fine sediment, this area is represented by high nutrient and organic matter supply that favour the establishment of a detritus-feeding community (Pan & Pratolongo, 2021; Stachowitsch, 1984; Zuschin & Stachowitsch, 2009), such as the observed smaller suspension-feeders (*Diplosoma spongiforme*, *Epizoanthus* spp., *Myxicola infundibulum*) and surface detritivores (*Paguristes eremita*, *Aporrhais pespelecani*). Furthermore, we observed an increase in the frequency of sediment mounds present on the surface of the sea floor from the transitional towards sandy-mud sea bottom type. The mounds are usually made by burrowing organisms, such as decapod crustaceans and polychaetes, by depositing the material used while building burrows or collecting surface particles from around the burrow opening (Pearson, 2001). The burrows are usually built for feeding and respiration by sub-surface deposit-feeders, which dominate in muddy sediments with high proportion of organic material associated with silt-clay sediment (Nasi *et al.*, 2020). Our observation of high frequency of sediment mounds on the sandy-mud sea bottom type go in hand with Zuschin & Stachowitsch (2009), who recorded a high intensity of bioturbation by burrowing organisms (Kristensen *et al.*, 2012; Pearson, 2001) in the northern part of the Gulf of Trieste.

The community structure in the observed area of muddy-sand sea bottom type correlates to the description of the biocenosis of the coastal detritic bottom described in this area (Lipej *et al.*, 2006). The biocenosis is characterised by diverse community of benthic invertebrates on sandy or muddy sediment, with high amount of organic detritus (Bellan-Santini *et al.*, 2015; Giaccone *et al.*, 2009; UNEP/MAP

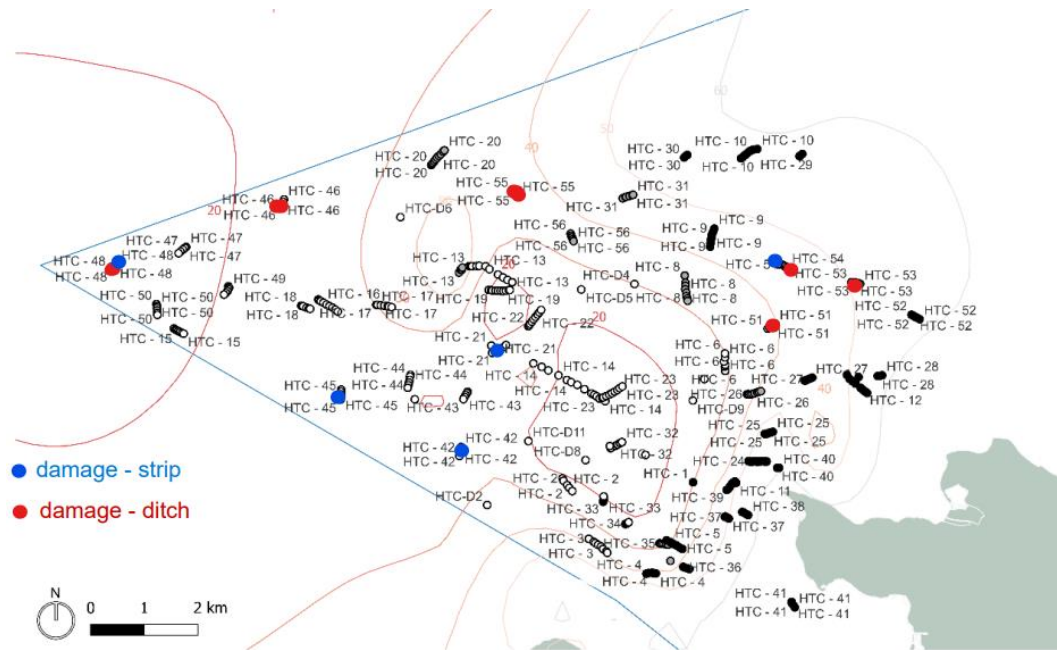
& SPA/RAC, 2021). The observation of *Peyssonnelia* beds and a higher abundance of coralligenous algae in the southern part of the study area could represent the association with *Peyssonnelia* spp. on coastal detritic bottoms with rhodoliths (Bellan-Santini *et al.*, 2015; Mavrič *et al.*, 2023; UNEP/MAP & SPA/RAC, 2021). The association is found in coastal detritic areas, represented by aggregations of living and dead thalli of various calcareous algae, including calcified (*P. rosamarina*) and non-calcified species (*P. squamaria*) (UNEP/MAP & SPA/RAC, 2021).

Although the transects in the northern part of the study area still coincide with the area of the biocenosis of coastal detritic bottom described in the area by Lipej *et al.* (2006, 2018), when observing the overall decrease in the amount of detritic component, abundance of epifaunal organisms and the changing topography of the bottom surface, the area could be under the influence of the neighbouring habitat of the muddy detritic bottom in the northeast, central part of the Gulf of Trieste (Lipej *et al.*, 2006). The circalittoral muddy detritic bottoms are present in the areas with high sediment input from rivers, covering the detritus bottom by layers of mud and sand, inhabited by sessile epifaunal organisms (*Hydrozoa*, *Pennatulacea*, *Ophiothrix* spp.) (UNEP/MAP & SPA/RAC, 2021). The overall area of the Gulf of Trieste was previously described by Vatova (1935) as the *Schizaster chiajei* zoocenosis, associated with silty and muddy sediments with different detrit quantities (Vatova, 1949). Gamulin-Brida (1967) then described it as the biocenosis of coastal detritic bottom mixed with "ooze" (*i.e.* mud), with some characteristics of the biocenosis of the coastal detritic of the Mediterranean (Gamulin-Brida, 1967; Pérès & Picard, 1964). The presence of *Ophiothrix quinquemaculata* was recognised as a characteristic of the muddy detritic sea bottom, where it appears in such high quantity, that it dominates over other species in abundance measures, constituting a separate facies (Bellan-Santini *et al.*, 2015; Gamulin-Brida, 1967; Pérès & Picard, 1964). If we take into account the high abundance of *Ophiothrix quinquemaculata* being a strong characteristic of muddy detritic bottom, we could conclude that the area of transitional sea bottom type should fall into the classification of muddy detritic bottoms (UNEP/MAP & SPA/RAC, 2021). However, when observing the high quantity of detritus material along with the high abundance of epifaunal suspension-feeder community observed on the sea bottom

type, the classification of transitional sea bottom type as coastal detritic bottoms (Giaccone *et al.*, 2009; UNEP/MAP & SPA/RAC, 2021) would also seem appropriate. Therefore the transitional sea bottom type accounts for its name, as the characteristics of the habitat such as the structure of the community, bottom morphology and the quantity of detritus material, could be assigned to both habitats of coastal detritic and muddy detritic bottoms, therefore representing a transitional stage between the described habitat classifications.

We observed a decrease in the abundance of *Ophiothrix quinquemaculata* towards the inner part of the Gulf of Trieste, in the area of the observed sandy-mud sea bottom type, which does not correlate to the description of Vatova or Gamulin-Brida. Fedra (1978) observed a similar decrease in the biomass of the suspension-feeding community, dominating in the southern area, in the east and northeast towards Trieste and an increase in the proportion of motile deposit feeders (*Holothuria* spp., *Ophiura lacertosa*, *Psammechinus microtuberculatus*). He also related the biocenosis in the central part of the Gulf to Vatova's biocenosis of *Schizaster turitella* rather to the assigned *Schizaster chiajei*. The biocenosis of *Schizaster turitella* was described in the Lim channel, north of Rovinj, characterized by high quantity of terrigenous mud covering the seafloor and the recognisable species of *Schizaster canaliferus* and *Turitella communis*, both species typical for the infaunal benthic community (Vatova, 1935). Although our observation of the community structure associated with sandy-mud sea bottom type, with low abundance of epifaunal species, high frequency of sediment mounds and high pelite component in the sediment, stood out from the descriptions of the biocenosis of coastal detritic bottoms described in the area (Lipej *et al.*, 2006), we could not relate it to the biocenosis described by Vatova (1935) as our sampling method was not applicable for the observation of the infaunal community, which is needed for the classification of the biocenosis. Although we did observe some infaunal species on the surface of the sea bottom (skeletal remains of Irregularia), they are not representable observations of the infaunal community, as they can be of foreign origin, transported by currents.





**Figure 18** The marked areas in the study site, where we observed damages on the seafloor. The type of damage is colour coded. (adapted from Mavrič *et al.* (2023))

Along with the observation of the epifaunal community and some sea bottom morphological and structural features, we were also able to detect some damages on the seafloor. Multiple strips and ditches were observed throughout the area, the strips were present mostly in the South and ditches in the Northeast and West of the study area (**Figure 18**). The most commonly used fishing gear for bottom trawling in the Slovenian Sea is the "volantina" otter trawl, which is a near-bottom net, dragged a few meters from the bottom (MKGP, 2021; RAC/SPA, 2003). The otter trawl uses weighted panels or "otter boards" to keep the net open horizontally, dragging the otter boards on the floor as it moves and leaving marks on the floor, which we observed as ditches (RAC/SPA, 2003). The observation of *Cereus pedunculatus* remaining in the area of the dredge strip can be explained by the ability of the anemone to retract into the sediment, therefore avoid being swept by the dredge (Riedel, Stachowitsch, *et al.*, 2008). Although we did not detect a significant difference in the community structure between the undisturbed and affected areas, fishing gears such as dredges and bottom trawls could have negative effects on the bottom community by removing the epifaunal growth, crushing multi-species clumps and disturbing the upper sediment layers (Stachowitsch & Fuchs, 1995; Thrush *et al.*, 2006). This could also be due to the fact that we did not collect enough data from disturbed areas. An increase of sampling locations with

intense fishing activities or traffic routes would provide an estimation of the disturbance rate and how it affects the benthic community.

This study provided an assessment of the structure of the epibenthic community in the Slovenian part of the Gulf of Trieste. We observed an overall gradient in epifaunal abundance from the offshore area towards the central part of the Gulf of Trieste; from an epifauna-rich southern area of muddy-sand sea bottom type, through a transitional area with highest abundance of *Ophiothrix quinquemaculata* and high quantity of detritus material present on the seafloor surface, towards the epifauna-depleted area of sandy-mud sea bottom type, associated to sediments with a high pelite content. Video transect recording with a video sledge SKIKAM proved useful as a non-invasive and time-efficient method for the observation of the epibenthic community on soft bottom. The method could be implemented in further mapping of the distribution of biocenoses (Matarrese *et al.*, 2004) and providing the knowledge on the structure of benthic communities (Maiorano *et al.*, 2011) thus defining a baseline for future research, conservation and management of the benthic habitats in the Slovenian Sea.

### **Acknowledgements**

I would like to thank my supervisors, Doc. dr. Borut Mavrič and Professoressa Laura Airoidi, for their guidance and support. I am grateful for the opportunity to work on this topic.

Data collection and analysis was made possible thanks to the team of Marine Biology Station Piran. Thank you to Tjaša for providing the first steps at taxa identification. Thank you to Ana and Domen for the help with bryozoa and fish identification and to Milijan for the help with statistical analysis. Thank you also to Prof. dr. Lipej for the discussion on biocenoses and the related topics.

A special thanks goes out to my family and friends for providing support and motivation throughout the process.

## References

- Ackers, R. G., Moss, D., Stone, S. M. K., & Morrow, C. C. (2007). Sponges of the British Isles (“Sponge V”) - A colour guide and working document (2007th ed.).
- Ahyong, S., Boyko, C. B., Bernot, J., Brandão, S. N., Daly, M., De Grave, S., de Voogd, N. J., Gofas, S., Hernandez, F., Hughes, L., Neubauer, T. A., Paulay, G., van der Meij, S., Boydens, B., Decock, W., Dekeyzer, S., Goharimanesh, M., Vandepitte, L., Vanhoorne, B., ... Zullini, A. (2024). World Register of Marine Species (WoRMS). WoRMS Editorial Board. Retrieved 12.10.2024, from <https://www.marinespecies.org>
- André, F. (2021). *Microcosmus polymorphus* Heller, 1877. DORIS. Retrieved 12.10.2024, from <https://doris.ffessm.fr/ref/specie/2549>
- Bakker, J. D. (2024). Applied Multivariate Statistics in R. University of Washington.
- Baldacconi, R., & Trainito, E. (2013). Spugne del Mediterraneo. Il Castello.
- Ballesteros, E. (2008). The Deep-Water Peyssonnelia Beds from the Balearic Islands (Western Mediterranean). *Marine Ecology*, 15, 233–253. <https://doi.org/10.1111/j.1439-0485.1994.tb00055.x>
- Bay-Nouailhat, A., & Bay-Nouailhat, W. (2020). Guide des Tuniciers de l’Europe del l’Ouest. M&L éditions, Melgven.
- Baynes, T. W., & Szmant, A. M. (1989). Effect of current on the sessile benthic community structure of an artificial reef. *Bulletin of Marine Science*, 44(2), 545–566.
- Bellan-Santini, D., Bellan, G., Bitar, G., Harmelin, J.-G., & Pergent, G. (2015). Handbook for interpreting types of marine habitat for the selection of sites to be included in the national inventories of natural sites of conservation interest (RAC/SPA (ed.)). United Nations Environment Programme, Mediterranean Action Plan, Regional Activity Centre for Specially Protected Areas (UNEP/MAP-RAC/SPA). [MedKey Habitats] Tunis, Tunisia. <https://doi.org/http://dx.doi.org/10.25607/OBP-1868>
- Bettoso, N., Faresi, L., Aleffi, F., & Pitacco, V. (2023). EPIBENTHIC MACROFAUNA ON AN ARTIFICIAL REEF OF THE NORTHERN ADRIATIC SEA: A FIVE-YEARS PHOTOGRAPHIC MONITORING.
- Blasnig, M., Riedel, B., Schiemer, L., Zuschin, M., & Stachowitsch, M. (2013). Short-term post-mortality scavenging and longer term recovery after anoxia in the northern Adriatic Sea. *Biogeosciences*, 10(11), 7647–7659. <https://doi.org/10.5194/bg-10-7647-2013>
- Boicourt, W. C., Kuzmić, M., & Hopkins, T. S. (1999). The Inland Sea: Circulation of Chesapeake Bay and the Northern Adriatic. In *Ecosystems at the Land-Sea Margin: Drainage Basin to Coastal Sea* (pp. 81–129). <https://doi.org/https://doi.org/10.1029/CE055p0081>
- Cardin, V., & Celio, M. (1997). Cluster analysis as a statistical method for identification of the water bodies present in the Gulf of Trieste (Northern Adriatic Sea). 38, 119–135.

- Cebrian, E., Uriz, M., Garrabou, J., & Ballesteros, E. (2011). Sponge Mass Mortalities in a Warming Mediterranean Sea: Are Cyanobacteria-Harboring Species Worse Off? *PloS One*, 6, e20211. <https://doi.org/10.1371/journal.pone.0020211>
- Clarke, K., & Warwick, R. (2001). Clarke KR, Warwick RM. Change in Marine Communities: An Approach to Statistical Analysis and Interpretation. Primer-E Ltd: Plymouth, UK (2nd ed.).
- Cozzi, S., Falconi, C., Comici, C., Čermelj, B., Kovac, N., Turk, V., & Giani, M. (2012). Recent evolution of river discharges in the Gulf of Trieste and their potential response to climate changes and anthropogenic pressure. *Estuarine, Coastal and Shelf Science*, 115, 14–24. <https://doi.org/https://doi.org/10.1016/j.ecss.2012.03.005>
- Craig, G. Y., & Jones, N. S. (1966). Marine benthos, substrata and paleoecology. *Paleontology*, 9(1), 30–38.
- Cushman-Roisin, B., Gačić, M., Poulain, P.-M., & Artegiani, A. (2001). Physical Oceanography of the Adriatic sea. Kluwer Academic Publishers: Dordrecht, The Netherlands. <https://doi.org/10.1007/978-94-015-9819-4>
- Davenport, J. (2017). DAVENPORT, J., GALLAGHER, M.C. & MCALLEN, R. (2017). Sponge-dwelling hermit crabs from the Clyde Sea. *Crustaceana* 90: 1533-1536. *Crustaceana*, 90, 1533–1536. <https://doi.org/10.1163/15685403-00003710>
- Davies, C. E., Moss, D., & Hill, M. O. (2004). EUNIS Habitat Classification Revised 2004. Technology, October, 310.
- Di Camillo, C., Coppari, M., Bartolucci, I., Bo, M., Betti, F., Bertolino, M., Calcinai, B., Cerrano, C., De Grandis, G., & Bavestrello, G. (2012). Temporal variations in growth and reproduction of *Tedania anhelans* and *Chondrosia reniformis* in the North Adriatic Sea. *Hydrobiologia*, 687. <https://doi.org/10.1007/s10750-011-0877-z>
- Díaz, J. A., Ordinas, F., Farriols, M. T., Melo-Aguilar, C., & Massutí, E. (2024). Sponge assemblages in fishing grounds and seamounts of the Balearic Islands (western Mediterranean). *Deep Sea Research Part I: Oceanographic Research Papers*, 203, 104211. <https://doi.org/https://doi.org/10.1016/j.dsr.2023.104211>
- Dworschak, P. (1987). Burrows of *Solecurtus strigilatus* (Linné) and *S. multistriatus* (Scacchi). *Senckenbergiana Maritima*, 19, 131–147.
- EEA. (2022). EUNIS marine habitat classification 2022 including crosswalks. <https://www.eea.europa.eu/data-and-maps/data/eunis-habitat-classification-1/eunis-marine-habitat-classification-review-2022/eunis-marine-habitat-classification-2022>
- Enrichetti, F., Dominguez-Carrió, C., Toma, M., Bavestrello, G., Betti, F., Canese, S., & Bo, M. (2019). Megabenthic communities of the Ligurian deep continental shelf and shelf break (NW Mediterranean Sea). *PLOS ONE*, 14(10), e0223949. <https://doi.org/10.1371/journal.pone.0223949>
- Fedra, K. (1978). On the ecology of the North Adriatic Sea. Wide-range investigations on the benthos: The Gulf of Triest. In *Memorie di biogeografia*

- Adriatica. Vol. 9. Supplemento (pp. 67–85). Istituto di Studi Adriatici.
- Fedra, K., Olscher, E. M., Scher, C., Jbel, /, Stachowitsch, M., & Wurzian, R. S. (1976). On the Ecology of a North Adriatic Benthic Community: Distribution, Standing Crop and Composition of the Macrobenthos. In *Marine Biology* (Vol. 38). Springer-Verlag.
- Folk, R. L. (1954). The Distinction between Grain Size and Mineral Composition in Sedimentary-Rock Nomenclature. *The Journal of Geology*, 62(4), 344–359. <https://doi.org/10.1086/626171>
- Gamulin-Brida, H. (1967). The benthic fauna of the Adriatic Sea. *Oceanography and Marine Biology: An Annual Review*, 5, 535–568.
- Giaccone, G., Giaccone, T., & Catra, M. (2009). Biocenosis of the coastal detritic bottom. In: Priority habitats according to the SPA/BIO protocol (Barcelona Convention) present in Italy. Identification sheets. *BIOLOGIA MARINA MEDITERRANEA*, 16 (suppl., 200–203.
- Goldstein, J., & Funch, P. (2022). A Review on Genus *Halichondria* (Demospongiae, Porifera). *Journal of Marine Science and Engineering*, 10, 1312. <https://doi.org/10.3390/jmse10091312>
- Haldar, S. K. (2020). Chapter 6 - Sedimentary rocks (S. K. B. T.-I. to M. and P. (Second E. Haldar (ed.); pp. 187–268). Elsevier. <https://doi.org/https://doi.org/10.1016/B978-0-12-820585-3.00006-5>
- Hammer, O., Harper, D., & Ryan, P. (2001). PAST: Paleontological Statistics Software Package for Education and Data Analysis. *Palaeontologia Electronica*, 4, 1–9.
- Harris, C. K., Sherwood, C. R., Signell, R. P., Bever, A. J., & Warner, J. C. (2008). Sediment dispersal in the northwestern Adriatic Sea. *Journal of Geophysical Research: Oceans*, 113(11), 1–18. <https://doi.org/10.1029/2006JC003868>
- Heller, C. (1877). Untersuchungen über die Tunicaten des Adriatischen und Mittelmeeres (Vol. 37). *Denkschriften der Kaiserlichen Akademie der Wissenschaften. Mathematisch-Naturwissenschaftliche Classe*, Wien. <https://www.biodiversitylibrary.org/item/31616>
- Ingrosso, G., Abbiati, M., Badalamenti, F., Bavestrello, G., Belmonte, G., Cannas, R., Benedetti-Cecchi, L., Bertolino, M., Bevilacqua, S., Bianchi, C. N., Bo, M., Boscarì, E., Cardone, F., Cattaneo-Vietti, R., Cau, A., Cerrano, C., Chemello, R., Chimienti, G., Congiu, L., ... Boero, F. (2018). Chapter Three - Mediterranean Bioconstructions Along the Italian Coast (C. B. T.-A. in M. B. Sheppard (ed.); Vol. 79, pp. 61–136). Academic Press. <https://doi.org/https://doi.org/10.1016/bs.amb.2018.05.001>
- JNCC. (2015). The Marine Habitat Classification for Britain and Ireland Version 15.03.
- Kolega, N., Žerjal, A., Poglajen, S., Rant, I., Jeklar, M., Lovrič, E., Vranac, D., Mozetič, D., Slavec, P., Berden-Zrimec, M., Poklar, M., Moškon, S., & Gregorič, P. (2014). Zajem naravnih geomorfoloških značilnosti morskega dna, analiza antropogenih fizičnih poškodb morskega dna in klasifikacija tipov morskega dna z določitvijo obsežnejšega morskega rastja na morskem

dnu.

- Kovačič, B., & Radovan, D. (2019). Prikaz stanja prostora za slovenski del Jadranskega morja in obalo.
- Kristensen, E., Penha-Lopes, G., Delefosse, M., Valdemarsen, T., Organo Quintana, C., & Banta, G. (2012). What is bioturbation? Need for a precise definition for fauna in aquatic science. *Marine Ecology Progress Series*, 446, 285–302. <https://doi.org/10.3354/meps09506>
- Kružić, P. (2002). Marine fauna of the Mljet National Park (Adriatic Sea, Croatia). 1. Anthozoa. *Natura Croatica*, 11, 265–292.
- Lipej, L., Orlando-Bonaca, M., & Mavrič, B. (2016). Biogenic formations in the Slovenian sea. Piran : National Institute of Biology, Marine Biology Station, 2016.
- Lipej, L., Orlando-Bonaca, M., Šiško, M., & Mavrič, B. (2018). Kartografski prikaz in opis bentoških habitatnih tipov v Slovenskem morju vključno s kartografskim prikazom in opredelitvijo najverjetnejših območij vpliva na habitatne tipe: I. fazno poročilo. Piran : National Institute of Biology, Marine Biology Station.
- Lipej, L., Turk, R., & Makovec, T. (2006). Endangered species and endangered habitat types in the Slovenian Sea. Zavod RS za varstvo narave, Ljubljana.
- Machan, R., & Fedra, K. (1975). A new towed underwater camera system for wide-range benthic surveys. *Marine Biology*, 33(1), 75–84. <https://doi.org/10.1007/BF00395004>
- Maiorano, P., Mastrototaro, F., Beqiraj, S., Costantino, G., Kashta, L., Gherardi, M., Sion, L., D'Ambrosio, P., Carlucci, R., D'Onghia, G., & Tursi, A. (2011). Bioecological Study of the Benthic Communities on the Soft Bottom of the Vlora Gulf (Albania). *Journal of Coastal Research*, 2011(10058), 95–105. [https://doi.org/10.2112/SI\\_58\\_9](https://doi.org/10.2112/SI_58_9)
- Malačič, V., & Petelin, B. (2009). Climatic circulation in the Gulf of Trieste (northern Adriatic). *Journal of Geophysical Research: Oceans*, 114(C7). <https://doi.org/https://doi.org/10.1029/2008JC004904>
- Manjón-Cabeza, M. E., & García Raso, J. E. (1999). Shell utilization by the hermit crabs *Diogenes pugilator* (Roux, 1829), *Paguristes eremita* (Linnaeus, 1767) and *Pagurus Forbesii* Bell, 1845 (Crustacea: Decapoda: Anomura), in a shallow-water community from southern Spain. *Bulletin of Marine Science*, 65(2), 391–405.
- Matarrese, A., Mastrototaro, F., D'onghia, G., Maiorano, P., & Tursi, A. (2004). Mapping of the benthic communities in the Taranto seas using side-scan sonar and an underwater video camera. *Chemistry and Ecology*, 20(5), 377–386. <https://doi.org/10.1080/02757540410001727981>
- Mavrič, B., Fortič, A., Lipej, L., Makovec, T., Orlando-Bonaca, M., Pitacco, V., Premrl, T., Šiško, M., & Zamuda, L. L. (2023). Nadgradnja poznavanja biotskih in abiotskih značilnosti ter obsega bentoških habitatnih tipov cirkalitoralni grobi sedimenti (MC3), cirkalitoralni premešani sedimenti (MC4) in cirkalitoralni peski (MC5). Končno poročilo, maj 2023. Poročila 216. Morska Biološka Postaja, Nacionalni inštitut za biologijo, Piran, 46 str.

- McCave, I. N. (1984). Erosion, transport and deposition of fine-grained marine sediments. Geological Society, London, Special Publications, 15(1), 35–69. <https://doi.org/10.1144/GSL.SP.1984.015.01.03>
- McKinney, F. (2007). The orthern Adriatic ecosystem : deep time in a shallow sea. Critical Moments and Perspectives in Earth History and Paleobiology. Columbia University Press.
- Miguez-Salas, O., Brandt, A., Knauber, H., & Riehl, T. (2024). Diversity and density relationships between lebensspuren and tracemaking organisms: a study case from abyssal northwest Pacific. Biogeosciences, 21(2), 641–655. <https://doi.org/10.5194/bg-21-641-2024>
- MKGP. (2021). Načrt upravljanja morskega gospodarskega ribištva v teritorialnih in notranjih morskih vodah Republike Slovenije.
- Monniot, C. (1962). LES MICROCOSMUS DES COTES DE FRANCE. Vie et Milieu. fh1-02923481f
- Montefalcone, M., Tunesi, L., & Ouerghi, A. (2021). A review of the classification systems for marine benthic habitats and the new updated Barcelona Convention classification for the Mediterranean. Marine Environmental Research, 169(105387). <https://doi.org/https://doi.org/10.1016/j.marenvres.2021.105387>
- Nasi, F., Ferrante, L., Alvisi, F., Bonsdorff, E., Auriemma, R., & Cibic, T. (2020). Macrofaunal bioturbation attributes in relation to riverine influence: What can we learn from the Po River lagoonal system (Adriatic Sea)? Estuarine, Coastal and Shelf Science, 232, 106405. <https://doi.org/https://doi.org/10.1016/j.ecss.2019.106405>
- Ogorelec, B., Mišič, M., & Faganeli, J. (1991). Marine geology of the Gulf of Trieste (northern Adriatic): Sedimentological aspects. Marine Geology, 99(1–2), 79–92. [https://doi.org/10.1016/0025-3227\(91\)90084-H](https://doi.org/10.1016/0025-3227(91)90084-H)
- Oksanen, J., Simpson, G., Blanchet, F., Kindt, R., Legendre, P., Minchin, P., O'Hara, R., Solymos, P., M, S., Szoecs, E., Wagner, H., Barbour, M., Bedward, M., Bolker, B., Borcard, D., Carvalho, G., Chirico, M., De Caceres, M., Durand, S., ... Weedon, J. (2024). vegan: Community Ecology Package (R package version 2.6-6.1). <https://vegandevs.github.io/vegan/>, <https://github.com/vegandevs/vegan>
- Orel, G., & Mennea, B. (1969). I popolamenti bentonici di alcuni tipi di fondo mobile del Golfo di Trieste. Pubblicazioni Della Stazione Zoologica Di Napoli, 37(2), 261–276.
- Orlić, M., Kuzmić, M., & Pasarić, Z. (1994). Response of the Adriatic Sea to the bora and sirocco forcing. Continental Shelf Research, 14(1), 91–116. [https://doi.org/10.1016/0278-4343\(94\)90007-8](https://doi.org/10.1016/0278-4343(94)90007-8)
- Pan, J., & Pratolongo, D. (2021). Soft-bottom Marine Benthos (pp. 180–210). <https://doi.org/10.1201/9780429399244-10>
- Park, C. (2007). A Dictionary of Environment and Conservation. Oxford University Press. <https://doi.org/10.1093/acref/9780198609957.001.0001>
- Parsons, T. R., Takahashi, M., & Hargrave, B. (1984). CHAPTER 6 - BENTHIC COMMUNITIES. In T. R. PARSONS, M. TAKAHASHI, & B. B. T.-B. O.

- P. (Third E. HARGRAVE (Eds.), Pergamon International Library of Science, Technology, Engineering and Social Studies (pp. 169–256). Pergamon.  
<https://doi.org/https://doi.org/10.1016/B978-0-08-030765-7.50011-8>
- Pearson, T. H. (2001). Functional group ecology in soft-sediment marine benthos: The role of bioturbation. *Oceanography and Marine Biology: An Annual Review*, 39, 233–267.
- Pérès, J. M., & Picard, J. (1964). Nouveau manuel de bionomie benthique de la Mer Méditerranée. (31 (47)). Recueil des Travaux de la Station marine d'Endoume.
- Petersen, C. G. J. (1915). On the Animal Communities of the Sea Bottom of the Skagerrak, the Christiania Fjord and the Danish Waters. Report from the Danish Biological Station, 23, 1–28.
- Picton, B. E., & Morrow, C. C. (2024). *Synarachnactis lloydii*. (Gosse, 1859). Encyclopedia of Marine Life of Britain and Ireland.  
<https://www2.habitas.org.uk/marbiop-ni/speciesaccounts.php?item=D10750>
- Poulain, P.-M., Kourafalou, V. H., & Cushman-Roisin, B. (2001). Northern Adriatic Sea. In B. Cushman-Roisin, M. Gačić, P.-M. Poulain, & A. Artegiani (Eds.), *Physical Oceanography of the Adriatic Sea: Past, Present and Future* (pp. 143–165). Springer Netherlands. [https://doi.org/10.1007/978-94-015-9819-4\\_5](https://doi.org/10.1007/978-94-015-9819-4_5)
- Premrl, T. (2024). Faunistic assessment of the coastal detritic bottom in the Slovenian Sea by using two different sampling approaches. University of Ljubljana, Biotechnical Faculty.
- R Core Team. (2024). R: A language and environment for statistical computing (4.4.1). R Foundation for Statistical Computing, Vienna, Austria.
- RAC/SPA. (2003). Effects of fishing practices on the Mediterranean sea: Impact on marine sensitive habitats and species, technical solution and recommendations.
- Riedel, B., Stachowitsch, M., & Zuschin, M. (2008). Sea anemones and brittle stars: Unexpected predatory interactions during induced in situ oxygen crises. *Marine Biology*, 153, 1075–1085. <https://doi.org/10.1007/s00227-007-0880-0>
- Riedel, B., Zuschin, M., & Stachowitsch, M. (2008). Dead zones: A future worst-case scenario for Northern Adriatic biodiversity. *Climate Warming and Related Changes in Mediterranean Marine Biota*, 35.
- Rosenberg, R. (1995). Benthic marine fauna structured by hydrodynamic processes and food availability. *Netherlands Journal of Sea Research*, 34(4), 303–317. [https://doi.org/https://doi.org/10.1016/0077-7579\(95\)90040-3](https://doi.org/https://doi.org/10.1016/0077-7579(95)90040-3)
- RStudio Team. (2019). RStudio: Integrated Development for R. RStudio, Inc., Boston, MA. <http://www.rstudio.com/>
- Schmidt, O. (1862). *Die Spongien des adriatischen Meeres*. Leipzig 1862.  
<https://www.marinespecies.org/aphia.php?p=sourcedetails&id=8175>
- Schönberg, C. H. L. (2021). No taxonomy needed: Sponge functional morphologies inform about environmental conditions. *Ecological Indicators*,



- 129, 107806. <https://doi.org/https://doi.org/10.1016/j.ecolind.2021.107806>
- Sigovini, M., Keppel, E., & Tagliapietra, D. (2016). Open Nomenclature in the biodiversity era. *Methods in Ecology and Evolution*, 7(10), 1217–1225. <https://doi.org/https://doi.org/10.1111/2041-210X.12594>
- Snelgrove, P. (2003). Marine Communities. In *Nature* (Vol. 280). <https://doi.org/10.1038/npg.els.0003175>
- Stachowitsch, M. (1980). The Epibiotic and Endolithic Species Associated with the Gastropod Shells inhabited by the Hermit Crabs *Paguristes Oculatus* and *Pagurus Cuanensis*. *Marine Ecology*, 1(1), 73–101. <https://doi.org/https://doi.org/10.1111/j.1439-0485.1980.tb00223.x>
- Stachowitsch, M. (1984). Mass Mortality in the Gulf of Trieste: The Course of Community Destruction. *Marine Ecology*, 5(3), 243–264. <https://doi.org/https://doi.org/10.1111/j.1439-0485.1984.tb00124.x>
- Stachowitsch, M., & Fuchs, A. (1995). Long-term changes in the benthos of the Northern Adriatic Sea. *Annales*, 7, 7–16.
- Syvitski, J. P. M., & Kettner, A. J. (2007). On the flux of water and sediment into the Northern Adriatic Sea. *Continental Shelf Research*, 27(3–4), 296–308. <https://doi.org/10.1016/j.csr.2005.08.029>
- Thorson, G. (1957). Chapter 17: Bottom Communities (Sublittoral or Shallow Shelf). In J. W. Hedgpeth (Ed.), *Treatise on Marine Ecology and Paleogeology* (p. 0). Geological Society of America. <https://doi.org/10.1130/MEM67V1-p461>
- Thrush, S., Gray, J., & Hewitt, J. (2006). Predicting the effects of habitat homogenization on marine biodiversity. *Ecological Applications : A Publication of the Ecological Society of America*, 16, 1636–1642. [https://doi.org/10.1890/1051-0761\(2006\)016\[1636:PTEOHH\]2.0.CO;2](https://doi.org/10.1890/1051-0761(2006)016[1636:PTEOHH]2.0.CO;2)
- Trincardi, F., Correggiari, A., & Roveri, M. (1994). Late Quaternary transgressive erosion and deposition in a modern epicontinental shelf: The Adriatic semiencloded basin. *Geo-Marine Letters*, 14(1), 41–51. <https://doi.org/10.1007/BF01204470>
- Trobec, A., Busetti, M., Zgur, F., Baradello, L., Babich, A., Cova, A., Gordini, E., Romeo, R., Tomini, I., Poglajen, S., Diviacco, P., & Vrabec, M. (2018). Thickness of marine Holocene sediment in the Gulf of Trieste (northern Adriatic Sea). *Earth System Science Data*, 10(2), 1077–1092. <https://doi.org/10.5194/essd-10-1077-2018>
- Trobec, A., Šmuc, A., Poglajen, S., & Vrabec, M. (2017). Submerged and buried Pleistocene river channels in the Gulf of Trieste (Northern Adriatic Sea): Geomorphic, stratigraphic and tectonic inferences. *Geomorphology*, 286, 110–120. <https://doi.org/https://doi.org/10.1016/j.geomorph.2017.03.012>
- UNEP/MAP, & SPA/RAC. (2021). Interpretation manual of the reference list of marine habitat types in the Mediterranean of the Barcelona convention. B.P. 337 - 1080 Tunis Cedex - Tunisia. [https://www.google.com/url?sa=t&source=web&rct=j&opi=89978449&url=https://www.rac-spa.org/meetings/nfp15/nfp\\_docs/inf/21wg502\\_inf04\\_en.pdf&ved=2ahUKE](https://www.google.com/url?sa=t&source=web&rct=j&opi=89978449&url=https://www.rac-spa.org/meetings/nfp15/nfp_docs/inf/21wg502_inf04_en.pdf&ved=2ahUKE)

wjxu6jD4qGGAxUyiP0HHanSAJ4QFnoECBQQAQ&usg=AOvVaw0nqNtI  
aBnlV2JQ64nlibxF

- UNEP/MED. (1998). Reference classification of marine benthic habitat types for the Mediterranean and draft list of Mediterranean marine habitat types of conservation interest.
- Vatova, A. (1935). Ricerche preliminari sulle biocenosi del Golfo di Rovigno: *Thalassia*. II, 1–30.
- Vatova, A. (1949). Nova *Thalassia*: La fauna bentonica dell' Alto e Medio Adriatico. *Nova Thalassia*, 1(3).
- Vazquez, E., Ramos-Espla, A. A., & Turon, X. (1995). The genus *Polycarpa* (Ascidacea, Styelidae) on the Atlantic and Mediterranean coasts of the Iberian Peninsula. *Journal of Zoology*, 237(4), 593–614.  
<https://doi.org/10.1111/j.1469-7998.1995.tb05017.x>
- VideoLan. (2006). VLC media player. <https://www.videolan.org/vlc/index.html>
- Volkenborn, N., Hedtkamp, S. I. C., van Beusekom, J. E. E., & Reise, K. (2007). Effects of bioturbation and bioirrigation by lugworms (*Arenicola marina*) on physical and chemical sediment properties and implications for intertidal habitat succession. *Estuarine, Coastal and Shelf Science*, 74(1), 331–343.  
<https://doi.org/https://doi.org/10.1016/j.ecss.2007.05.001>
- Watling, L. (2019). Macrofauna (J. K. Cochran, H. J. Bokuniewicz, & P. L. B. T.-E. of O. S. (Third E. Yager (eds.); pp. 728–734). Academic Press.  
<https://doi.org/https://doi.org/10.1016/B978-0-12-409548-9.11069-3>
- Wentworth, C. K. (1922). A Scale of Grade and Class Terms for Clastic Sediments. *The Journal of Geology*, 30(5), 377–392.  
<https://doi.org/10.1086/622910>
- Wickham, H., Averick, M., Bryan, J., Chang, W., McGowan, L., François, R., Grolemund, G., Hayes, A., Henry, L., Hester, J., Kuhn, M., Pedersen, T., Miller, E., Bache, S., Müller, K., Ooms, J., Robinson, D., Seidel, D., Spinu, V., ... Yutani, H. (2019). Welcome to the tidyverse. *Journal of Open Source Software*, 4(43), 1686. <https://doi.org/10.21105/joss.01686>
- Zavatarelli, M., Pinardi, N., Kourafalou, V. H., & Maggiore, A. (2002). Diagnostic and prognostic model studies of the Adriatic Sea general circulation: Seasonal variability. *Journal of Geophysical Research: Oceans*, 107(C1), 2–20. <https://doi.org/10.1029/2000JC000210>
- Zuschin, M., & Stachowitsch, M. (2009). Epifauna-dominated benthic shelf assemblages: Lessons from the modern Adriatic Sea. *Palaios*, 24(4), 211–221. <https://doi.org/10.2110/palo.2008.p08-062r>

## Appendix A

### Data collected during sampling

**Table 8** Overview of video transects, sampled with the SKIKAM video sledge. The information on the sampling procedure is given with transect ID, date and location of sampling, along with the speed of trawling. The information about the division of video transects into sub-transects is given with a timestamp, marking the beginning of each sub-transects within a video transect and the duration of the sub-transect. The calculated surface of the sub-transects analysed during video analysis is given. Additionally, the pelite content present on the sampling location of the transects and the observed sea bottom type from video analysis assigned to each sub-transect is presented.

Transect ID	Date	Latitude (N)	Longitude (E)	Speed [m/s]	Sub-transect N	Time on video [hh:mm:ss]	Duration of sub-transect [s]	Length of sub-transect [m]	Surface of sub-transect [m <sup>2</sup> ]	Pelite content [%]	Sea bottom type (MS, T, SM)
<b>HTC-15</b>	23/03/2022	45°33,348'	13°24,998'	0.21	1	00:03:50	160	0.43	49.00	20	MS
				0.21	2	00:06:30	180	0.81	55.13	20	MS
				0.21	3	00:09:30	201	1.33	61.56	20	MS
				0.21	4	00:12:51	40	0.36	12.25	20	MS
				0.21	5	00:13:31	180	1.69	55.13	20	MS
		45°33,298'	13°25,140'	0.21	6	00:16:31	136	1.56	41.65	20	MS
<b>HTC-16</b>	23/03/2022	45°33,667'	13°27,064'	0.36	1	00:02:43	197	0.37	103.43	30	MS
				0.36	2	00:06:00	35	0.15	18.38	30	MS
				0.36	3	00:06:35	125	0.57	65.63	30	MS
				0.36	4	00:08:40	51	0.31	26.78	30	MS
				0.36	5	00:09:31	180	1.19	94.50	30	MS

				0.36	6	00:12:31	170	1.48	89.25	30	MS
				0.36	7	00:15:21	143	1.52	75.08	30	MS
		45°33,550'	13°27,347'	0.36	8	00:17:44	183	2.25	96.08	30	MS
<b>HTC-17</b>	23/03/2022	45°33,625'	13°27,898'	0.36	1	00:02:45	180	0.34	94.50	30	MS
				0.36	2	00:05:45	180	0.72	94.50	30	MS
				0.36	3	00:08:45	161	0.98	84.53	30	MS
				0.36	4	00:11:36	137	1.10	71.93	30	MS
				0.36	5	00:14:21	125	1.25	65.63	30	MS
		45°33,604'	13°28,121'	0.36	6	00:16:36	166	1.91	87.15	30	MS
<b>HTC-18</b>	23/03/2022	45°33,602'	13°26,821'	0.31	1	00:02:34	161	0.29	72.79	30	MS
				0.31	2	00:05:15	50	0.18	22.60	30	MS
				0.31	3	00:06:05	89	0.38	40.24	30	MS
				0.31	4	00:07:34	58	0.30	26.22	30	MS
				0.31	5	00:08:32	79	0.47	35.71	30	MS
		45°33,572'	13°26,949'	0.31	6	00:09:51	17	0.12	7.69	30	MS
<b>HTC-19</b>	23/03/2022	45°33,796'	13°29,508'	0.31	1	00:02:17	183	0.29	82.73	20	MS
				0.31	2	00:05:20	180	0.67	81.38	20	MS
				0.31	3	00:08:20	162	0.94	73.24	20	MS
				0.31	4	00:11:02	139	1.07	62.84	20	MS
				0.31	5	00:13:21	225	2.09	101.72	20	MS
				0.31	6	00:17:06	180	2.14	81.38	20	MS

		45°33,799'	13°29,812'	0.31	7	00:20:06	105	1.47	47.47	20	MS
<b>HTC-20</b>	24/03/2022	45°35,041'	13°28,649'	0.21	1	00:03:48	180	0.48	55.13	40	T
				0.21	2	00:06:48	180	0.85	55.13	40	T
				0.21	3	00:09:48	170	1.16	52.06	40	T
				0.21	4	00:12:48	50	0.44	15.31	40	T
				0.21	5	00:13:45	161	1.54	49.31	40	T
				0.21	6	00:16:45	158	1.84	48.39	40	T
				0.21	7	00:19:45	162	2.22	49.61	40	T
		45°35,192'	13°28,835'	0.21	8	00:22:45	159	2.51	48.69	40	T
<b>HTC-21</b>	24/03/2022	45°33,164'	13°29,575'	0.31	1	00:02:47	180	0.35	81.38	30	MS
				0.36	2	00:05:47	180	0.72	94.50	30	MS
				0.36	3	00:08:47	60	0.37	31.50	30	MS
				0.36	4	00:09:47	44	0.30	23.10	30	MS
				0.31	5	00:10:31	131	0.96	59.22	30	MS
				0.21	6	00:12:53	116	1.04	35.53	30	MS
				0.21	7	00:15:38	6	0.07	1.84	30	MS
				0.21	8	00:15:56	40	0.44	12.25	30	MS
				0.21	9	00:16:36	15	0.17	4.59	30	MS
<b>HTC-22</b>	24/03/2022	45°33,438'	13°30,089'	0.31	1	00:03:25	180	0.43	81.38	30	MS
				0.31	2	00:06:25	109	0.49	49.28	30	MS
				0.31	3	00:08:14	57	0.33	25.77	30	MS

				0.31	4	00:09:11	40	0.26	18.08	30	MS
				0.31	5	00:09:51	30	0.21	13.56	30	MS
				0.31	6	00:10:21	164	1.18	74.14	30	MS
				0.31	7	00:13:21	165	1.53	74.59	30	MS
				0.31	8	00:16:21	126	1.43	56.96	30	MS
		45°33,605'	13°30,267'	0.31	9	00:19:03	154	2.04	69.62	30	MS
<b>HTC-23</b>	24/03/2022	45°32,724'	13°31,129'	0.26	1	00:02:53	156	0.31	59.15	20	MS
				0.26	2	00:05:53	149	0.61	56.50	20	MS
				0.31	3	00:08:53	163	1.01	73.69	20	MS
				0.31	4	00:11:53	163	1.35	73.69	20	MS
				0.36	5	00:14:53	169	1.75	88.73	20	MS
				0.31	6	00:17:53	180	2.24	81.38	20	MS
		45°32,851'	13°31,453'	0.31	7	00:20:53	219	3.18	99.01	20	MS
<b>HTC-24</b>	25/03/2022	45°32,122'	13°33,283'	0.10	1	00:05:30	180	0.69	26.25	60	SM
				0.10	2	00:08:30	180	1.06	26.25	60	SM
				0.10	3	00:11:30	180	1.44	26.25	60	SM
				0.10	4	00:14:30	180	1.81	26.25	60	SM
				0.10	5	00:17:30	180	2.19	26.25	60	SM
				0.15	6	00:20:30	180	2.56	39.38	60	SM
				0.15	7	00:23:30	180	2.94	39.38	60	SM
				0.15	8	00:26:30	180	3.31	39.38	60	SM

				0.15	9	00:29:30	180	3.69	39.38	60	SM
				0.15	10	00:32:30	180	4.06	39.38	60	SM
				0.15	11	00:35:30	180	4.44	39.38	60	SM
				0.15	12	00:38:30	180	4.81	39.38	60	SM
		45°32,122'	13°33,543'	0.15	13	00:41:30	215	6.20	47.03	60	SM
<b>HTC-25</b>	25/03/2022	45°32,400'	13°33,509'	0.21	1	00:03:30	180	0.44	55.13	60	T
				0.21	2	00:06:30	180	0.81	55.13	60	T
		45°32,422'	13°33,625'	0.21	3	00:09:30	189	1.25	57.88	60	T
<b>HTC-26</b>	25/03/2022	45°32,795'	13°33,245'	0.21	1	00:02:06	180	0.26	55.13	50	T
				0.21	2	00:05:06	180	0.64	55.13	50	T
				0.21	3	00:08:06	180	1.01	55.13	50	T
				0.21	4	00:11:06	180	1.39	55.13	50	T
				0.21	5	00:14:06	159	1.56	48.69	50	T
		45°32,828'	13°33,444'	0.26	6	00:17:06	184	2.19	69.77	50	T
<b>HTC-27</b>	25/03/2022	45°32,943'	13°34,069'	0.21	1	00:02:30	180	0.31	55.13	50	SM
				0.21	2	00:05:30	168	0.64	51.45	50	SM
				0.21	3	00:08:30	180	1.06	55.13	50	SM
		45°32,974'	13°34,177'	0.21	4	00:11:30	39	0.31	11.94	50	SM
<b>HTC-28</b>	25/03/2022	45°33,002'	13°35,116'	0.31	1	00:02:14	194	0.30	87.70	60	SM
<b>HTC-29</b>	25/03/2022	45°35,199'	13°33,938'	0.21	1	00:02:20	185	0.30	56.66	60	SM
<b>HTC-30</b>	25/03/2022	45°35,164'	13°32,281'	0.31	1	00:02:07	173	0.25	78.21	60	SM

<b>HTC-31</b>	25/03/2022	45°34,743'	13°31,409'	0.36	1	00:02:30	180	0.31	94.50	50	T
				0.36	2	00:05:30	180	0.69	94.50	50	T
		45°34,780'	13°31,557'	0.31	3	00:08:30	40	0.24	18.08	50	T
<b>HTC-32</b>	25/03/2022	45°32,228'	13°31,300'	0.26	1	00:02:10	230	0.35	87.21	20	MS
				0.26	2	00:06:00	191	0.80	72.42	20	MS
				0.26	3	00:09:11	180	1.15	68.25	20	MS
				0.26	4	00:12:11	180	1.52	68.25	20	MS
				0.26	5	00:15:11	21	0.22	7.96	20	MS
		45°32,291'	13°31,462'	0.26	6	00:15:32	104	1.12	39.43	20	MS
<b>HTC-33</b>	28/03/2022	45°31,686'	13°31,209'	0.21	1	00:03:34	180	0.45	55.13	20	MS
				0.10	2	00:06:34	180	0.82	26.25	20	MS
				0.10	3	00:09:34	180	1.20	26.25	20	MS
		45°31,741'	13°31,214'	0.10	4	00:12:34	87	0.76	12.69	20	MS
<b>HTC-34</b>	28/03/2022	45°31,467'	13°31,533'	0.50	1	00:03:40	180	0.46	131.25	30	T
				0.10	2	00:06:40	173	0.80	25.23	30	T
		45°31,486'	13°31,579'	0.10	3	00:09:40	227	1.52	33.10	30	T
<b>HTC-35</b>	28/03/2022	45°31,280'	13°32,028'	0.21	1	00:03:06	180	0.39	55.13	30	T
				0.21	2	00:06:06	172	0.73	52.68	30	T
				0.21	3	00:08:58	180	1.12	55.13	30	T
		45°31,269'	13°32,153'	0.21	4	00:11:58	209	1.74	64.01	30	T
<b>HTC-36</b>	28/03/2022	45°31,047'	13°32,375'	0.31	1	00:02:08	180	0.27	81.38	50	SM



				0.26	2	00:05:08	180	0.64	68.25	50	SM
		45°31,027'	13°32,463'	0.26	3	00:08:08	35	0.20	13.27	50	SM
<b>HTC-37</b>	28/03/2022	45°31,559'	13°32,957'	0.21	1	00:04:04	170	0.48	52.06	50	SM
		45°31,541'	13°33,016'	0.21	2	00:07:04	101	0.50	30.93	50	SM
<b>HTC-38</b>	28/03/2022	45°31,610'	13°33,207'	0.26	1	00:03:05	180	0.39	68.25	60	SM
		45°31,580'	13°33,292'	0.31	2	00:06:05	110	0.46	49.73	60	SM
<b>HTC-39</b>	28/03/2022	45°31,829'	13°32,978'	0.26	1	00:02:14	178	0.28	67.49	50	SM
				0.26	2	00:05:14	180	0.65	68.25	50	SM
		45°31,901'	13°33,061'	0.36	3	00:08:14	118	0.67	61.95	50	SM
<b>HTC-40</b>	28/03/2022	45°32,060'	13°33,698'	0.36	1	00:02:47	88	0.17	46.20	60	SM
<b>HTC-41</b>	21/02/2023	45°30,714'	13°33,938'	0.20	1	00:03:48	197	0.52	57.46	60	SM
				0.20	2	00:07:05	27	0.13	7.88	60	SM
		45°30,660'	13°33,984'	0.20	3	00:07:32	161	0.84	46.96	60	SM
<b>HTC-42</b>	21/02/2023	45°32,211'	13°29,153'	0.50	1	00:02:15	86	0.13	62.71	30	MS
				0.50	2	00:03:48	16	0.04	11.67	30	MS
				0.50	3	00:04:04	172	0.49	125.42	30	MS
				0.50	4	00:06:56	115	0.55	83.85	30	MS
		45°32,120'	13°29,133'	0.50	5	00:08:51	204	1.25	148.75	30	MS
<b>HTC-43</b>	21/02/2023	45°32,768'	13°29,234'	0.50	1	00:02:10	107	0.16	78.02	30	MS
				0.50	2	00:03:57	187	0.51	136.35	30	MS
				0.50	3	00:07:04	20	0.10	14.58	30	MS

				0.50	4	00:07:24	108	0.56	78.75	30	MS
		45°32,693'	13°29,175'	0.50	5	00:09:12	159	1.02	115.94	30	MS
<b>HTC-44</b>	21/02/2023	45°32,927'	13°28,410'	0.53	1	00:03:26	94	0.22	71.97	30	MS
				0.53	2	00:05:00	236	0.82	180.69	30	MS
				0.53	3	00:08:56	180	1.12	137.81	30	MS
		45°32,797'	13°28,373'	0.53	4	00:11:56	233	1.93	178.39	30	MS
<b>HTC-45</b>	21/02/2023	45°32,765'	13°27,418'	0.50	1	00:02:30	140	0.24	102.08	30	MS
				0.50	2	00:04:50	60	0.20	43.75	30	MS
				0.50	3	00:05:50	181	0.73	131.98	30	MS
				0.50	4	00:08:51	95	0.58	69.27	30	MS
		45°32,667'	13°27,414'	0.50	5	00:10:26	77	0.56	56.15	30	MS
<b>HTC-46</b>	21/02/2023	45°34,667'	13°26,544'	0.50	1	00:03:15	85	0.19	61.98	30	MS
				0.50	2	00:04:40	5	0.02	3.65	30	MS
				0.50	3	00:04:45	189	0.62	137.81	30	MS
				0.50	4	00:07:54	158	0.87	115.21	30	MS
				0.50	5	00:10:32	25	0.18	18.23	30	MS
		45°34,577'	13°26,472'	0.50	6	00:10:57	97	0.74	70.73	30	MS
<b>HTC-47</b>	21/02/2023	45°34,170'	13°25,152'	0.48	1	00:02:04	262	0.38	181.49	20	MS
				0.48	2	00:06:26	64	0.29	44.33	20	MS
				0.48	3	00:07:30	180	0.94	124.69	20	MS
		45°34,105'	13°25,046'	0.48	4	00:10:30	67	0.49	46.41	20	MS

<b>HTC-48</b>	21/02/2023	45°33,983'	13°24,162'	0.50	1	00:02:07	179	0.26	130.52	20	MS
				0.50	2	00:05:06	180	0.64	131.25	20	MS
		45°33,924'	13°24,067'	0.50	3	00:08:06	183	1.03	133.44	20	MS
<b>HTC-49</b>	21/02/2023	45°33,783'	13°25,768'	0.40	1	00:02:37	155	0.28	90.42	30	T
		45°33,699'	13°25,710'	0.40	2	00:05:37	194	0.76	113.17	30	T
<b>HTC-50</b>	21/02/2023	45°33,590'	13°24,742'	0.45	1	00:03:40	180	0.46	118.13	20	MS
				0.45	2	00:06:40	180	0.83	118.13	20	MS
				0.45	3	00:09:40	180	1.21	118.13	20	MS
		45°33,481'	13°24,758'	0.45	4	00:12:40	191	1.68	125.34	20	MS
<b>HTC-51</b>	22/02/2023	45°33,458'	13°33,524'	0.43	1	00:03:57	166	0.46	104.90	40	T
				0.43	2	00:06:57	173	0.83	109.33	40	T
				0.43	3	00:09:57	180	1.24	113.75	40	T
		45°33,509'	13°33,633'	0.43	4	00:12:57	123	1.11	77.73	40	T
<b>HTC-52</b>	22/02/2023	45°33,582'	13°35,704'	0.48	1	00:03:55	180	0.49	124.69	60	SM
				0.48	2	00:06:55	167	0.80	115.68	60	SM
				0.48	3	00:09:42	195	1.31	135.08	60	SM
		45°33,624'	13°35,587'	0.48	4	00:12:57	50	0.45	34.64	60	SM
<b>HTC-53</b>	22/02/2023	45°33,926'	13°34,841'	0.48	1	00:02:33	117	0.21	81.90	60	SM
				0.48	2	00:04:30	50	0.16	35.00	60	SM
				0.48	3	00:05:20	130	0.48	91.00	60	SM
				0.48	4	00:07:30	157	0.82	109.90	60	SM

		45°33,941'	13°34,716'	0.48	5	00:10:07	89	0.63	62.30	60	SM
<b>HTC-54</b>	22/02/2023	45°34,077'	13°33,797'	0.45	1	00:03:05	180	0.39	118.13	50	T
				0.45	2	00:06:05	145	0.61	95.16	50	T
				0.45	3	00:08:30	151	0.89	99.09	50	T
				0.45	4	00:11:01	90	0.69	59.06	50	T
		45°34,107'	13°33,655'	0.45	5	00:12:31	166	1.44	108.94	50	T
<b>HTC-55</b>	22/02/2023	45°34,796'	13°29,826'	0.42	1	00:03:23	145	0.34	88.11	40	T
				0.42	2	00:06:23	180	0.80	109.38	40	T
				0.42	3	00:09:23	180	1.17	109.38	40	T
		45°34,751'	13°29,906'	0.42	4	00:12:23	77	0.66	46.79	40	T
<b>HTC-56</b>	22/02/2023	45°34,378'	13°30,670'	0.43	1	00:02:47	180	0.35	112.50	40	T
				0.43	2	00:05:47	103	0.41	64.38	40	T
				0.43	3	00:07:30	116	0.60	72.50	40	T
		45°34,302'	13°30,714'	0.43	4	00:09:26	160	1.05	100.00	40	T





## Appendix B







### List of species with comments on identification process







The presented list of species with comments should not be considered as an identification key and should not be cited in further works. The list provides an explanation on the process of identification, with the help of descriptions of morphological features of organisms in literature. The identification of organisms during video analysis is not supported by observation of the described organisms with any other observation methods. Dredge samples collected in the course of this project in sampling area (Mavrič *et al.*, 2023), support the presence of certain species in the area, however, it is not guaranteed that the forms observed during video analysis correlate to the species identified from dredge samples. Although the classification of forms, observed during video analysis, cannot match the confidence level of classification using microscopy methods, it still provides a consistent labelling of similar forms, that can be identified subsequently using other sampling methods, *e. g.* combining sampling by hand (SCUBA) and video/photo documentation.

The classification used in this study is marked with "cf." as an indication of the correlation of identifying factors of the specimen with the given species. The identification can be verified after further analysis of the specimen and reference material (Sigovini *et al.*, 2016). The "Possible misidentification" section provides information on the possibility of confusing the given taxa with any other taxa on the list. The descriptions of taxa are based on combining the information from literature and personal comments about the observed forms from the observer. The "NOTE" section in the organism description provides the information on the presence of the organisms in the dredge samples. The description is supported by a screenshot photo of a representable organism. The taxa to which we compared our classification is provided as written in World Register of Marine Species (WoRMS (Ahyong *et al.*, 2024)).








*Table 9 List of species with comments.*




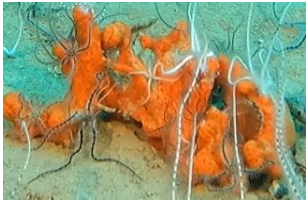

The classification used in this study	Description of taxa	Photographic representation of taxa	Assigned taxa as written in WoRMS
<i>PORIFERA</i>			
<i>Aplysina aerophoba</i>	Erect form with oscula on the terminal side of finger-like structures The colouration of the surface is dark yellow, which can be darkened in damaged areas. The consistency of the surface is leather-like.  NOTE: <i>A. aerophoba</i> identified from dredge samples		<i>Aplysina aerophoba</i> (Nardo, 1833)
cf. <i>Clathria compressa</i>  Possible misidentification: can be confused with <i>U. digitata</i> , <i>T. anhelans</i>	Massive lobed form with visible mesh-like internal structure. The tunic is transparent with channel-like structures flowing on the surface towards the oscula. The colouration is light orange.		<i>Clathria (Clathria) compressa</i> Schmidt, 1862
<i>Cliona celata</i>	Massive form with the surface covered in small oscula. The colouration is light yellow. The form often overgrows hard structures such as detritus material (shells, rocks).		<i>Cliona celata</i> Grant, 1826
<i>Crella sp.</i>	Massive or in the form of epiphyte on bivalve shells. The colouration is pale purple with transparent tunic observed at the opening of oscula and transparent channels flowing towards the oscula.  NOTE: <i>C. rosea</i> identified from dredge samples		<i>Crella</i> Gray, 1867





<p>cf. <i>Dysidea avara</i></p> <p>Possible misidentification: can be confused with <i>D. fragilis</i></p>	<p>Massive erect with oscula on the terminal side of finger-like structures. The colouration is light purple or pink. Protuberances are present on the surface, which appears spiky.</p> <p>NOTE: <i>D. avara</i> identified from dredge samples</p>		<p><i>Dysidea avara</i> (Schmidt, 1862)</p>
<p>cf. <i>Dysidea fragilis</i></p> <p>Possible misidentification: can be confused with <i>D. avara</i></p>	<p>Form of epiphyte on other organisms (sponges, tunicates). The colouration is beige. Protuberances are present on the surface, which appears spiky.</p>		<p><i>Dysidea fragilis</i> (Montagu, 1814)</p>
<p><i>Haliclona</i> spp.</p>	<p>Massive lobed form with oscula distributed irregularly on the surface The colouration is purple to light grey.</p> <p>NOTE: <i>H. simulans</i> identified from dredge samples</p>		<p><i>Haliclona</i> Grant, 1841</p>
<p><i>Halichondria panicea</i></p> <p>Possible misidentification: can be confused with <i>T. anhelans</i>, <i>M. tunicata</i></p>	<p>Erect palmate or creeping form, which resembles a hollow tube with small oscula distributed on the surface. The colouration is light yellow.</p>		<p><i>Halichondria</i> (<i>Halichondria</i>) <i>panicea</i> (Pallas, 1766)</p>
<p><i>Hemimyscale columella</i></p>	<p>Massive with pore-like surface with large craters various in size. The colouration is pale orange to yellow.</p>		<p><i>Hemimyscale columella</i> (Bowerbank, 1874)</p>
<p><i>Phorbast fictitius</i></p>	<p>Massive or in the form of epiphyte on <i>Paguroidea</i> shells. Small circular openings on the surface give it a pore-like appearance. The colouration is red to dark orange</p> <p>NOTE: <i>P. fictitius</i> identified from dredge samples</p>		<p><i>Phorbast fictitius</i> (Bowerbank, 1866)</p>





<i>Polymastia penicillus</i>	Massive form. Observed buried in the sediment floor with finger-like transparent tubes protruding from underneath the sediment.		<i>Polymastia penicillus</i> (Montagu, 1814)
<i>Porifera</i> idet.	Branching (dichotomous growth). Observed to move when hit with the video sledge. The colouration is dark yellow.		<i>Porifera</i> Grant, 1836
<i>Mycale</i> cf. <i>lingua</i>	Massive, lobed form often covered in sediment, with multiple sulci present on the surface. The colouration is dark yellow.		<i>Mycale</i> ( <i>Mycale</i> ) <i>lingua</i> (Bowerbank, 1866)
<i>Mycale tunicata</i>  Possible misidentification: can be confused with <i>H. panicea</i>	Erect branching form with small bumps/protuberances on the surface. The colouration is dark yellow or brown.  NOTE: <i>M. tunicata</i> identified from dredge samples		<i>Mycale</i> ( <i>Aegogropila</i> ) <i>tunicata</i> (Schmidt, 1862)
<i>Raspailia viminalis</i>	Branching form with oscula distributed on the surface of branches. The colouration is dark brown, with the appearance of a fluffy surface.  NOTE: <i>R. viminalis</i> identified from dredge samples		<i>Raspailia</i> ( <i>Raspailia</i> ) <i>viminalis</i> Schmidt, 1862
<i>Suberites massa</i>  Possible misidentification: can be confused with <i>U. digitata</i> , <i>T. anhelans</i>	Erect branching form, growing from a common base. The colouration is light orange with darkened areas.  NOTE: <i>S. massa</i> identified from dredge samples		<i>Suberites massa</i> Nardo, 1847









<i>Suberites domuncula</i>	<p>Massive or in the form of epiphyte on <i>Paguroidea</i> shells. The surface is smooth and often covered in sediment. The colouration is dark orange.</p> <p>NOTE: <i>S. domuncula</i> identified from dredge samples</p>		<i>Suberites domuncula</i> (Olivi, 1792)
<i>Suberitidae</i>	<p>Thin encrusting layer on bivalve shells. The colouration is light orange.</p>		<p><i>Suberitidae</i> Schmidt, 1870</p> <p>Argument: (Baldacconi &amp; Trainito, 2013)</p>
<i>Dictyoceratida</i>	<p>Simple massive or lobed with oscula irregularly distributed on the surface. Observed slight protuberances on the surface, which is often covered in sediment. The colouration is dark brown to black.</p> <p>NOTE: species identified from dredge samples:  <i>Spongia officinalis</i>  <i>Sarcotragus spinosulus</i>  <i>Chondrosia reniformis</i></p>	 	<i>Dictyoceratida</i> Minchin, 1900
<i>Sycon sp.</i>	<p>Tube-like form with oscula on the terminal side. Presence of a bundle of spicules near the oscula. Observed protuberances on the surface. The colouration is white to beige.</p>		<i>Sycon</i> Risso, 1827
<p><i>Tedania anhelans</i></p> <p>Possible misidentification: many forms, can be confused with <i>H. panicea</i>, <i>C. compressa</i>, <i>U. digitata</i></p>	<p>Massive erect or lobed form, with oscula on the terminal side of finger-like structures. The colouration ranges from black or dark brown to orange or dark yellow.</p> <p>NOTE: <i>T. anhelans</i> identified from dredge samples</p>	 	<i>Tedania (Tedania) anhelans</i> (Vio in Olivi, 1792)






<i>Tethya citrina</i>	<p>Massive, spherical shape with protuberances on the surface, giving it a spiky appearance. The colouration is light yellow.</p> <p>NOTE: <i>T. citrina</i> identified from dredge samples</p>		<i>Tethya citrina</i> Sarà & Melone, 1965
<p><i>Ulosa digitata</i></p> <p>Possible misidentification: different forms, can be confused with <i>C. compressa</i>, <i>T. anhelans</i>, <i>S. massa</i>, <i>S. domuncula</i></p>	<p>Observed forms:</p> <p>Form 1: Massive lobed form with oscula distributed irregularly on the surface. The surface appears leather-like and is often covered in fine sediment. The colouration is dark red.</p> <p>Form 2: The form observed as "crawling" on the bottom surface with oscula distributed irregularly on the surface. The colouration is dark orange.</p> <p>Form 3: Erect irregularly branched form with oscula distributed irregularly on the surface. The consistency appears crumbly. The colouration is bright orange.</p> <p>Form 4: Finger-like branched form with oscula distributed irregularly on the sides of the branches. The colouration is light orange.</p> <p>NOTE: <i>U. digitata</i> identified from dredge samples</p>	<p>Form 1:</p>  <p>Form 2:</p>  <p>Form 3:</p>  <p>Form 4:</p> 	<i>Ulosa digitata</i> (Schmidt, 1866)
<b>CNIDARIA</b>			
<i>Actiniaria</i>	<p>Solitary organisms with one type of tentacles surrounding the mouth, positioned in the centre of the oral disc. Observed on soft bottoms, buried or with uncovered body extending into the water column.</p>		<i>Actiniaria</i> Hertwig, 1882





<i>Andresia partenopea</i>	Buried with only the oral disc above the sediment. Great size in comparison to other taxa. Transparent, thick tentacles with no colour pattern.		<i>Andresia partenopea</i> (Andrès, 1883)
<i>Calliactis palliata</i>	Observed as an epibiont on <i>Pagurus prideaux</i> . The colouration of the body is beige to slight pink with purple dots. The oral disc is usually contracted and cannot be seen.  NOTE: <i>C. palliata</i> identified from dredge samples		<i>Calliactis palliata</i> (Müller, 1776)
<i>Calliactis parasitica</i>	Observed as an epibiont on <i>Paguriodea</i> shells. The body colouration is bright brown or beige with white longitudinal stripes.  NOTE: <i>C. parasitica</i> identified from dredge samples		<i>Calliactis parasitica</i> (Couch, 1842)
<i>Cereus pedunculatus</i>	Buried in sediment or with the body above the surface. If the anemone is contracted, the colouration of the body is dark brown with white dots. The colouration of the oral disc varies from dark green to light brown with marbled pattern. The tentacles are positioned only on the brim of the oral disc.  NOTE: <i>C. pedunculatus</i> identified from dredge samples		<i>Cereus pedunculatus</i> (Pennant, 1777)
<i>Ceriantharia</i>	Solitary organisms with two distinct types of tentacles: short labial in the middle and long marginal on the rim of the oral disc. The body is surrounded by a tube, that can be membranous or covered with sand. Observed on soft bottoms, buried or with uncovered		<i>Ceriantharia</i> Perrier, 1893

	body extending into the water column.		
<i>Cerianthus membranaceus</i>	<p>The organism is positioned above the sediment floor in a hard tube. Numerous thin and long rim tentacles extending from the tube.</p> <p>The colouration of tentacles varies from dark to light.</p>		<i>Cerianthus membranaceus</i> (Gmelin, 1791)
<i>Cladocora caespitosa</i>	<p>Colonial organism with multiple polyps arranged in a cushion-like form. The colouration is pale brown and indicated live polyps. The structure is often covered in sediment.</p> <p>NOTE: at first glance can be confused with <i>T. citrina</i> when covered in sediment</p>		<i>Cladocora caespitosa</i> (Linnaeus, 1767)
<i>Corymorpha nutans</i>	Long, translucent stalk fixed in sediment on one side and with a rosette of long, thin tentacles on the other.		<i>Corymorpha nutans</i> M. Sars, 1835
<i>Edwardsia clapedii</i>  Possible misidentification: can be confused with <i>M. mitchellii</i> , <i>P. cylindrica</i> or <i>S. lloydii</i> in low visibility conditions	Buried in sediment with only the oral disc above the sediment. The oral disc is surrounded by 16 tentacles in 2 rows. The tentacles are transparent, the oral disc beige with protruding mouth in the middle.		<i>Edwardsia clapedii</i> (Panceri, 1869)








<i>Epizoanthus</i> spp.	Zooids growing on shells of <i>Paguroidea</i> . (Stachowitsch, 1980)		<i>Epizoanthus</i> Gray, 1867
<i>Hydrozoa</i>	Branched, fern-like structures. Occasionally individual zooids can be observed.		<i>Hydrozoa</i> Owen, 1843
<i>Mesacmaea mitchellii</i>	The organism is positioned above the sediment or buried in some cases. The oral disk surrounded by 36 tentacles in 2 rows, of them 7 inner ones typically erect over the mouth. The tentacles are transparent with brown transversal stripes.		<i>Mesacmaea mitchellii</i> (Gosse, 1853)
<i>Pachycerianthus solitarius</i>  Possible misidentification: can be confused with <i>C. membranaceus</i> , <i>S. lloydii</i>	The organism is positioned above the sediment or partially buried. Thin, long tentacles vary from beige to black.		<i>Pachycerianthus solitarius</i> (Rapp, 1829)
<i>Peachia cylindrica</i>  Possible misidentification: can be confused with <i>E. clapedii</i>	Buried in sediment with the oral disk surrounded by 12 tentacles in one row. The colouration of tentacles is transparent with brown transversal stripes.		<i>Peachia cylindrica</i> (Reid, 1848)
<i>Phymanthus pulcher</i>	Buried in sediment with the tentacles positioned on the brim of the disc except for one row of tentacles, which erect inside the disc. The tentacles are not smooth (unlike <i>C. pedunculatus</i> ), the colouration is dark brown to beige in the centre of the disc.		<i>Phymanthus pulcher</i> (Andrès, 1883)






<p><i>Sagartia undata</i></p> <p>Possible misidentification: can be confused with <i>P. solitarius</i> in low visibility conditions</p>	<p>The organism is positioned above the sediment, with white longitudinal stripes. The long and beige coloured tentacles are positioned on the rim of the oral disc.</p>		<p><i>Sagartia undata</i> (Müller, 1778)</p>
<p>cf. <i>Synarachnactis lloydii</i></p> <p>Argument: difficult observation due to size and visibility</p>	<p>The organism can be buried or positioned above the sediment. The tentacles are thin and beige coloured, with transversal brown stripes.</p>		<p><i>Synarachnactis lloydii</i> (Gosse, 1859)</p>
<b>POLYCHAETA</b>			
<p><i>Aphrodita aculeata</i></p>	<p>Flat, oval shaped body with scale-like dorsal side and black, thick bristles on the side. The body is usually covered in sediment.</p>		<p><i>Aphrodita aculeata</i> Linnaeus, 1758</p>
<p><i>Filograna</i> sp./<i>Salmacina</i> sp.</p> <p>Argument: cannot distinguish between genus <i>in situ</i></p>	<p>A complex of white to beige tubes, attached to a hard substrate (<i>Bryozoa</i>, detritus material). The form resembles a bush.</p>		<p><i>Filograna</i> Berkeley, 1835</p> <p><i>Salmacina</i> Claparède, 1870</p>
<p><i>Myxicola infundibulum</i></p>	<p>The organisms can be burrowed or extended above the sediment. The dark purple tentacles are on the surface of the sediment and connected by a mucilaginous membrane, which remains visible when the animal retracts.</p>		<p><i>Myxicola infundibulum</i> (Montagu, 1808)</p>





<i>Sabella pavonina</i>	The organism is positioned above the sediment in a narrow hard tube. The gill plume extending from the tube is arranged in one-dimensional circle. The appendages are transparent with transversal stripes.		<i>Sabella pavonina</i> Savigny, 1822
<i>Sabella spallanzanii</i>	The organism is positioned above the sediment in a narrow hard tube. The gill plume is arranged in a spiral, the appendages are transparent with transversal stripes.		<i>Sabella spallanzanii</i> (Gmelin, 1791)
<i>Sabellidae</i>	The organism is observed in narrow tubes with attached mud, sand or shell debris. The gill plume, extending from the tube, is arranged in one-dimensional circle.  NOTE: including also the tubes with no gill plume visible		<i>Sabellidae</i> Latreille, 1825
<i>Sedentaria</i>	Sediment mound made up of swirls of excretions.  NOTE: counted but excluded from the analysis		<i>Sedentaria</i> Lamarck, 1818












<i>Serpulidae</i>	White, hard tubes, not covered in sand particles. The colouration of the gill plume is brown to orange and arranged in one-dimensional circle.		<i>Serpulidae</i> Rafinesque, 1815
<b>GASTROPODA</b>			
<i>Aporrhais pespelecani</i>  Comment: observation of the shell <i>in situ</i> does not provide confidence in the inhabitant's identification	Shells with palm-like digitization on the last turn, with 3 flaps and a long siphonal channel.  NOTE: <i>A. pespelecani</i> identified from dredge samples		<i>Aporrhais pespelecani</i> (Linnaeus, 1758)
<i>Bolinus brandaris</i>	Globular shell with spines and a long siphonal channel extending on one side.  NOTE: <i>B. brandaris</i> identified from dredge samples		<i>Bolinus brandaris</i> (Linnaeus, 1758)
<i>Diodora</i> cf. <i>gibberula</i>  Argument: can be confused with other species of <i>Diodora</i> ( <i>D. graeca</i> , <i>D. italica</i> )	Cone-shaped shell with a hole on the top and slight circular striations on the surface.  NOTE: <i>D. gibberula</i> , <i>D. graeca</i> , <i>D. italica</i> identified from dredge samples		<i>Diodora gibberula</i> (Lamarck, 1822)
<i>Eubbranchus tricolour</i>	<i>Nudibranchia</i> species with white colouration. Numerous cerata ending in bright yellow point. Found on <i>Hydrozoa</i> .		<i>Eubbranchus tricolour</i> Forbes, 1838







Gastropoda	Includes gastropod shells that could not be classified to a lower level due to low video quality.		
<i>Hexaplex trunculus</i>	Massive shells with short spines on the surface and short siphonal channel curved upwards.  NOTE: <i>H. trunculus</i> identified from dredge samples		<i>Hexaplex trunculus</i> (Linnaeus, 1758)
<i>Dendrodoris limbata</i>	<i>Nudibranchia</i> species with a smooth mantel surface and colouration combination of orange and black in different patterns (spotted, full black with orange rim).		<i>Dendrodoris limbata</i> (Cuvier, 1804)
<i>Doris pseudoargus</i> / <i>Geitodoris planata</i>  Argument: difficult to distinguish between the species <i>in situ</i>	<i>Nudibranchia</i> species with variable colour patterns and small bumps on the mantel surface.  NOTE: <i>D. pseudoargus</i> , <i>G. planata</i> identified from dredge samples		<i>Doris pseudoargus</i> Rapp, 1827  <i>Geitodoris planata</i> (Alder & Hancock, 1846)
<i>Jorunna tomentosa</i>  Argument: <i>in situ</i> observation does not provide enough information for classification	<i>Nudibranchia</i> species with mostly white colouration and small bumps present on the mantel surface.  NOTE: <i>J. tomentosa</i> identified from dredge samples		<i>Jorunna tomentosa</i> (Cuvier, 1804)
<i>Muricinae</i>	Globular shells with spines and long siphonal channel.		







<b>BIVALVIA</b>			
<i>Aequipecten opercularis</i>	<p>Rounded, almost circular shell with symmetrical valves and pronounced dense radiant ribs on the surface.</p> <p>NOTE: <i>A. opercularis</i> identified from dredge samples</p>		<i>Aequipecten opercularis</i> (Linnaeus, 1758)
<i>Flexopecten sp.</i>	<p>Round shells with strong radiant ribs, which cannot be classified as <i>F. flexuosus</i> or <i>F. glaber</i> due to low visibility and low video quality.</p>		<i>Flexopecten</i> Sacco, 1897
<i>Flexopecten flexuosus</i>	<p>Rounded shell with pronounced, smooth radiant ribs, separated by deep furrows. Smaller in size when compared to <i>F. glaber</i> and <i>A. opercularis</i>.</p> <p>NOTE: <i>F. flexuosus</i> identified from dredge samples</p>		<i>Flexopecten flexuosus</i> (Poli, 1795)
<i>Flexopecten glaber</i>	<p>Rounded shell with flattened, less pronounced radiant ribs than in <i>F. flexuosus</i>, and less frequent than <i>A. opercularis</i>.</p> <p>NOTE: <i>F. glaber</i> identified from dredge samples</p>		<i>Flexopecten glaber</i> (Linnaeus, 1758)
<i>Mimachlamys varia</i>	<p>Oval shell with asymmetrical ears and spikes on the surface of the shell. The radiant ribs are dense, similarly to <i>A. opercularis</i>.</p>		<i>Mimachlamys varia</i> (Linnaeus, 1758)







	NOTE: <i>M. varia</i> identified from dredge samples		
<i>Solecurtus strigilatus</i>	two clear holes in the sediment floor, approximately 3cm in diameter and 2cm apart  NOTE: uncountable, not included in the analysis		<i>Solecurtus strigilatus</i> (Linnaeus, 1758)
<b>CEPHALOPODA</b>			
<i>Sepia officinalis</i>	Dark brown body with variable pattern. The pupil is in the form of "W".		<i>Sepia officinalis</i> Linnaeus, 1758
<b>BRYOZOA</b>			
<i>Bryozoa</i>	Bryozoan forms, which could not be identified due to low visibility and low video quality.		
<i>Bugulina</i> cf. <i>turbinata</i>  Possible misidentification: can be confused with <i>B. spicata</i>	The structure is attached to hard substrate ( <i>Paguroidea</i> shells, detritic material), arranged in a spiral form. The colouration is brown to yellow.  NOTE: <i>B. cf. spicata</i> identified from dredge samples		<i>Bugulina turbinata</i> (Alder, 1857)






<p><i>Chartella</i> cf. <i>tenella</i></p> <p>Possible misidentification: can be confused with <i>C. papyrea</i></p>	<p>The structure is attached to hard substrate (<i>Paguroidea</i> shells, detritic material), arranged in erect flat blades, rounded at the end with a pale rim. The colouration is light brown to beige.</p>		<p><i>Chartella tenella</i> (Hincks, 1887)</p>
<p><i>Frondipora verrucosa</i></p>	<p>The structure is attached to hard substrate (<i>Paguroidea</i> shells, detritic material) and in the form of erect short branches. The colouration is light yellow to beige.</p> <p>NOTE: <i>F. verrucosa</i> identified from dredge samples</p>		<p><i>Frondipora verrucosa</i> (Lamouroux, 1821)</p>
<p><i>Schizobrachiella sanguinea</i></p>	<p>The structure is attached to hard substrate (<i>Paguroidea</i> shells, detritic material) and in the form of encrusting colons, that can form smaller horns. The colouration is dark red with white spots on the surface (retracted zooids).</p> <p>NOTE: <i>S. sanguinea</i> identified from dredge samples</p>		<p><i>Schizobrachiella sanguinea</i> (Norman, 1868)</p>
<p><i>Schizomavella</i> sp.</p> <p>Possible misidentification: can be confused with <i>F. verrucosa</i>, <i>S. dunkeri</i> and other species of the genus</p>	<p>The structure is attached to hard substrate (<i>Paguroidea</i> shells, detritic material) and in the form of encrusting colony with nipple-like bumps on the surface. The colouration is bright yellow.</p>		<p><i>Schizomavella</i> (<i>Schizomavella</i>) <i>mamillata</i> (Hincks, 1880)</p>
<p><i>Schizoporella dunkeri</i></p> <p>Possible misidentification: can be confused with <i>S. mamillata</i>, <i>S. sanguinea</i></p>	<p>The structure is attached to hard substrate (<i>Paguroidea</i> shells, detritic material) and in the form of a smooth encrusting colony glued to the surface. The colouration is light orange.</p> <p>NOTE: <i>S. dunkeri</i> identified from dredge samples</p>		<p><i>Schizoporella dunkeri</i> (Reuss, 1848)</p>







<i>Smittina cervicornis</i>	The structure is attached to hard substrate ( <i>Paguroidea</i> shells, detritic material) and in the form of erect branches with dichotomal pattern, forming bush-like structures. The colouration is dark orange to bright red.		<i>Smittina cervicornis</i> (Pallas, 1766)
<b>CRUSTACEA</b>			
<i>Corystes cassivelaunus</i>	Oval carapace, wider anterior part, with spines on the edge. Anterior part continues into narrow rostrum. The antennae are longer than the carapace. The organism is observed buried in the sand with only anterior part exposed.		<i>Corystes cassivelaunus</i> (Pennant, 1777)
<i>Ethusa mascarone</i>  Possible misidentification: can be confused with <i>M. lanata</i>	Rectangular carapace and slender appendages. The organism is observed carrying other organisms on their head (sponges, bivalve shells).  NOTE: <i>E. mascarone</i> identified from dredge samples		<i>Ethusa mascarone</i> (Herbst, 1785)
<i>Ilia nucleus</i>	Round almost spherical carapace with eyes raised above the carapace in the anterior region. The appendages are elongated and thin. The organism is observed buried in the sand with only anterior part exposed.  NOTE: <i>I. nucleus</i> identified from dredge samples		<i>Ilia nucleus</i> (Linnaeus, 1758)


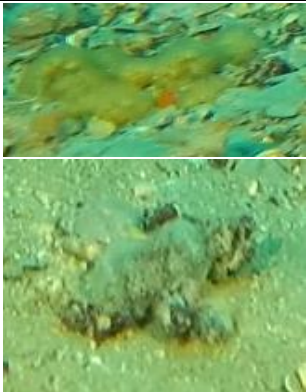


			
<p><i>Inachus spp.</i></p> <p>Argument: species distinguished by close observation of the spines in the dorsal part of the carapace</p>	<p>Triangular carapace, narrowing in the anterior region. A pair of appendages longer than the other. The elongated appendages are often covered in pieces of sponges (decorator crabs).</p> <p>NOTE: species identified from dredge samples:  <i>I. dorsettensis</i>  <i>I. thoracicus</i></p>		<p><i>Inachus</i> Weber, 1795</p>
<p><i>Macropodia sp.</i></p> <p>Argument: species distinguished by close observation of the rostrum</p>	<p>Slim carapace, which appears longer than wider. Long and slim appendages with attached epibionts on the surface (decorator crabs)</p> <p>NOTE: <i>M. rostrata</i> identified from dredge samples</p>		<p><i>Macropodia</i> Leach, 1814</p>
<p><i>Maja sp.</i></p> <p>Argument: species distinguished by the shape of the carapace</p>	<p>Robust, triangular carapace with thick appendages. The carapace and appendages are covered with epibionts (decorator crabs)</p>		<p><i>Maja</i> Lamarck, 1801</p>
<p><i>Medorippe lanata</i></p>			<p><i>Medorippe lanata</i> (Linnaeus, 1767)</p>
<p><i>Paguristes eremita</i></p>	<p>Individuals bearing a shell (decorated or not), with appendages visible underneath: two enlarged bright red chelae, stalked blue eyes and long red antennae.</p>		<p><i>Paguristes eremita</i> (Linnaeus, 1767)</p>






	NOTE: <i>Paguristes eremita</i> identified from dredge samples		
<i>Pagurus prideaux</i>	Right chela bigger than the left and distinguished based on the presence of the anemone <i>Adamsia palliata</i> .  NOTE: <i>P. prideaux</i> identified from dredge samples		<i>Pagurus prideaux</i> Leach, 1815
<i>Pilumnus sp.</i>  Argument: species distinguished by the presence of spines on the carapace	Wide, flat carapace, covered in bristles. One pair of appendages is enlarged.  NOTE: <i>P. spinifer</i> identified from dredge samples		<i>Pilumnus</i> Leach, 1816
<b>ECHINODERMATA</b>			
<i>Astropecten sp.</i>	The dorsal side is covered with scale-like skeletal pieces. The arms lined with rigid spines on the side.  NOTE: <i>A. aranciatus</i> identified from dredge samples		<i>Astropecten</i> Gray, 1840
<i>Ocnus planci</i>	Leather-like body surface with rows of ambulacral podia along the body. The colour of the extended mouth tentacles is dark brown.  NOTE: <i>O. planci</i> identified from dredge samples		<i>Ocnus planci</i> (Brandt, 1835)
<i>Echinaster sepositus</i>	Long, rounded arms with small, irregular protuberance on the surface. The colouration is red or dark orange.  NOTE: <i>E. sepositus</i> identified from dredge samples		<i>Echinaster</i> ( <i>Echinaster</i> ) <i>sepositus</i> (Retzius, 1783)
<i>Holothuroidea</i>	Elongated cylindrical body, covered with large papillae. The colouration is dark brown. The surface		<i>Holothuroidea</i> de Blainville, 1834






	is usually covered in sediment.		
<i>Ophiothrix quinquemaculata</i>	<p>The central disc with five spiny arms, found lying flat on the bottom surface or on top of other organisms (sponges, tunicates). The arms are usually extended into the water column. The colouration varies from white, yellow, black to red and is usually a combination of colours.</p> <p>NOTE: <i>O. quinquemaculata</i> identified from dredge samples</p>		<i>Ophiothrix quinquemaculata</i> (Delle Chiaje, 1828)
<i>Ophioderma longicaudum</i>	<p>Large central disc with long arms (compared to <i>O. quinquemaculata</i>). The surface appears smooth, without bristles. The colouration is black.</p> <p>NOTE: <i>O. longicaudum</i> identified from dredge samples</p>		<i>Ophioderma longicaudum</i> (Bruzellius, 1805)
<i>Ophiura</i> sp.	<p>Rounded disc and short arms (compared to <i>O. longicaudum</i>). The arms are thick at the base and narrowing in the ends. The surface is covered in scales and appears smooth. The colouration is light brown to beige.</p>		<i>Ophiura</i> Lamarck, 1801
<i>Paracentrotus lividus</i>	<p>Dark purple colour with visible pattern of the test. The dark spikes are long and thin.</p>		<i>Paracentrotus lividus</i> (Lamarck, 1816)






	NOTE: <i>P. lividus</i> identified from dredge samples		
<i>Psammechinus microtuberculatus</i>	Dark green to light brown colour with visible pattern of the test. The colouration of the spikes is beige. The size is smaller than <i>P. lividus</i>  NOTE: <i>P. microtuberculatus</i> identified from dredge samples		<i>Psammechinus microtuberculatus</i> (Blainville, 1825)
<i>Sphaerechinus granularis</i>	Large round test with short spikes. The colouration of the spikes is dark purple with white tips.  NOTE: <i>S. granularis</i> identified from dredge samples		<i>Sphaerechinus granularis</i> (Lamarck, 1816)
<b>TUNICATA</b>			
<i>Aplidium conicum</i>  Possible misidentification: can be confused with other <i>Aplidium</i>	The structure is attached to hard substrate ( <i>Paguroidea</i> shells, detritic material) and in the form of rounded firm colony with smooth surface. The pattern of the zooids, arranged around the siphons, is observed on the surface. The colouration is light orange.		<i>Aplidium conicum</i> (Olivi, 1792)
<i>Aplidium</i> cf. <i>elegans</i>  Possible misidentification: can be confused with <i>A. tabarquensis</i>	The structure is attached to hard substrate ( <i>Paguroidea</i> shells, detritic material) and in the form of rounded gelatinous colony. The zooid openings in the shape of crown teeth give the impression of "soft" surface. The tunic is transparent with channel-like structures flowing towards the exhaling siphons.		<i>Aplidium elegans</i> (Giard, 1872)


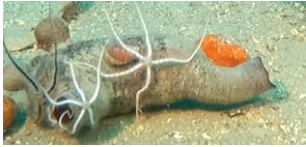



			
<i>Aplidium</i> spp.	<p>Structures attached to hard substrate (<i>Paguroidea</i> shells, detritic material) and in the form of spherical colonies. The zooid siphons are crown shaped, giving the impression of "soft" surface. The zooids are arranged around a common siphon.</p> <p>NOTE: includes all unidentifiable colonial tunicates that could not be identified with confidence due to low visibility and low video quality, where the defining characters were hard to observe</p>		<i>Aplidium</i> Savigny, 1816
<i>Aplidium</i> cf. <i>ocellatum</i>	The structure is attached to hard substrate (detritic material) and in the form of rounded colony. The zooids are attached at the base and not submerged in a common tunic. The zooid siphons are bordered with a white line.		<i>Aplidium ocellatum</i> Monniot C. & Monniot F., 1987
<i>Ascidia</i> spp.  Argument: species distinguished based on the colour of the tunic	The structure is attached to hard substrate (detritic material) and in a solitary form, fixed by the base, with smooth and a white tunic, usually covered in epibionts. The terminal siphon is longer than the one positioned on 1/3 of the body. The siphons are lined with a crown of white or dark teeth.		<i>Ascidia</i> Linnaeus, 1767



	NOTE: <i>A. mentula</i> identified from dredge samples		
<i>Ascidella</i> spp.	<p>The structure is attached to hard substrate (detritic material) and in a solitary form, fixed by the base, with rough white to light brown tunic often covered in sediment. The siphons are short and stubby, one terminal and one positioned on 1/3 of the body. The siphon opening resembles a crown.</p> <p>NOTE: <i>A. aspersa</i> identified from dredge samples</p>	 	<i>Ascidella</i> Roule, 1884
<i>Botrylloides</i> sp.	The structure is attached to hard substrate (detritic material) and in a form of a colony. The zooids are connected by a transparent tunic and organized in parallel rows separated by channels, flowing towards the common siphons.		<i>Botrylloides</i> Milne Edwards, 1841
<i>Botryllus</i> sp.	<p>The structure is attached to hard substrate (detritic material) and in a form of a colony. The zooids are connected by a transparent tunic and grouped around the exhaling siphons in a shape of a star.</p> <p>NOTE: <i>B. schlosseri</i> identified from dredge samples</p>		<i>Botryllus</i> Gaertner, 1774

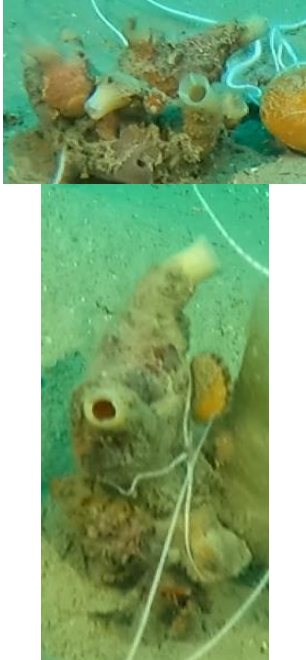


<i>Ciona intestinalis</i>	<p>The structure is attached to hard substrate (detritic material) and in a solitary form, fixed by the base. The intestine can be seen through the translucent tunic. Both siphons are positioned on the terminal side, bordered with a yellow line and a small dark dot in between the lobes.</p> <p>NOTE: <i>C. intestinalis</i> identified from dredge samples</p>		<i>Ciona intestinalis</i> (Linnaeus, 1767)
<i>Didemnidae</i>	<p>Includes structures attached to hard substrate (<i>Paguroidea</i> shells, detritic material) and in a form of a colony. The colouration is black and the zooid arrangement cannot be observed.</p>		<i>Didemnidae</i> Giard, 1872
<i>Didemnum</i> cf. <i>drachi</i>  Possible misidentification: can be confused with other <i>Didemnum</i> species; also with encrusting sponges	<p>The structure is attached to hard substrate (<i>Paguroidea</i> shells, detritic material) and in a form of a colony. The tunic is light orange with a smooth surface. The zooids are arranged in lines with channels flowing towards the exhaling siphons on the surface.</p>	 	<i>Didemnum drachi</i> Lafargue, 1975
<i>Didemnum</i> cf. <i>maculosum</i>	<p>The structure is attached to hard substrate (<i>Paguroidea</i> shells, detritic material) and in a solitary form of a colony. The colour of the tunic varies from brown to dark green. The zooids are arranged in a marbled</p>		<i>Didemnum maculosum</i> (Milne Edwards, 1841)





	<p>pattern with channels flowing towards the exhaling siphons on the surface.</p> <p>NOTE: <i>D. maculosum</i> identified from dredge samples</p>		
<p>cf. <i>Diplosoma spongiforme</i></p> <p>Possible misidentification: can be confused with other <i>Didemnidae</i></p>	<p>The structure is attached to hard substrate (detritic material) and in a form of a colony, resembling a massive lobed form of <i>Porifera</i>. The colouration varies from grey, green to beige, sometimes white and transparent, where zooids can be seen below the tunic. The surface appears "soft" and "fluffy". Big exhaling siphons on the surface resemble oscula in sponges.</p> <p>NOTE: <i>D. spongiforme</i> identified from dredge samples</p>		<p><i>Diplosoma spongiforme</i> (Giard, 1872)</p>
<p><i>Distomus variolosus</i></p>	<p>The structure is attached to hard substrate (<i>Paguroidea</i> shells, detritic material) and in a form of a colony, where the zooids attached at the base. The two siphons of the zooid are positioned close together. The colouration of the zooids is dark red with white stripes on the siphons.</p> <p>NOTE: <i>D. variolosus</i> identified from dredge samples</p>		<p><i>Distomus variolosus</i> Gaertner, 1774</p>
<p><i>Microcosmus</i> cf. <i>nudistigma</i></p> <p>Possible misidentification: can be confused with <i>M. vulgaris</i></p>	<p>The structure is attached to hard substrate (detritic material) and in a solitary form, fixed on the ventral side (opposite the siphons), with wrinkled dark red to purple tunic, often covered with epibionts. The terminal siphon is longer than the one positioned on the dorsal side. The siphons are far apart and between them runs a longitudinal</p>		<p><i>Microcosmus nudistigma</i> Monniot C., 1962</p>




	ridge. The colouration of the siphons is dark purple with thin white stripes. Open siphons resemble a trumpet.		
<p><i>Microcosmus</i> cf. <i>vulgaris</i></p> <p>Possible misidentification: can be confused with <i>M. nudistigma</i></p>	<p>The structure is attached to hard substrate (detritic material) and in a solitary form, fixed on the ventral side, with smooth dark red tunic (resembles elephant's trunk), seldom covered with epibionts. The terminal siphon is longer than the one positioned on the dorsal side. The siphons are positioned far apart with wide, straight opening. The colouration of the tunic and the siphons is dark red.</p>	 	<p><i>Microcosmus vulgaris</i> Heller, 1877</p>
<p><i>Molgula</i> spp.</p> <p>Argument: species distinguished by the sediment grain coverage on the tunic</p>	<p>The structure is attached to hard substrate (detritic material) and in a solitary form, almost completely buried in the sediment with only the siphons visible. The tunic is soft covered with sediment grains. The siphons are short and positioned close together.</p>	 	<p><i>Molgula</i> Forbes, 1848</p>








<p><i>Phallusia mammillata</i></p>	<p>The structure is attached to hard substrate (detritic material) and in a solitary form, fixed by the base, with a thick white tunic with irregular bumps on the surface. The terminal siphon is longer than the one positioned on 1/3 of the body.</p>		<p><i>Phallusia mammillata</i> (Cuvier, 1815)</p>
<p><i>Polycarpa cf. gracilis</i></p> <p>Possible misidentification: can be confused with <i>P. mamillaris</i> if covered with epibionts; other species distinguished based on the morphology of the digestive tract</p>	<p>The structure is attached to hard substrate (detritic material) and in a solitary form, fixed by the ventral side, with soft yellow tunic, which is seldom overgrown with epibionts. The siphons are positioned far apart. The colouration of the siphons is yellow with beige or white stripes.</p>		<p><i>Polycarpa gracilis</i> Heller, 1877</p>







<p><i>Polycarpa</i> cf. <i>mamillaris</i></p> <p>Possible misidentification: can be confused with <i>P. pomaria</i>, distinguished by the morphology of the gonads and branchial structures; can be confused with <i>P. gracilis</i></p>	<p>The structure is attached to hard substrate (detritic material) and in a solitary form, fixed by the ventral side, with rough tunic, often covered with epibionts. The terminal siphon is longer than the one positioned on 1/3 of the body. The colouration of the siphons is light beige with white stripes.</p>		<p><i>Polycarpa mamillaris</i> (Pallas, 1774)</p>
<p><i>Polycarpa pomaria</i></p> <p>Possible misidentification: can be confused with <i>P. mamillaris</i>, <i>Ascidella</i> spp. if covered in epibionts</p>	<p>The structure is attached to hard substrate (detritic material) and in a solitary form, fixed by the base, with smooth red tunic, covered in epibionts or sediment. The siphons are short and stubby, one terminal and the other slightly lower. The colouration of the siphons is bright red, occasionally with white stripes.</p>		<p><i>Polycarpa pomaria</i> (Savigny, 1816)</p>
<p><i>Polycitor adriaticus</i></p>	<p>The structure is attached to hard substrate (<i>Paguroidea</i> shells, detritic material) and in a form of a colony. The colouration of the test is white. The zooids are distributed irregularly, embedded in the test, which gives the surface of the test a smooth appearance. The zooid siphons have a pigment spot in each lobe, which can be observed as dark</p>		<p><i>Polycitor adriaticus</i> (Drasche, 1883)</p>



	spots on the surface of the colony.		
<p>cf. <i>Polysyncraton lacazei</i></p> <p>Argument: can be confused with other <i>Didemnidae</i>; distinguished by microscopic observation of zooids</p>	<p>The structure is attached to hard substrate (<i>Paguroidea</i> shells, detritic material) and in a form of a colony with a firm dark orange test. The zooids are distributed on the surface in rows, flowing towards common exhaling siphons, which surrounded by small white dots.</p>		<p><i>Polysyncraton lacazei</i> (Giard, 1872)</p>
<p><i>Pyura</i> spp.</p> <p>Possible misidentification: can be confused with <i>M. vulgaris</i>; species distinguished by the morphology of the digestive tract</p>	<p>The structure is attached to hard substrate (detritic material) and in a solitary form, fixed by the ventral side, with rough, wrinkled tunic, covered with epibionts and sediment. The short and stubby siphons are positioned on each side of the body. The colouration of the siphons is red with occasional white lines inside.</p>		<p><i>Pyura</i> Molina, 1782</p>

<i>Salpidae</i>	<p>Solitary or colonial individuals connected by side in a chain-like form.</p> <p>Each zooid has a cylindrical transparent tunic, where a small globular dark red mass can be observed. The chain of individuals dwell near the bottom floor.</p> <p>Solitary individuals observed on top of sponges or anemones.</p> <p>NOTE: uncountable, not included in the analysis</p>		<i>Salpidae</i> Lahille, 1888
<b>OSTEICHTHYES</b>			
<i>Cepola macrophthalma</i>	<p>Ribbon-like body, gradually narrowing towards the tail. The dorsal fin is unsegmented.</p> <p>The animals are observed near the bottom, swimming in and out of holes, made in the sediment.</p>		<i>Cepola macrophthalma</i> (Linnaeus, 1758)
<i>Chelidonichthys</i> spp.  Argument: species distinguished based on size, head shape and pectoral fin colouration	<p>Massive head, flattened under the mouth. The snout is rounded, the eyes are positions on the top.</p> <p>The three free rays from pectoral fins can be observed.</p>		<i>Chelidonichthys</i> Kaup, 1873

<i>Gobius niger</i>	Marble colouration of the body. The eyes are close together and protuberant. The animal is observed dwelling on the bottom surface.		<i>Gobius niger</i> Linnaeus, 1758
<i>Pleuronectiformes</i>	Flat fish observed dwelling on the surface of the sediment. The colouration is similar to sand.		
<i>Scorpaenidae</i>  Argument: lower classifications distinguished based on the size and shape of scales on the skin	Massive head with thorns. The animal is observed dwelling on the sediment surface, often in hiding behind clumps of organisms (sponges, bivalves, tunicates).		<i>Scorpaenidae</i> Risso, 1827
<i>Serranus hepatus</i>	Narrow body with light and dark transversal stripes. The fins are transparent except for the darker pelvic fins. A dark spot can be observed on the dorsal fin.	 	<i>Serranus hepatus</i> (Linnaeus, 1758)
<i>Symphodus cinereus</i>	Marble colouration of the body with light longitudinal stripes present occasionally. The colouration of the body is beige to light green. A black spot can be observed on the bottom side of the caudal fin.		<i>Symphodus cinereus</i> (Bonnaterre, 1788)
<i>Teleostei</i>	Fish, which we could not identify due to low visibility and low quality video, where the		

	classifications signs were hard to observe.		
<i>Trachinus draco</i>	Big head with eyes on the top and upward inclined mouth. The flattened body gradually narrows towards the tail. The animal is observed partially buried in sediment.		<i>Trachinus draco</i> Linnaeus, 1758
<i>Pseudoceros maximus</i>	Flat oval body with small undulations on the mantle edge. A longitudinal ridge extends along the body on the dorsal side with two tentacles in the anterior part. The colouration is dark brown with white specs on the surface.		<i>Pseudoceros maximus</i> -type A Lang, 1884
<i>Yungia aurantiaca</i>	Flat oval body with small undulations on the mantle edge. A longitudinal ridge extends along the body on the dorsal side. The colouration is dark orange with white line along the mantle edge.		<i>Yungia aurantiaca</i> (Delle Chiaje, 1822)
<b>MACROALGAE</b>			
<i>Corallinales</i>	Round structures covered in encrusting red algae, found on the bottom floor; resemble pink rocks.		<i>Corallinales</i> P.C. Silva & H.W. Johansen, 1986
<i>Peyssonnelia squamaria</i>	Dark red, flat and leaf shaped thalli, attached to hard substrate (organisms with shells, detritic material), forming dense beds and covering the bottom floor.  NOTE: <i>P. squamaria</i> identified from dredge samples		<i>Peyssonnelia squamaria</i> (S.G.Gmelin) Decaisne ex J.Agardh, 1842
<i>Valonia</i> spp.  Argument: species distinguished based on the branching of vesicles	Dark green thalli form colonies of vesicles. The colonies are attached to hard substrate (detritic material), partially covered in sediment		<i>Valonia</i> C.Agardh, 1823

## Porifera

Classification of forms is based on the observed morphological features, correlated to the description of organisms in literature. However, due to high polymorphism of some species (*Ulosa digitata*, *Tedania anhelans*) (Ackers *et al.*, 2007; Di Camillo *et al.*, 2012), some classifications include more than one form which can be taken as different form of one species or as individuals of different species. Furthermore, some of the observed taxa did not match the description of growth form in literature. The growth form of *Raspailia viminalis* is described as erect and branching (Schmidt, 1862), however, we observed the specimens lying flat on the bottom surface. *Halichondria panicea* is described as encrusting with a smooth, leathery surface and oscula only slightly protuberant on the surface (Baldacconi & Trainito, 2013), however we observed a hollow growth form, with oscula distributed irregularly on the surface. Although a variety of growth forms have been observed (Goldstein & Funch, 2022), a more detailed observation of the internal structure is required for improving the confidence of identification.

The classification of Suberitidae is based on Baldacconi & Trainito (2013), describing the encrusting organisms on bivalves. However, the classification should be considered with discretion, as the observation method does not provide enough information for a clear distinction between Suberitidae and other species of encrusting sponges.

The classification of Dictyoceratida includes species with high resemblance (*Spongia officinalis*, *Sarcotragus spinosulus*, *Chondrosia reniformis*), which have been identified from dredge samples (Mavrič *et al.*, 2023) but cannot be distinguished by the method of observation during video analysis.

Although the observed forms of *Ulosa digitata* are here considered under the same classification, further investigation of morphology of the internal structures is required to consider the forms as one species. Furthermore, a repeated analysis of the video material is required for separate quantification of each growth form.

Some taxa were also found in association with organisms of other taxa, which served as an identification characteristic *e. g.* *Suberites domuncula* with *Paguristes eremita*, Suberitidae with *Aequipecten opercularis* and *Mimachlamys varia*.

## Cnidaria



The observation method hindered the identification of organisms especially in low visibility conditions, where the transparent nature of the tentacles of anemones made them hard to distinguish from the sediment. Furthermore, the number of tentacles was usually not a reliable characteristic and was used only as "more than" or "less than" when comparing two observations *e. g. Edwardsia claparedii* has more tentacles than *Peachia cylindrica* but less than *Mesacmaea mitchellii*. Additional characteristics such as the arrangement of tentacles and their thickness was used when determining the classification of observed forms. Some taxa were also found in association with organisms of other taxa, which served as an identification characteristic *e. g. Calliactis palliata* with *Pagurus prideaux*, *Calliactis parasitica* and *Epizoanthus* spp. with *Paguristes eremita*.

### Polychaeta

Classification of taxa is mostly based on the observation of secondary structures made by animals (tubes), which were counted regardless the presence of the gill plume in some species (*Filograna* sp./*Salmacina* sp., Sabellidae, Serpulidae). The observation of excrements on the sediment surface were correlated to the subclass Sedentaria (Kristensen *et al.*, 2012; Volkenborn *et al.*, 2007). Even though the excrement structures were counted during video analysis, they have been excluded from the data analysis and are only used as additional observations in community descriptions, as they represent a group of infaunal species and cannot be observed with a method using video sledge.

### Gastropoda

Taxa with a recognisable shell structure were not difficult to spot, however the inhabitants of the shells could not be recognised easily, as hermit crabs have a preference for *Hexaplex trunculus*, *Bolinus brandaris* shells (Manjón-Cabeza & García Raso, 1999) and *Aporrhais pespelecani* shells (Davenport, 2017). Furthermore, a great deal of shells were abandoned, covered with epibionts or partially buried in sediment. Therefore, one of the main recognisable characteristics, when the animal in the shell could not be seen, were "lebensspuren" (*i.e.* marks, left in the sediment, indicating movement of the animal in the shell) (Blasnig *et al.*, 2013; Miguez-Salas *et al.*, 2024). Regarding the classification of sea

slugs, the level of uncertainty comes from the morphological polymorphism of the animals (*Doris pseudoargus* and *Geitodoris planata*) and the inability of recognising morphological characteristics using video analysis.

### Bivalvia

The living organisms were recognised easily by the open shells in filtration and were startled by the sledge and "swam" away by rapid opening and closing of the valves (*Aequipecten opercularis*, *Mimachlamys varia*, *Flexopecten flexuosus*, *F. glaber*). The association of holes in the sediment with *Solecurtus strigilatus* was made based on the description of burrow shape of the animal (Dworschak, 1987); only presence and absence of the holes is documented as *S. strigilatus* is an infaunal species and therefore cannot be observed with a method using video sledge.

### Bryozoa

Identification and classification of the observed forms was based on previous records of organisms obtained from dredge samples (Mavrič *et al.*, 2023), overall species present in the area and expert opinion. However, the classification should still be taken with caution, as the species are distinguished by the observation of zooids, using microscopy methods.

### Crustacea

Identification of organisms was based on the observed morphological features (size and shape of appendages, carapace characteristics) which were limited by the observation method. Hermit crabs (*Paguristes eremita*) were easily recognised by the shell with two enlarged bright red appendages poking out from underneath. However, other taxa were harder to spot until they startled and fled (*Pagurus prideaux*), hid in the sediment (*Coristes cassivelaunus*, *Ilia nucleus*), underneath a bigger sponge or tunicate (*Pilumnus* sp., *Medorippe lanata*, *Ethusa mascarone*) or took a defensive stand (*Inachus* spp.). Some taxa were found in association with organisms of other taxa, which served as an identification characteristic *e.g.* *P. eremita* with *Suberites domuncula*, *P. prideaux* with *Calliactis palliata*.

## Echinodermata

Both *Ophiothrix quinquemaculata* and *Ophiothrix fragilis* have been documented in the Northern Adriatic, however more literature records mention *O. quinquemaculata* (Fedra *et al.*, 1976; Mavrič *et al.*, 2023; Riedel, Zuschin, *et al.*, 2008; Stachowitsch, 1984; Vatova, 1935) than *O. fragilis* (Bettoso *et al.*, 2023), which could mean that the classifications are used as synonyms. Nevertheless, the classification of *O. quinquemaculata* is used in this study, supported by dredge samples collected in the area (Mavrič *et al.*, 2023). With the exception of *Ophiura longicaudum*, all other ophiurids with the appearance of a smooth surface are classified under *Ophiura* sp.

## Tunicata

Classification of *Ascidiella* forms to the species level was mostly based on colouration of the organisms, which varied greatly and could not always be observed due to the low video quality. Therefore, all forms were classified under the common genus, however, the form with white stripes on the inner side of the siphons (cf. *Ascidiella aspersa*) prevailed greatly in density over the form with red colouration of the siphons (cf. *Ascidiella scabra*). Further classification would be possible using additional sampling methods.

Classification of the *Microcosmus* spp. species was based on descriptions of morphological features found in literature of species descriptions. However, this proved difficult due to inconsistent labelling and multiple dissimilar descriptions of one species *e.g.* the description of *M. vulgaris* by Heller (1877) and Monniot (1962). In both, the form is described as solitary and fixed on the ventral side, opposite the siphons, which are dark red and have a circular opening. One siphon is longer than the other. However, Heller (1877) mentions a distinct longitudinal ridge on the dorsal side, from one siphon to the other, which is not described for this species by Monniot (1962). Furthermore, Monniot (1962) presents the longitudinal ridge as a characteristic of *M. nudistigma*, along with dark purple colouration of siphons with bright stripes on the inside. The observed forms of *M. nudistigma* and *M. vulgaris* during video analysis are classified based on the descriptions of the species in Monniot (1962) and Heller (1877).



*M. vulgaris* is often confused with *M. polymorphus* in descriptions of external morphology (André, 2021) or only mentioned briefly (Bay-Nouailhat & Bay-Nouailhat, 2020). Furthermore, *M. polymorphus* can easily be confused with species of *Pyura* when observing external morphology, therefore the classification of *Pyura* sp. during video analysis cannot be considered with great confidence and should be verified after the observation of internal morphology of specimens. Both *M. polymorphus* and two species of *Pyura* (*P. microcosmus*, *P. dura*) are mentioned in previous records (Fedra *et al.*, 1976) and are considered present in the area.

Furthermore, Fedra *et al.* (1976) recorded two species of *Polycarpa* (*P. gracilis*, *P. pomaria*) in the area, which provided a level of confidence for the classification of the observed forms following the description of Vazquez *et al.* (1995). However, due to incomplete and often confusing morphological descriptions of the species (Heller, 1877; Vazquez *et al.*, 1995), further identification using microscopy is needed. The observed form assigned to *P. gracilis* was also considered similar to *Microcosmus sabatieri* regarding the structure and colouration of the tunic, however due to the lack of the typical red and purple striation of the siphons, this correlation was discarded.

A more detailed observation of forms described as *Polycarpa mamillaris* and *Polycarpa pomaria* is required, as the observed forms are classified based only on description of morphology in literature (Bay-Nouailhat & Bay-Nouailhat, 2020), which did not correlate entirely to the observed forms. Especially regarding *P. mamillaris*, where the classification of the observed form is an approximation of the form described by Bay-Nouailhat and Bay-Nouailhat (2020) and Vazquez *et al.* (1995).

#### Osteichthyes

The classification includes demersal fish observed during video analysis. Although the video analysis method does not provide sufficient details for species identification, the classification is based on previous records of distribution and dredge samples carried out in the area (Mavrič *et al.*, 2023).

Macroalgae: Corallinales, rhodoliths

The term "corallinales" used to classify the rhodolith structures, counted upon occurrence, (1 "corallinales" = 1 biogenic nodule/rhodolith structure). However, the counting was irregular, as a lot of the structures were lost in either *Peyssonnelia* beds or dense *Ophiothrix* covers, therefore the method of counting should be changed to the method used for the estimation of *Peyssonnelia* abundance (presence/absence). The rhodolith structure identification is not supported with dredge samples as the rhodolith particles proved to be too small to get caught up in the dredge net (Mavrič *et al.*, 2023), therefore the species composition as well as the proportion of the volume made up by the coralline algae in one nodule remains unknown.

Macroalgae: *Peyssonnelia squamaria*

*Peyssonnelia* beds observed in the video analysis consisted of *P. squamaria*, which was identified by dredge samples in the area (Mavrič *et al.*, 2023). Although other species described in the Slovenian Sea (*P. rosa-marina*, *P. polymorpha*) (Lipej *et al.*, 2016) were mostly present in the biogenic formations on the infralittoral hard substrate, they can still be present on soft-bottom circalittoral beds.